



**Universidade do Minho**  
Escola de Ciências

Patrícia Manuela Hilário Oliveira **Color preference for simple and complex compositions**

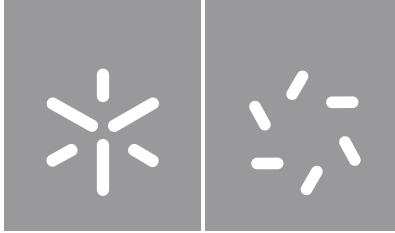
Patrícia Manuela Hilário Oliveira

**Color preference for simple  
and complex compositions**

UMinho | 2023

outubro de 2023





**Universidade do Minho**  
Escola de Ciências

Patrícia Manuela Hilário Oliveira

**Color preference for simple  
and complex compositions**

Dissertação de Mestrado  
Mestrado em Optometria Avançada

Trabalho efetuado sob a orientação do  
**Professor Doutor Sérgio Miguel Cardoso Nascimento**

## **DIREITOS DE AUTOR E CONDIÇÕES DE UTILIZAÇÃO DO TRABALHO POR TERCEIROS**

Este é um trabalho académico que pode ser utilizado por terceiros desde que respeitadas as regras e boas práticas internacionalmente aceites, no que concerne aos direitos de autor e direitos conexos.

Assim, o presente trabalho pode ser utilizado nos termos previstos na licença abaixo indicada.

Caso o utilizador necessite de permissão para poder fazer um uso do trabalho em condições não previstas no licenciamento indicado, deverá contactar o autor, através do RepositóriUM da Universidade do Minho.



**Atribuição-NãoComercial-SemDerivações CC BY-NC-ND**

<https://creativecommons.org/licenses/by-nc-nd/4.0/>

## **ACKNOWLEDGMENT**

I want to start by thanking my advisor Professor Sérgio Miguel Cardoso Nascimento for the tremendous support and guidance given throughout this time and all the insightful information and advice offered.

I would like to thank my friends and family for all the motivational and encouraging words given.

Everyone who is a part of the Color Science Lab thanks for always being available to help and being supportive friends and colleagues. Particularly thank you to Professor João Manuel Maciel Linhares for suggesting that I join the Starter project of the Lab.

Very importantly many thanks to all the participants who took time out of their lives to do the experiments their collaboration made this work possible.

Last but not least I want to express gratitude to Fundação para a Ciência e a Tecnologia for the grant (26/ECUM/CFUM/2022 - UIDB/04650/2020) awarded to me that supported the work carried out.

## **STATEMENT OF INTEGRITY**

I hereby declare having conducted this academic work with integrity. I confirm that I have not used plagiarism or any form of undue use of information or falsification of results along the process leading to its elaboration.

I further declare that I have fully acknowledged the Code of Ethical Conduct of the University of Minho.

## **RESUMO**

### **Preferência de cor para composições simples e complexas.**

A preferência por cores isoladas tem sido estudada empirica e teoricamente há muito tempo e é relativamente bem caracterizada. A preferência por combinações de cores é mais difícil de estudar e menos compreendida.

Este trabalho teve dois objetivos principais. O primeiro foi investigar como a educação artística e as deficiências de cor vermelho-verde influenciam o padrão de preferência para cores isoladas, usando um paradigma clássico. O segundo foi desenvolver e aplicar um novo paradigma experimental para caracterizar as preferências para composições de cores complexas.

Foram selecionadas 46 amostras físicas do Natural Color System (NCS) para as experiências. Estas representam 10 tonalidades, três níveis de luminosidade e dois níveis de saturação. As amostras acromáticas também foram selecionadas com três níveis de luminosidade. Participaram cinquenta indivíduos sem formação artística, cinquenta com formação artística e cinco dicromatas vermelho-verde nas experiências.

Na primeira experiência, os participantes visualizaram cada amostra colorida isoladamente e classificaram o quanto gostavam ou não gostavam da cor, apontando para uma escala de -10 a +10. Os resultados revelaram o padrão clássico de preferência, ou seja, uma maior preferência por azuis e uma menor preferência por amarelos escuros. Para os participantes com formação artística, um padrão de preferência diferente foi obtido entre as amostras.

Na segunda experiência, os participantes usaram as amostras do NCS para criar várias combinações: 2x1, 2x2, 3x3 e 4x4. As combinações de cores foram analisadas computacionalmente e caracterizadas com diversos parâmetros quantitativos. O padrão dos dados colorimétricos obtidos a partir da experiência foi comparado com os padrões obtidos simulando diferentes tipos de seleções aleatórias. Descobriu-se que as combinações feitas não eram aleatórias. Foram reveladas algumas diferenças importantes significativas entre os participantes com formação artística e aqueles sem formação artística.

**Palavras chave:** Combinações de Cores, Estética das Cores, Preferência por Cores, Visão de Cores,

## **ABSTRACT**

### **Color preference for simple and complex compositions**

Color preference for single colors has been empirically and theoretically studied for a long time and is relatively well characterized. Color preference for combinations of colors is more difficult to study and less well understood.

This work had two main goals. To use a classical paradigm to investigate how artistic education and red-green color deficiencies influence the pattern of preference for single colors and to develop and apply a new experimental paradigm to characterize preferences for complex color compositions.

Forty-six physical samples of the Natural Color System (NCS) were selected for the experiments. They represent 10 hues, three lightness levels, and two saturation levels. Achromatic samples were also selected with three lightness levels. Fifty participants without artistic education, fifty with artistic education and five red-green dichromats carried out the experiments.

In the first experiment, participants viewed each colored sample isolated and rated how much they liked or disliked the color by pointing to a scale from -10 to +10. Results revealed the classical pattern of preference, i.e., higher preference for blues and lower for dark yellows. For the participants with artistic education, a different pattern of preference across the samples was obtained.

In the second experiment, participants used the NCS samples to make several combinations: 2x1, 2x2, 3x3, and 4x4. The color combinations were computationally analyzed and characterized with several quantitative parameters. The pattern of colorimetric data obtained from the experiment was compared with the patterns obtained simulating different types of random selections. It was found that the way combinations were done was not random. Some important differences between participants with artistic education and those without were revealed.

**Keywords:** Color Aesthetics, Combinations of Colors, Color Preference, Color Vision



## Index

RESUMO .....	v
ABSTRACT.....	vi
ABBREVIATIONS AND ACRONYMS.....	xi
INDEX OF FIGURES .....	xiii
INDEX OF TABLES.....	xviii
1.INTRODUCTION .....	1
2.FUNDAMENTALS OF COLOR VISION SCIENCE .....	2
2.1.The Eye.....	2
2.1.1.The Cornea .....	2
2.1.2.The Lens.....	3
2.1.3.The Humors .....	4
2.1.4.The Iris.....	4
2.1.5.The Retina.....	5
2.1.6.The Fovea and Foveola .....	7
2.1.7.The Macula .....	8
2.1.8.The Optic Nerve and the Blind Spot .....	8
2.2.Lateral geniculate nucleus (LGN) and Cortical processing.....	9
2.3.Color Vision .....	10
2.3.1.Light and Color.....	10
2.3.2.Color Vision Theory.....	11
2.3.2.1.Trichromatic Theory.....	11
2.3.2.2.Opponent Color Theory.....	11
2.3.3.Color Vision Deficiencies.....	12
2.3.3.1.Inherited Deficiencies .....	13
2.3.3.2.Acquired Deficiencies .....	14

2.3.3.3. Color Confusion Lines.....	15
2.3.4. Color Vision Tests .....	15
2.3.4.1. Ishihara Plates Test .....	15
2.3.4.2. Farnsworth-Munsell 100-Hue Test.....	16
2.3.4.3. Anomaloscopes .....	17
2.4. Color Spaces .....	18
2.4.1. Tristimulus and Color Matching Functions .....	18
2.4.2. CIE 1931 (x,y) .....	20
2.4.3. CIE 1976 (LAB) .....	21
2.4.4. CIECAM02-UCS.....	23
2.5. Natural color system.....	24
3. LITERATURE REVIEW: COLOR PREFERENCE .....	27
4. GENERAL METHODS.....	33
4.1. Selection of the samples and illumination.....	33
4.2. Making the physical samples .....	37
5. PILOT EXPERIMENTS .....	39
5.1. Color preference for single colors without the achromatic samples .....	39
5.1.1. Objective .....	39
5.1.2. Methods.....	39
5.1.3. Results and conclusions .....	42
5.1.4. Discussion.....	45
5.2. Color preference for color combinations without repetition .....	46
5.2.1. Objective .....	46
5.2.2. Methods.....	46
5.2.3. Results and conclusions .....	50
5.2.4. Discussion.....	57

6.COLOR PREFERENCE FOR SINGLE COLORS .....	59
6.1.Objective .....	59
6.2.Methods.....	59
6.3.Results and conclusions .....	61
6.4.Discussion.....	64
7.COLOR PREFERENCE FOR COLOR COMBINATIONS .....	66
7.1.Objective .....	66
7.2.Methods.....	66
7.3.Results and conclusions .....	67
7.4.Discussion.....	74
8.EFFECTS OF ARTISTIC EDUCATION ON COLOR PREFERENCE FOR SINGLE COLORS .....	76
8.1.Objective .....	76
8.2.Methods.....	76
8.3.Results and conclusion .....	77
8.4.Discussion.....	79
9.EFFECTS OF ARTISTIC EDUCATION ON COLOR PREFERENCE FOR COLOR COMBINATIONS	80
9.1.Objective .....	80
9.2.Methods.....	80
9.3.Results and conclusion .....	80
9.4.Discussion.....	87
10.EFFECTS OF RED-GREEN COLOR VISION DEFICIENCIES ON COLOR PREFERENCE FOR SINGLE COLORS .....	89
10.1.Objective .....	89
10.2.Methods.....	89
10.3.Results and conclusions .....	89
10.4.Discussion.....	91

11.EFFECTS OF RED-GREEN COLOR VISION DEFICIENCIES ON COLOR PREFERENCE FOR COLOR COMBINATIONS .....	93
11.1.Objective .....	93
11.2.Methods.....	93
11.3.Results and conclusions .....	93
11.4.Discussions .....	100
12.CONCLUSIONS AND FUTURE WORK .....	102
13.OUTPUTS OF THIS WORK .....	103
REFERENCES.....	104
APPENDIX .....	109

## **ABBREVIATIONS AND ACRONYMS**

NCS: Natural Color System

cones/mm<sup>2</sup>: Cones per square millimeter

S: Short wavelength

M: Medium wavelength

L: Long wavelength

nm: Nanometers

°: degrees

LGN: Lateral geniculate nucleus

R: Red

G: Green

B: Blue

fMRI: Functional magnetic resonance imaging

CIE: Commission Internationale de l'Éclairage (French) – International Commission on Illumination (English)

$V(\lambda)$ : Photopic luminance function

K: Kelvin

$\Delta E$ : Color difference

$L^*$ : Perceived lightness in the CIELAB color space

$a^*$ : Red and green chroma perceptions in the CIELAB color space

$b^*$ : Yellow and blue chroma perceptions in the CIELAB color space

$J'$ : Lightness in the CIECAM02-UCS color space

$a'_M$ : Redness-greenness in the CIECAM02-UCS color space

$b'_M$ : yellowness-blueness in the CIECAM02-UCS color space

S: Blackness

W: Whiteness

C: Chromaticness

CCT: Correlated color temperature

cm: Centimeter

cd/m<sup>2</sup>: candela per square meter

$E_n$ : Illuminance

CEICVS 052/2021: Comissão de Ética para a Investigação em Ciências da Vida e da Saúde da  
Unniversidade do Minho

## INDEX OF FIGURES

Figure 1 - Schematic diagram of the human eye with some key components labeled. Adapted from [1]. .....	2
Figure 2 - Schematic illustration of the cornea with all five layers labeled. Adapted from [3]. .....	3
Figure 3 - Schematic diagram of the retina cells. Adapted from [1]. .....	5
Figure 4 - Log <sub>10</sub> S- (white squares), M- (gray diamonds), and L- (black circles) cone photopigment spectra for different templates. Adapted from [9]. .....	6
Figure 5 - Plot of the visual acuity variation with eccentricity. Adapted from [15]. .....	7
Figure 6 - Absorption spectrum of macular pigment. Adapted from [17]. .....	8
Figure 7 - Fundus image of a healthy eye. Adapted from [20]. .....	9
Figure 8 - Diagram of the functional segregation of the primate visual system. Adapted from [22]. .....	10
Figure 9 - The electromagnetic spectrum. Adapted from [23]. .....	10
Figure 10 - Stimulus for the demonstration of opponent after images. Adapted from [1]. .....	12
Figure 11 - Color confusion lines for tritanopia (top left), protanopia (top right), and deuteranopia (bottom). Adapted from [30]. .....	15
Figure 12 - Ishihara plates test. ....	16
Figure 13 - Farnsworth–Munsell 100-Hue Test. ....	17
Figure 14 - Example of an Anamoscope. ....	17
Figure 15 - Color matching functions of R (represented with red), G (represented with green), and B (represented with blue). Adapted from [30]. .....	18
Figure 16 - CIE 1931 color matching functions for the x, y, and z primaries R. Adapted from [46]. .....	19
Figure 17 - Photopic luminance function. Adapted from [30]. .....	19
Figure 18 - CIE chromaticity diagram. Adapted from [30]. .....	20
Figure 19 - CIELAB diagram. Adapted from [49]. .....	23
Figure 20 - Hue circle. Adapted from [51]. .....	25
Figure 21 - Triangle used to illustrate nuance. Adapted from [47]. .....	26
Figure 22 - (A) The 32 chromatic colors (B) The projections of the 32 colors onto an isoluminant plane in CIELAB color space. (C) Color preferences of all 48 participants (D) WAVEs for the 32 chromatic colors. Adapted from [65]. .....	28
Figure 23 - Mean hue preference curves. (A) British subjects. (B) Chinese subjects. Adapted from [62]. .....	31

Figure 24 - sRGB representation of the selected NCS samples illuminated by the Solux lamp with the diffuser used. ....	34
Figure 25 - Spectra of the solux lamp with (black line) and without (gray line) diffuser. ....	36
Figure 26 - Two-dimensional representation of the CIECAM02-UCS of the selected samples solux lamp divided by lightness level. ....	37
Figure 27 - Sample making. ....	37
Figure 28 - Example of sample with name and symbol. ....	38
Figure 29 - Visual angle representation. ....	41
Figure 30 - Experiment setup. ....	42
Figure 31 - Mean ratings across all participants. ....	43
Figure 32 - sRGB computational representation of samples S 6030-Y (lowest rated) on the left and S 2050-B (highest rated) on the right. ....	43
Figure 33 - Mean ratings across males (on the top); Mean ratings across females (on the bottom). ....	44
Figure 34 - sRGB computational representation of samples S 1030-R, S 2020-G40Y, S 1020-B50G, S 1020-B, S 1030-R50B, and S 1030-R30B (from left to right). ....	45
Figure 35 - sRGB computational representation of samples S 3030-R, S 3020-G, S 3030-R50B, and S 3030-R30B (from left to right). ....	45
Figure 36 - sRGB computational representation of samples S 5540-G40Y, and S 6020-R70B (from left to right). ....	45
Figure 37 - Grids used. ....	48
Figure 38 - Setup used. ....	49
Figure 39 - Example of ellipse. ....	50
Figure 40 - Plot of the number of observers for the rating order. ....	51
Figure 41 - Difference of color for the lightness axis. ....	51
Figure 42 - Difference of color for the chromatic axis. ....	52
Figure 43 - Angle results for the 2x2 grid. ....	52
Figure 44 - Axis ratio results for the 2x2 grid. ....	53
Figure 45 - Area results for the 2x2 grid. ....	53
Figure 46 - Angle results for the 3x3 grid. ....	54
Figure 47 - Axis ratio results for the 3x3 grid. ....	54
Figure 48 - Area results for the 3x3 grid. ....	55
Figure 49 - Angle results for the 4x4 grid. ....	55



Figure 50 - Axis ratio results for the 4x4 grid. ....	56
Figure 51 - Area results for the 4x4 grid. ....	56
Figure 52 - Mean satisfaction for each grid. ....	57
Figure 53 - Experiment setup. ....	61
Figure 54 - Mean rating across all observers. ....	61
Figure 55 - Mean ratings across females (on the top); Mean ratings across males (on the bottom). ....	62
Figure 56 - sRGB computational representation of samples S 1030-R, S 1030-R50B, S 1030-R30B, S 2020-G40Y, and S0525-R70B (from left to right). ....	63
Figure 57 - sRGB computational representation of samples S 3030-R, S 4030-Y, S 3030-R50B, and S 3030-R30B (from left to right). ....	63
Figure 58 - sRGB computational representation of samples S 3060-Y and S 2050-R30B (from left to right). .....	63
Figure 59 - sRGB computational representation of samples S 5030-R, S 6030-Y, S 5540-G40Y, and S 6020-R70B (from left to right). ....	64
Figure 60 - Lids and black cardboard used. ....	66
Figure 61 - Setup used. ....	67
Figure 62 - Plot of the number of observers for the rating order. ....	68
Figure 63 - Difference of color for the lightness axis. ....	68
Figure 64 - Difference of color for the chromatic axis. ....	69
Figure 65 - Angle results for the 2x2 grid. ....	69
Figure 66 - Axis ratio results for the 2x2 grid. ....	70
Figure 67 - Area results for the 2x2 grid. ....	70
Figure 68 - Angle results for the 3x3 grid. ....	71
Figure 69 - Axis ratio results for the 3x3 grid. ....	71
Figure 70 - Area results for the 3x3 grid. ....	72
Figure 71 - Angle results for the 4x4 grid. ....	72
Figure 72 - Axis ratio results for the 4x4 grid. ....	73
Figure 73 - Area results for the 4x4 grid. ....	73
Figure 74 - Mean satisfaction for each grid. ....	74
Figure 75 - Mean rating across all participants. ....	77
Figure 76 - sRGB computational representation of samples S 4030-Y (lowest rated) on the left and S 9000-N (highest rated) on the right. ....	77

Figure 77 - sRGB computational representation of samples S 1030-R, S 1020-G, S 1020-B50G, S1030-R30B (from left to right). .....	78
Figure 78 - sRGB computational representation of sample S 3030-G40Y. ....	78
Figure 79 - sRGB computational representation of samples S 1060-R, S 3060-Y (from left to right). ...	78
Figure 80 - sRGB computational representation of samples S 5030-R and S 6030-Y40R, S 6030-Y, S 5540-G40Y, S 5030-B50G, S 6020-R70B and S 5030-R50B, S5030-R30B (from left to right). ..	79
Figure 81 - Plot of the number of observers for the rating order. ....	80
Figure 82 - Color difference for the lightness axis. ....	81
Figure 83 - Color difference for the chromatic axis.....	81
Figure 84 - Angle results for the 2x2 grid.....	82
Figure 85 - Axis ratio results for the 2x2 grid. ....	82
Figure 86 - Area results for the 2x2 grid. ....	83
Figure 87 - Angle results 3x3 grid.....	83
Figure 88 - Axis ratio results for the 3x3 grid. ....	84
Figure 89 - Area results for the 3x3 grid. ....	84
Figure 90 - Angle results for the 4x4 grid.....	85
Figure 91 - Axis ratio results for the 4x4 grid. ....	85
Figure 92 - Area results for the 4x4 grid. ....	86
Figure 93 - Mean satisfaction for each grid.....	86
Figure 94 - Mean ratings across all dichromats. ....	90
Figure 95 - Mean ratings across all protanopes (on the top); Mean ratings across all deuteranopes (on the bottom). ....	91
Figure 96 - Difference of color for the lightness axis.....	94
Figure 97 - Difference of color for the chromatic axis. ....	94
Figure 98 - Angle results for the 2x2 grid.....	95
Figure 99 - Axis ratio results for the 2x2 grid. ....	95
Figure 100 - Area results for the 2x2 grid. ....	96
Figure 101 - Angle results for the 3x3 grid.....	96
Figure 102 - Axis ratio results for the 3x3 grid. ....	97
Figure 103 - Area results for the 3x3 grid. ....	97
Figure 104 - Angle results for the 4x4 grid.....	98
Figure 105 - Axis ratio results for the 4x4 grid. ....	98

Figure 106 - Area results for the 4x4 grid ..... 99  
Figure 107 - Mean satisfaction for each grid..... 99

**INDEX OF TABLES**

Table 1 - Values of mean, standard deviation, maximum, and minimum  $\Delta E$  for the Solux lamp without a diffuser. .... 34

Table 2 - Values of mean, standard deviation, maximum, and minimum  $\Delta E$  for the D65 lamp without a diffuser. .... 35

Table 3 - Values of mean, standard deviation, maximum, and minimum  $\Delta E$  for the Solux lamp with a diffuser. .... 36

Table 4 - Luminance and illuminance result for 15 by 15 cm square. .... 40

Table 5 - Luminance and illuminance result for the 12 by 12 cm square. .... 47

Table 6 - Luminance and illuminance result for the box lid..... 48

Table 7 - Luminance and illuminance result for 12 by 12 cm square. .... 60

## **1. INTRODUCTION**

Color preference is an important aspect of human life. It influences many of our daily decisions, from the selection of clothes to the purchase of art. Preference for single colors has been scientifically studied for a long time and is relatively well understood. Blues are the most preferred colors and browns are the least preferred. Several theories explain to different degrees the pattern of preferences across the color space. There seems to be an influence of gender and culture on preference, but the influence of artistic education has not been investigated. Preference for combinations of colors is more difficult to study and is less well understood. Most of the studies are based on passive evaluation of color compositions and the results are interpreted in relation to theories related to color naturalness, e.g. how much compositions resemble natural color compositions, or color harmony.

The first goal of this work was to reproduce a classical experiment in color preference for single colors but using physical samples from the Natural Color System (NCS) instead of colors on a monitor display. This implied the selection of color samples, its manufacture, and the development of a testing technique. The experimental technique developed was applied to two groups of participants to study the effects of artistic education on the pattern of preference across the color space.

The second goal was to develop and test a new active experimental procedure to study color preference for complex color compositions together with appropriate computational instruments to analyze the results quantitatively. The technique - physical samples, procedure, and computational tools - was first tested in a set of pilots and then applied in its final tuned version to the same groups described above for single colors.

This research approach combines an exploratory innovative methodology with more classical techniques and allows collecting data to test models of color preference.

## 2. FUNDAMENTALS OF COLOR VISION SCIENCE

### 2.1. The Eye

The anatomical structure of the eye (Figure 1) affects visual perception.

A camera is often used to exemplify how the eye components work. They all have important roles in vision in particular color perception. Small variations in these components can lead to changes in visual perception.

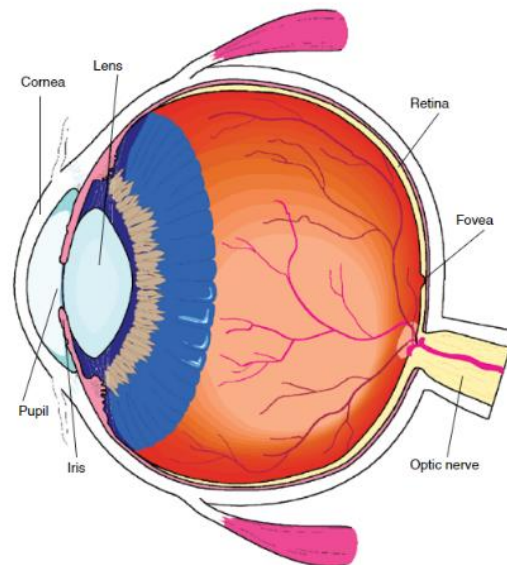


*Figure 1 - Schematic diagram of the human eye with some key components labeled. Adapted from [1].*

#### 2.1.1. The Cornea

The cornea is a transparent surface that allows light to pass through. It is the most anterior surface of the eye. It is avascular, i.e., without blood vessels. For that reason, the surrounding blood vessels and fluids provide the nutrients that it needs [1].

It is considered the most important element when it comes to image formation. Shape variations can be related to myopia, hyperopia, or astigmatism conditions which can be corrected by reshaping the cornea usually using a laser [1].

Figure 2 represents the layers of the cornea. They are named epithelium, Bowman's membrane, stroma, Descemet's membrane, and endothelium from the anterior layer to the posterior layer [2], [3].

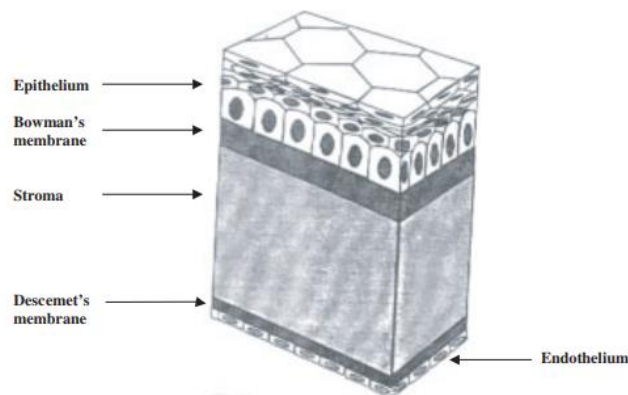


*Figure 2 - Schematic illustration of the cornea with all five layers labeled. Adapted from [3].*

The epithelium is the most superficial layer. Consists of five cell layers that have a thickness of around 50 to 60 microns. Complete cell turnover of the epithelium takes approximately seven to 10 days [4] its regenerative power makes this component extremely important.

The Bowman's membrane measures around eight to 12 microns in thickness [2], [4] and is the one below the epithelium.

The stroma is the largest layer of the cornea and consists of thousands of lamellar layers of collagen that are parallel to the surface [2], [4]. The disposition of the lamellar layers is crucial for maintaining the transparency of the cornea.

Descemet's membrane measures around 10 microns in thickness [2], [4] and separates the stroma and the endothelium.

The endothelium is a single layer of cells that have a polygonal shape and are connected by plasma membranes [2], [4]. As age advances the endothelium suffers a decrease in its number of cells. As a result, two phenomena can occur those are pleomorphism (the cells change their shape) and polymegathism (the cells modify their size), this happens so that spaces left by the decrease of cells can be filled [4].

### **2.1.2. The Lens**

The main function of the lens is to accommodate, i.e., to change its shape to increase or decrease the optical power. For distant stimulus, the lens becomes thinner which causes a

decrease in optical power, for near stimulus it becomes thicker causing an increase in optical power [5].

The ciliary muscles control changes in the shape of the lens [1].

The cornea and the lens act together to form an inverted image of the external stimulus that is projected on the retina.

With age, the lens loses flexibility which causes problems focusing near objects and eventually the complete inability to do it, a condition called presbyopia [1]. The lens scatters and absorbs short wavelengths, this phenomenon increases with the hardening of the lens. As a result, the lens becomes yellower. The yellow filter appears in everyone even though it differs from person to person [1]. The change of color in the lense is gradual and due to chromatic adaptation, these variations are little or not perceived.

### **2.1.3. The Humors**

The aqueous humor fills the space between the cornea and the lens and as the name suggests is mostly water-based.

The vitreous humor fills the space between the lens and the retina. Its consistency is usually compared to gelatin. These elements have refraction indices similar to the one of water, so they represent small optical power [1].

### **2.1.4. The Iris**

The iris is a sphincter muscle that controls pupil size. Pupil size changes according to the level of illumination on the retina in darker conditions the pupil size increases (mydriasis), and in bright conditions, the pupil size decreases (miosis) [5]. Other aspects like viewing emotionally arousing pictures result in larger pupil sizes whether pleasant or unpleasant pictures are being shown [6].

The individual unique eye color is affected by the different amounts of melanin and the way it is distributed [1] as well as light scattering from the iris [7].



### 2.1.5. The Retina

The retina is a light-sensitive layer of the eye and has multiple layers (Figure 3) of cells: ganglion cells, amacrine cells, bipolar cells, horizontal cells, photoreceptors, and the cells making the pigmented epithelium [1]. It can be divided into two parts, the inner layer which contains a neurosensory layer, and an outer pigmented layer.

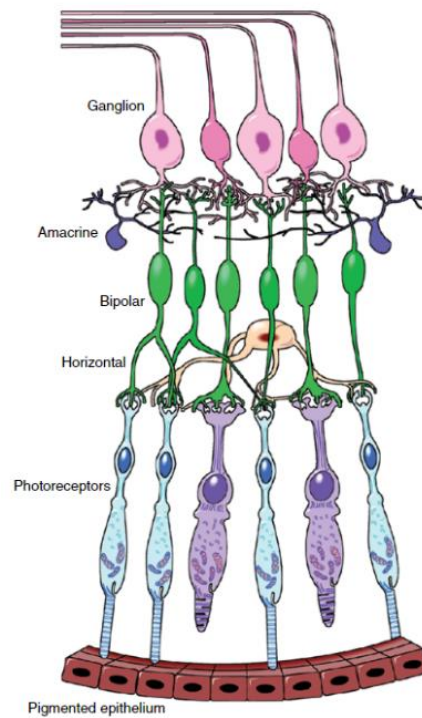


Figure 3 - Schematic diagram of the retina cells. Adapted from [1].

The two types of photoreceptors named rods and cones have different properties. They transduce the information of a stimulus into chemical and electrical [1] signals that are then processed by the later stages of the visual system.

The ratio of cones and rods depends on the area evaluated. The eye has an average of 92 million rods (ranging from 77.9 to 107.3 million rods) and 4.6 million cones (ranging from 4.08 to 5.29 million cones) [8].

Rods are more predominant in the peripheral area and are absent in the fovea area [1], [8]. Rods are active at low light levels and they mediate the type of vision referred to as scotopic vision [1].

Cones density is maximum in the foveola (central part of the fovea) area and averages 199,000 cones per square millimeter (cones/mm<sup>2</sup>) (ranging from 100,000 to 324,000

cones/mm<sup>2</sup>) [8]. Cones are active at high light levels (where rods are saturated) and mediate the type of vision referred to as photopic vision [1].

For intermediate light levels, both photoreceptor types are active, mediating the type of vision referred to as mesopic vision [1].

There are three types of cones classified according to their sensitivity to light: long, medium, and short wavelength (L, M, and S). Represented in Figure 4 are the peaks for different templates [9].

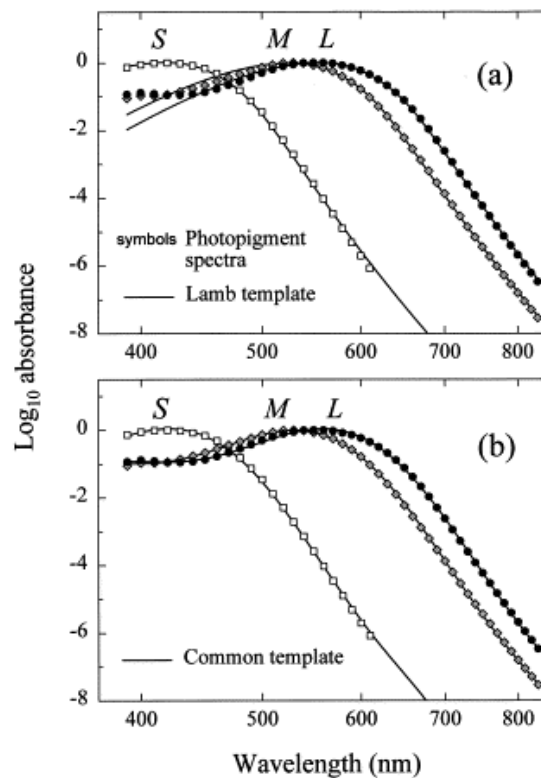


Figure 4 - Log<sub>10</sub> S- (white squares), M- (gray diamonds), and L- (black circles) cone photopigment spectra for different templates. Adapted from [9].

Represented with a continuous line in Figure 4a) is the Lamb [10] template with peak values of 418.1, 526.2, and 555.7 nm for S, M, and L cones, respectively. Because the correspondence to the photopigment spectra represented using symbols is lower for smaller wavelength values a different template was used. This is represented by a line in Figure 4b) and has peak values of 420.7, 530.3, and 558.9 nm for S, M, and L cones, respectively [9].

There is only one type of rods, and the peak of their absorption spectrum is 500 nm [11]. Because of the region where the peak sensitivity of the L, M, and S cones is, they are sometimes referred to as red, green, and blue cones, respectively [1]. This is not the correct way of referring

to them because although the cones' response peaks near the wavelength values that correspond to these colors they are active to a wide range of wavelength values as seen in Figure 4. The cone system is the one responsible for color perception.

The retina has photosensitive ganglion cells that are important in pupillary light reflex and modulating sleep/alertness and mood [12]. These cells express a photopigment called melanopsin [13].

The pigmented epithelium is a layer located behind the retina that absorbs light and prevents light scattering through the retina [1].

### 2.1.6. The Fovea and Foveola

The fovea is the retina area with the best spatial acuity and color perception and occupies around two degrees ( $2^\circ$ ) of the central visual field. When fixating on a stimulus the visual axis is aligned with the fovea [1], [14]. The foveola is the center part of the fovea [5], [14].

The visual acuity changes drastically according to eccentricity in the foveal area. Figure 5 shows the result of eccentricity for the temporal and nasal sides, the variations are the same for these sides apart from the area where the blind spot is located. The visual acuity is maximum in the foveola and rapidly decreases even when the distance to the fovea is small, but for larger distances to the center of the fovea the visual acuity is very low [15].

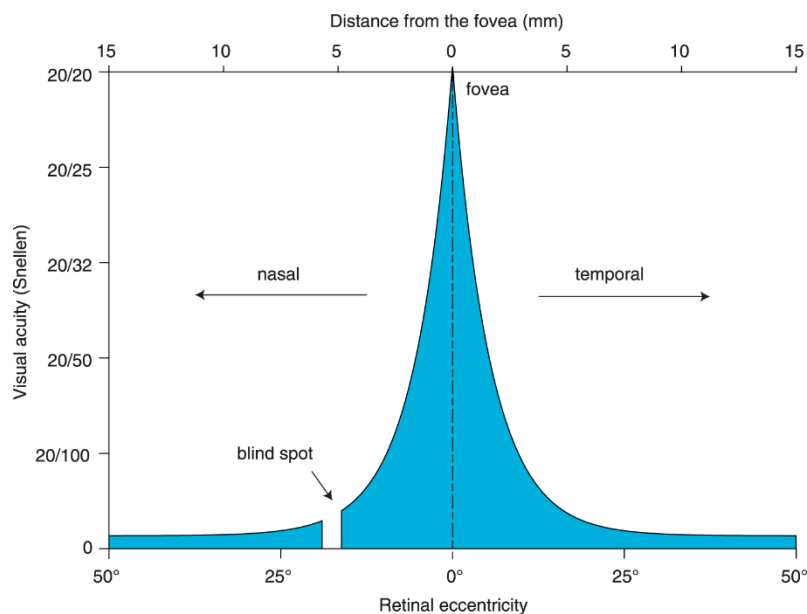


Figure 5 - Plot of the visual acuity variation with eccentricity. Adapted from [15].

### 2.1.7. The Macula

The macula is a yellow filter that protects the retina from short-wavelength energy [5], [16]. This filter differs from individual to individual and is one of the reasons given to explain color perception variability in different observers with normal color vision. This yellow filter does not suffer any modifications with age [16].

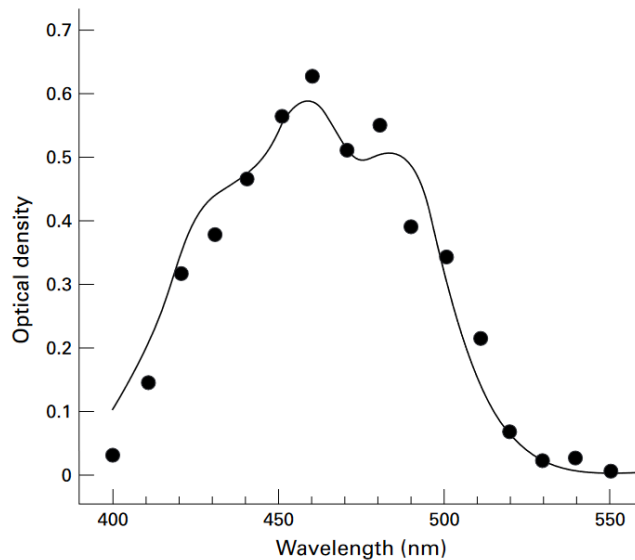


Figure 6 - Absorption spectrum of macular pigment. Adapted from [17].

Figure 6 illustrates the absorption spectrum of macular pigment as plotted by Wyszecki and Stiles (line) and Werner et al. (points). The peak of the macular pigment is at around 460 nm [17].

### 2.1.8. The Optic Nerve and the Blind Spot

The optic nerve is located in the back of the eye and is made of axons of ganglion cells. There are about one million fibers that carry information to higher levels of the visual system [1].

The optic disc was reported as having a mean vertical and horizontal disc diameter of 1.88 and 1.77 mm, respectively when measured on 60 eye bank eyes [18].

The blind spot is a place where no visual information exists, this happens because the optic nerve fills that spot and prevents photoreceptors from forming there [19].

Figure 7 represents the fundus of a healthy eye and the arrow indicates the optic nerve [20].

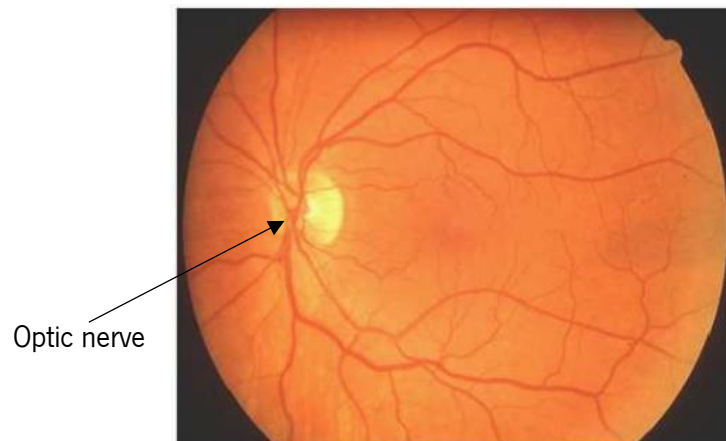


*Figure 7 - Fundus image of a healthy eye. Adapted from [20].*

## **2.2. Lateral geniculate nucleus (LGN) and Cortical processing**

The LGN is a six-layer structure that has three pathways [21]. The parvocellular pathway has four dorsal layers and the magnocellular pathway has two ventral layers [22]. The two divisions are also called what and where pathways correspond to, the ventral and dorsal pathways respectively. In between each layer are the koniocellular pathways which have small cells and receive the signal of the S cones [21], [23].

Each layer of the different pathways is projected into different layers of V1 [21].

The parvocellular layers are sensitive to color and respond faster than magno cells do. This research paper [22] also reports the findings of Shapley et al. of parvo cells being sensitive to low contrast while magnocellular layers are sensitive to high contrast. The receptive fields of magno cells are larger which results in a system with lower resolution, the opposite occurs in parvo cells.

The LGN receives input from the ganglion cells, they then project the input onto the primary visual cortex (also referred to as V1). The LGN modulates visual signals that use feedback from higher visual areas (V2, V3, V4, and Middle temporal also called MT) [1]. The diagram in Figure 8 allows visualization of the previous information.

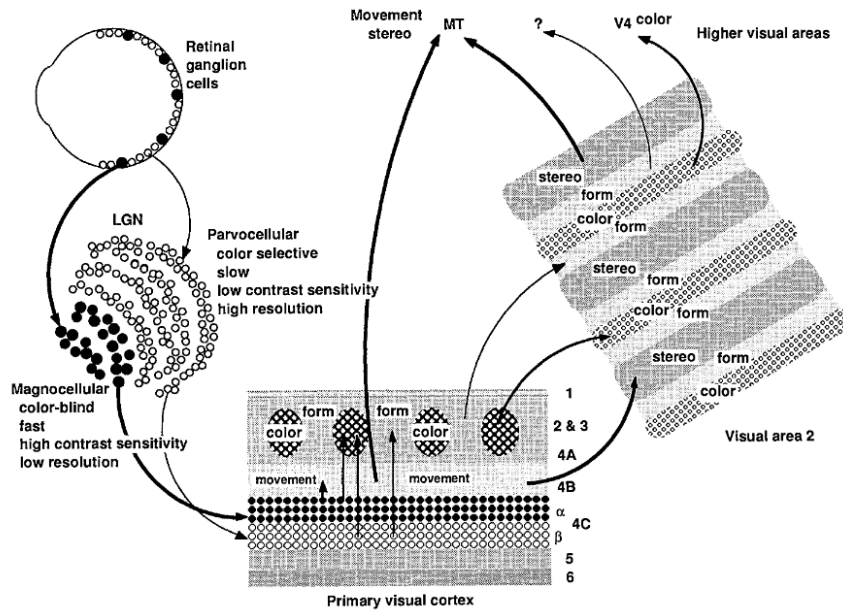


Figure 8 - Diagram of the functional segregation of the primate visual system. Adapted from [22].

The V4 area is reported in studies as being involved in color decoding for activities that use colored stimuli [24], [25].

## 2.3. Color Vision

### 2.3.1. Light and Color

Light is the stimulus for vision. The light reflected from an object (or emitted by a light source) enters the eye through the pupil and is focused onto the retina by the lens and cornea. It is then absorbed by the cones and rods that produce the electrical signals that are processed by the neural retina, before traveling to the optical nerve and reaching the brain.

The electromagnetic spectrum and the visible range are represented in Figure 9 [23].

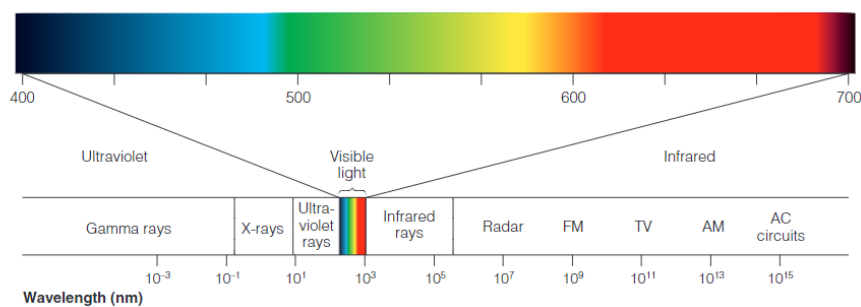


Figure 9 - The electromagnetic spectrum. Adapted from [23].

The visible light wavelength ranges from around 400 to 700 nm [26], other authors say from around 380 to 700 nm [27]. The wavelengths from 400 to 450 nm are the violet light, 450

to 490 nm are the blue light, 500 to 575 nm are the green light, 575 to 590 nm are the yellow light, 590 to 620 nm are the orange light, and 620 to 700 nm are the red light [23].

## **2.3.2. Color Vision Theory**

### **2.3.2.1. Trichromatic Theory**

A simple description of this theory is that color vision perception depends on three mechanisms, Thomas Young and Hermann von Helmholtz were the most influential researchers to describe and study this theory [28], [29].

Hermann von Helmholtz did color-matching experiments. The observer's task in this experiment was to adjust the amount of three different wavelengths of light mixed until the color of this mixture matched the color of the monochromatic test field. He found that it was possible to match the test field when using the three different wavelengths available to adjust. The other finding was that observers with normal color vision could match the test field but could not do it using only two out of the three wavelengths for all the colors of the spectrum [23].

Thomas Young in 1802 proposed that for normal color vision, three wavelengths are needed. He also did color-matching experiments to reach this conclusion [29].

The idea of the three active mechanisms continued to be studied and eventually measuring the absorption spectrum (Figure 4) of the three cones (L, M, and S) validated the theory [1], [23], [30].

### **2.3.2.2. Opponent Color Theory**

Ewald Hering noticed that certain hues were never perceived together, he noted that color perception was never described as reddish-green or yellowish-blue. For that reason, he believed that there was something fundamental about the red-green and yellow-blue pairs that caused them to oppose one another. He considered that red, green, yellow, and blue were unique hues [31].

A simple demonstration of that is Figure 10 where if you fixate on the black spot of the left image for 30 seconds and then look at the black spot in the right, the post image of red is green and vice versa, and of yellow is blue and vice versa [1], [23], [30].



*Figure 10 - Stimulus for the demonstration of opponent after images. Adapted from [1].*

To explain these observations, Hering proposed the existence of three types of mechanisms, and he said that they had opponent responses, these were the light and dark, the red and green, and the yellow and blue mechanisms. At the time Hering's theory was not accepted but findings of experiments over the years helped validate and update his theory. That is how the modern opponent color theory emerged [1], [30], [31].

At the beginning of the 1950s, Svaetichin found opposite electrophysiological signals in the retina of goldfish [1], [32]. Later DeValois et al. also found opposite signals in the lateral geniculate nucleus in monkeys [33].

Jameson and Hurvich did hue cancellation experiments. These contributed to the possibility of spectral sensitivities of opponent pathways being measured [34].

### **2.3.3. Color Vision Deficiencies**

Most color deficiencies only cause a partial loss of color perception and are associated with the photoreceptors in the retina [23].

John Dalton used his color perception to describe his color deficiency. He said, "All crimsons appear to me to consist chiefly of dark blue: but many of them seem to have a tinge of dark brown. I have seen specimens of crimson, claret, and mud, which were very nearly alike"[35]. Even though he didn't understand exactly why his color perception was different, his description of it led to the term Daltonism used when referring to color vision deficiency [23].



### **2.3.3.1. Inherited Deficiencies**

This type of deficiency affects 8% of males and 0.4% of females in the European caucasian population [36]. Inherited deficiencies do not progress over time, do not affect the visual system's performance, and do not represent any risk to vision [30], except for S cones monochromats where poor visual acuity was been reported [37]. These deficiencies are divided into three groups: anomalous trichromats, dichromats, and monochromats [38].

Anomalous trichromats have anomalies in the spectral sensitivity of the pigments in their cones. The anomalies in the different cones have different names. For anomalies in the L cone, the term used is protanomaly which affects 1.0 to 1.2% of European males, for anomalies in the M cone the term used is deuteranomaly, which affects 4.6 to 5.1% of European males, for anomalies in the S cone the term used is tritanomaly, it is a very rare condition that was never been documented in a way that satisfies the scientific community so it is now believed that such condition does not exist what indeed exists is incomplete tritanopia (not complete loss of s cones function) [1], [36], [39]. The percentages reported are the prevalence when the Nagel anomaloscope was used and can suffer variations according to different authors. A study [40] that used functional magnetic resonance imaging (fMRI) in anomalous trichromats showed that these observers have bold responses to color in V2 and V3 but not in V1 and have neural compensation for their anomalous color vision in the early visual cortex. The results found show that anomalous trichromats strongly compensate for color losses through the amplification of cortical responses to chromatic contrast.

Dichromats lack one of the three cones and see a smaller range of colors than trichromats [36]. Dichromatic conditions are named according to the missing cone when the L cone is missing the term used is protanopia, which affects 0.8 to 1.2% of European males, when the M cone is missing the term used is deuteranopia, which affects 0.9 to 1.3% of European males, when the S cone is missing the term used is tritanopia [1], [36]. The percentages reported are the prevalence when the Nagel anomaloscope was used and can suffer variations according to different authors.

Individuals who suffer from protanopia and deuteranopia struggle to discriminate between reddish and greenish hues since the red and green opponent mechanism cannot be constructed. These two conditions differ in their relative luminous sensitivity for the protanopia condition the luminous sensitivity is shifted in the direction of shorter wavelengths. Those who suffer from

tritanopia struggle to discriminate between yellowish and blueish hues since the yellow and blue opponent mechanism cannot be constructed [1], [30].

Protanopia and deuteranopia are more common in males because men only have one X chromosome and this condition affects the X chromosome. Both X chromosomes need to carry the condition for a woman to express the deficiency [36].

Monochromats only have one type of photoreceptor. If they only have cones the condition is called cone monochromatism it is a very rare condition and if they only have rods the condition is called rod monochromatism, which affects 0,003% of males and 0,002% of females [1]. Rod monochromatism causes poor visual acuity, these individuals are sensitive to light and only see in shades of lightness (gray, white, and black) [23].

### **2.3.3.2. Acquired Deficiencies**

Acquired deficiencies are secondary to diseases and can also occur due to drug toxicity. These deficiencies are equally prevalent in males and females and can change throughout life and differ from eye to eye [41].

Verriest [42] classified them into three types: The red-green type I causes decreases in visual acuity, and changes in luminosity and chromatic confusion in the red and green axis often related to choroidal atropic processes. The red-green type II causes major decreases in color discrimination in the red and green axis and has minor decreases in color discrimination in the blue and yellow axis often related to optic nerve disease and optic neuritis among others. The blue-yellow type III causes a decrease in color discrimination in the blue and yellow axis and variations in visual acuity often are related to glaucoma and papilledema among others [41], [42].

Diabetes and retinitis pigmentosa affects the S-cone and there is also evidence that they are affected by other pathologies like retinal detachment [41], [42].

### 2.3.3.3. Color Confusion Lines

Figure 11 represents the colors confused by the dichromats. The lines vary according to the type of color vision deficiency [43].

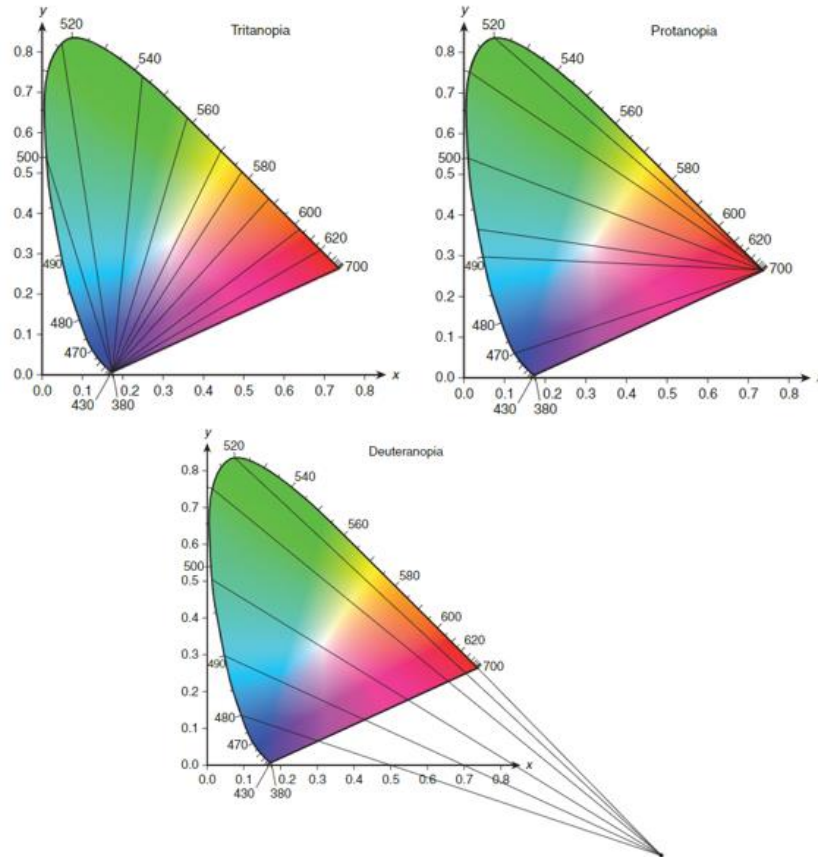


Figure 11 - Color confusion lines for tritanopia (top left), protanopia (top right), and deuteranopia (bottom). Adapted from [30].

### 2.3.4. Color Vision Tests

There are multiple tests available to characterize the different types of color vision deficiencies, and all have benefits and disadvantages. Only the main ones will be described here.

The one used in the experiments reported here was the Ishihara.

#### 2.3.4.1. Ishihara Plates Test

Test that consists of plates with colorful dots of random lightness that together make a specific number or pattern. Both the background and the pattern or number have the same reflectance [1], [44].

There are different types of plates with different purposes.

The plates where observers with normal color vision see one number or pattern but the ones with color vision deficiencies see a different number or pattern are called transformation plates, other authors called them alteration plates [44], [45]. In the vanishing plates, the observers with color vision deficiencies do not see anything but the ones with normal color vision do, the opposite occurs in the hidden-digit plates. Diagnostic plates are the ones where deuteranopes and protanopes see different numbers or patterns. There is also a demonstration plate that all observers can see, this is the first plate that is presented [45].

To administer this test, observers see the plates under controlled lights and say the number they see or follow the pattern with their hands.

The Ishihara plates test is used to detect congenital red-green deficiencies quickly [44], [46].

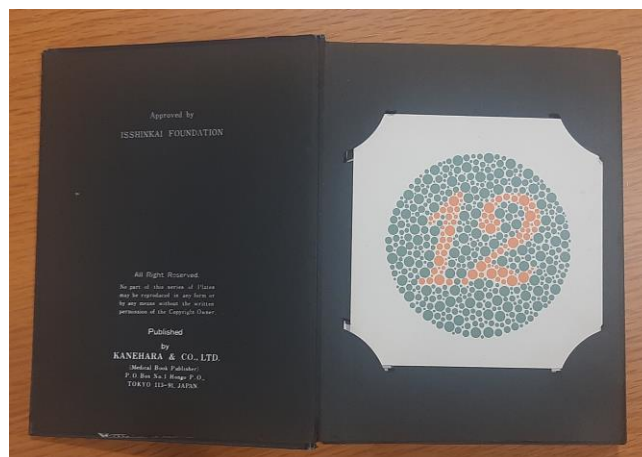


*Figure 12 - Ishihara plates test.*

#### **2.3.4.2. Farnsworth-Munsell 100-Hue Test**

The Farnsworth-Munsell 100-Hue test is an arrangement test. It has four sets of chips, the observer's task is to arrange them in a progressive order of hue according to the two reference points placed in the extremities. When color vision deficiencies exist, mistakes will be made in the order of specific hues that will allow the person administering the test to identify the type of color vision deficiency. A special feature of the Farnsworth–Munsell 100-Hue test is that it allows the severity of color vision deficiency to be identified [1], [44], [45].



*Figure 13 - Farnsworth–Munsell 100-Hue Test.*

### **2.3.4.3. Anomaloscopes**

Anomaloscopes are color-matching tests. They consist of instruments that can identify deuteranopia, protanopia, protanomaly, and deuteranomaly [44], [45]. The instrument has a divided field with a part that is fixed and another that is a mixture of two primary colors. The second part of the field can be changed by observers until it matches the other part of the field [44].



*Figure 14 - Example of an Anamoloscope.*

## 2.4. Color Spaces

### 2.4.1. Tristimulus and Color Matching Functions

The color matching functions for the red, green, and blue systems represent the quantity of the three primaries (R, G, and B) necessary to match a given stimulus of a certain wavelength. This function was defined for the average observer [47].

Negative tristimulus values in the red, green, and blue systems (R, G, B systems) (Figure 15) represent a stimulus that can only be matched by adding color to the actual stimulus. The peaks of these primaries are at 645 nm for red, 444 nm for blue, and 526 nm for green [1], [5], [30].

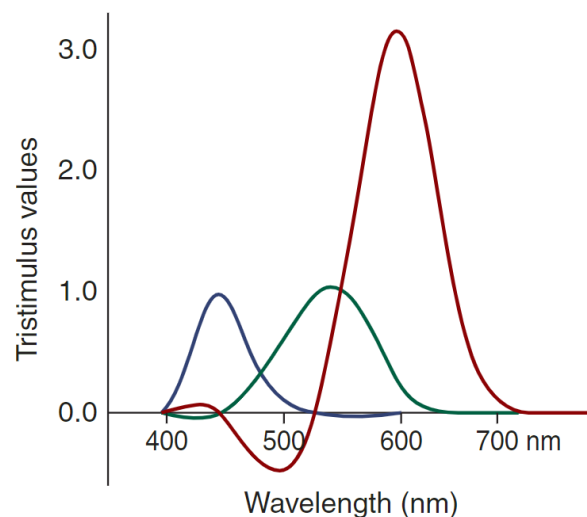


Figure 15 - Color matching functions of R (represented with red), G (represented with green), and B (represented with blue). Adapted from [30].

After some mathematical transformations, the International Commission on Illumination (CIE) recommended the color matching functions. Figure 16 [48] represents the primaries: x, y, and z created with the goal of removing negative values and having one of the color matching functions equal the photopic luminance function ( $V(\lambda)$ ) [1], [5], [30].

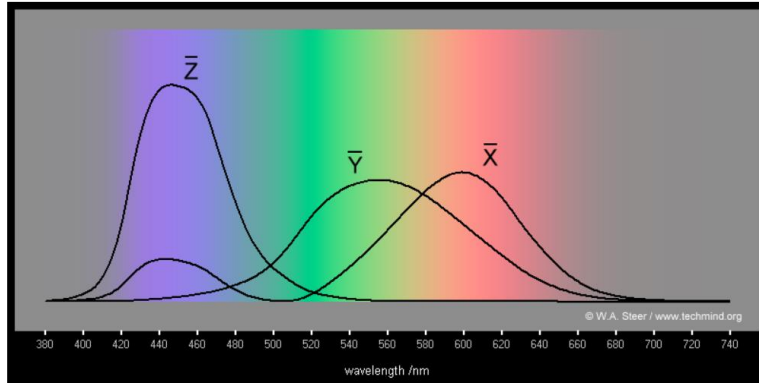


Figure 16 - CIE 1931 color matching functions for the  $x$ ,  $y$ , and  $z$  primaries  $R$ . Adapted from [46].

The  $V(\lambda)$  was developed to describe the photopic perception of brightness. [30].

In Figure 17 is possible to observe that some wavelengths stimulate the visual system more than others and the peak of this sensibility is 555 nm [1], [5], [30].

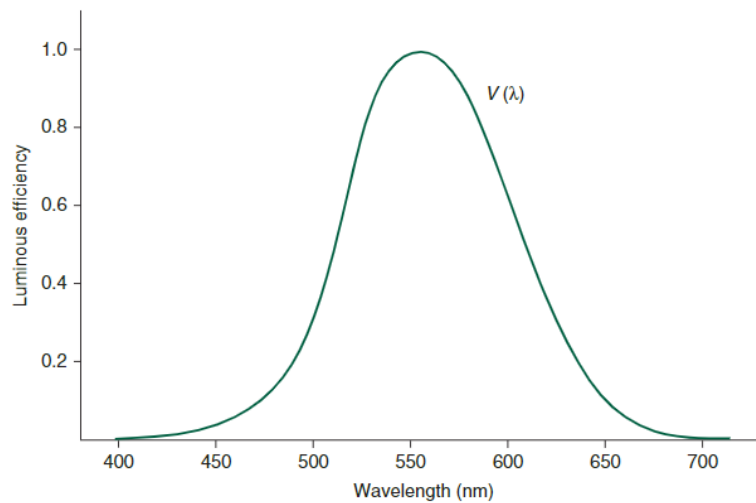


Figure 17 - Photopic luminance function. Adapted from [30].

The XYZ tristimulus is obtained using Equation 1, Equation 2, and Equation 3 [47]:

$$X = k \int_{\lambda} \Phi(\lambda) \bar{x}(\lambda) d\lambda \quad \text{Equation 1}$$

$$Y = k \int_{\lambda} \Phi(\lambda) \bar{y}(\lambda) d\lambda \quad \text{Equation 2}$$

$$Z = k \int_{\lambda} \Phi(\lambda) \bar{z}(\lambda) d\lambda \quad \text{Equation 3}$$

Where  $\Phi(\lambda)$  is the spectral power distribution of the stimulus,  $\bar{x}(\lambda)$ ,  $\bar{y}(\lambda)$ , and  $\bar{z}(\lambda)$  are the color matching functions.  $k$  is a normalizing constant calculated using Equation 4 [47]:

$$k = \frac{100}{\int_{\lambda} S(\lambda)\bar{y}(\lambda)d\lambda} \quad \text{Equation 4}$$

Where  $S(\lambda)$  is the relative spectral power distribution of the light source or illuminant of interest.

Both the color-matching functions and the tristimulus values are essential to define color spaces.

### 2.4.2. CIE 1931 (x,y)

This color space uses the CIE XYZ tristimulus obtained from the imaginary primaries (x, y, z).

The diagram (Figure 18) is constructed by converting the tristimulus values into relative units that are called chromaticity coordinates (x, y, z) they do not take into consideration the chromatic adaptation [47].

The chromaticity diagram creates a map of the relationship between color stimuli, not between color perception [5].

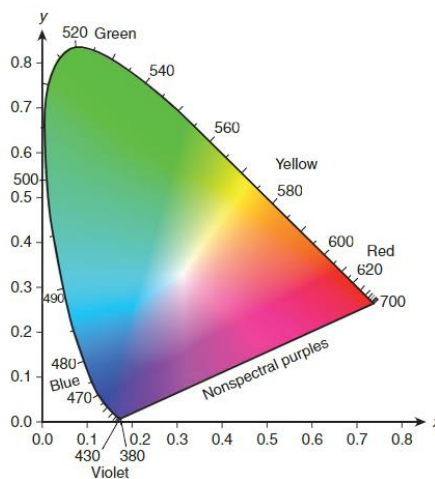


Figure 18 - CIE chromaticity diagram. Adapted from [30].

The x and y coordinates are calculated using Equation 5, Equation 6, and Equation 7 [47]:



$$x = \frac{X}{X + Y + Z} \quad \text{Equation 5}$$

$$y = \frac{Y}{X + Y + Z} \quad \text{Equation 6}$$

$$z = \frac{Z}{X + Y + Z} \quad \text{Equation 7}$$

The sum of  $x$ ,  $y$ , and  $z$  is one. Some important characteristics of this color space are that the monochromatic hues are represented along the arc of the diagram usually referred to as spectral locus. Also, the straight line along the bottom that connects the 380 nm to the 700 nm represents the purples that cannot be represented using only one wavelength but by mixing wavelengths [47].

The Planckian locus is an arc in the diagram that contains various color temperatures and the standard illuminants fall on that arc. This was named after Max Planck, an impactful physicist who developed Planck's radiation law [43], [47].

Standard illuminants (A, B, D65, ...) are variations of white light. Illuminants have different color temperatures, for example, illuminant A has a color temperature of 2855.5 Kelvin (K). An example of an illuminant A is an incandescent light but for illuminant D65 the color temperature is 6500 K, which is the illuminant that better represents daylight [47].

The CIE  $xy$  is not a uniform color space so the distance between colors is not always correct. It represents a standard observer and a visual field of  $2^\circ$  [47].

### **2.4.3. CIE 1976 (LAB)**

The CIELAB color space is a simple uniform color space that contains chromatic adaptation transformations and predictors of lightness, chroma, and hue [1].

It was developed to be used for the specification of color differences. The Euclidean distance between two points in CIELAB is a measure of their color difference ( $\Delta E$ ) and is calculated using Equation 8 [1], [47]:

$$\Delta E = [(\Delta L^*)^2 + (\Delta a^*)^2 + (\Delta b^*)^2]^{1/2} \quad \text{Equation 8}$$

For calculating the CIELAB coordinates is necessary to have some parameters of the CIE xy model and those are the tristimulus values (XYZ) and the reference white point ( $X_n, Y_n, Z_n$ ) [47].

After using Equation 9, Equation 10, and Equation 11, the parameters  $L^*$ ,  $a^*$  and  $b^*$  are obtained [47]:

$$L^* = 116 f(Y/Y_n) - 16 \quad \text{Equation 9}$$

$$a^* = 500 [f(X/X_n) - f(Y/Y_n)] \quad \text{Equation 10}$$

$$b^* = 200 [f(Y/Y_n) - f(Z/Z_n)] \quad \text{Equation 11}$$

with

$$f(X/X_n) = (X/X_n)^{1/3} \text{ if } (X/X_n) > (6/29)^3$$

$$f(X/X_n) = (841/108)(X/X_n) + 4/29 \text{ if } (X/X_n) \leq (6/29)^3$$

$$f(Y/Y_n) = (Y/Y_n)^{1/3} \text{ if } (Y/Y_n) > (6/29)^3$$

$$f(Y/Y_n) = (841/108)(Y/Y_n) + 4/29 \text{ if } (Y/Y_n) \leq (6/29)^3$$

$$f(Z/Z_n) = (Z/Z)^{1/3} \text{ if } (Z/Z_n) > (6/29)^3$$

$$f(Z/Z_n) = (841/108)(Z/Z_n) + 4/29 \text{ if } (Z/Z_n) \leq (6/29)^3$$

$L^*$  is the perceived lightness ranging from zero for black to 100 for diffused white. The  $a^*$  and  $b^*$  coordinates are red-green and yellow-blue chroma perceptions, respectively [47].

In the  $a^*$  axis, positive values are red chroma perceptions, and negative values are green chroma perceptions.

In the  $b^*$  axis, positive values are yellow chroma perceptions, and negative values are blue chroma perceptions.

These three parameters are combined as cartesian coordinates and form a three-dimensional color space (Figure 19) [49].

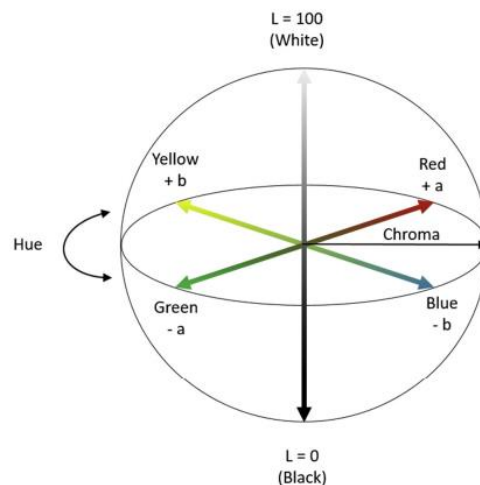


Figure 19 - CIELAB diagram. Adapted from [49].

#### 2.4.4. CIECAM02-UCS

The CIECAM02 model was recommended in 2002 after being tested by several people, with this model it became possible to correct some previous limitations of the previous CIECAM97s model [42],

CIECAM02 was quickly accepted and used in the industry, performing well when compared to other models available. The Technical Committee of CIE Division 8 was created to solve issues that appeared, and this group is still active [1], [47].

The CIECAM02 model suffered further improvements and the CIECAM02-UCS model was created providing a more uniform color space [47].

CIECAM02-UCS aims to combine color difference and color appearance predictions into a single model.

This model provides parameters of lightness,  $J'$ , redness-greenness,  $a'_M$ , and yellowness-blueness,  $b'_M$ , and they are equivalent to the parameters of  $L^*$ ,  $a^*$ , and  $b^*$  in the CIELAB model [47].

Equation 12, Equation 13, Equation 14, and Equation 15 show how to obtain these parameters:

$$J' = \frac{1.7J}{1 + 0.07J} \quad \text{Equation 12}$$

$$M' = \frac{1}{0.0228} \log_{10}(1 + 0.0228M) \quad \text{Equation 13}$$

$$a'_M = M' \cos(h) \quad \text{Equation 14}$$

$$b'_M = M' \sin(h) \quad \text{Equation 15}$$

The CIECAM02-UCS model allows the calculation of  $\Delta E$  to be done with the  $J'$  parameter, the  $a'_m$  parameter, and the  $b'_m$  parameter. The equation is expressed below:

$$\Delta E = [(\Delta J')^2 + (\Delta a'_M)^2 + (\Delta b'_M)^2]^{1/2} \quad \text{Equation 16}$$

## 2.5. Natural color system

Color-ordered systems are collections of colored samples, arranged and labeled according to perceptual attributes of color. This allows an intuitive search between samples [50].

For the selection of the colored samples used in this study, the color system used was the NCS. This system uses colored pigments to manufacture the color samples and therefore there are limitations on the colors of samples available [50].

The NCS was developed in 1964 by the Swedish Color Center Foundation and is considered a standard for color description [50]. It is based on the opponent colors theory of Hering [1].

In this system, color is described based on the number of basic colors such as yellow, red, blue, green, black, and white that are perceived in a sample. The number of colors is represented using percentages. It also requires the use of the hue circle and the triangle [1], [5].

The hue circle (Figure 20) has four quadrants, each representing unique hues such as yellow, red, blue, and green. These unique hues are arranged orthogonally and have an equal number of steps but different magnitudes in each quadrant. This occurs because there are more visually distinct hues between unique red and unique blue than between unique yellow and unique green [1].

To describe a hue that is between two unique hues a relative perceptual composition is given, for example, an orange that is perceived to fall midway to unique red and unique yellow would be Y50R [1].

Hue is always described in a clockwise direction [51].

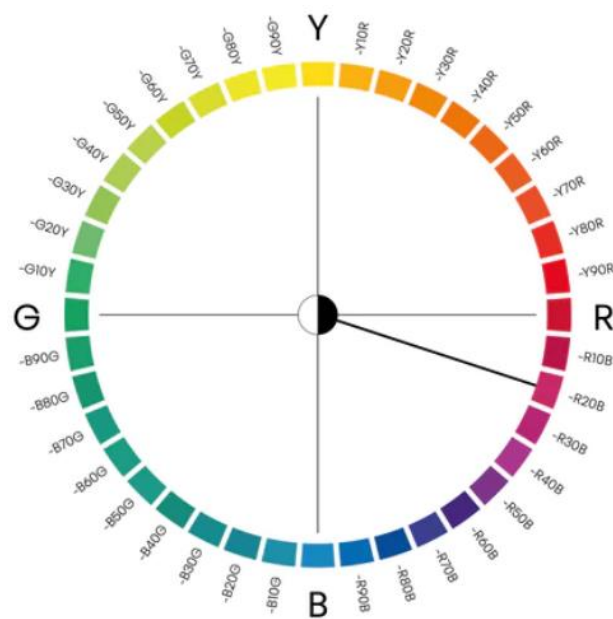


Figure 20 - Hue circle. Adapted from [51].

The triangle (Figure 21) is used for describing nuance [51].

The three corners of the triangle represent colors with the maximum quantity of blackness (S), whiteness (W), and chromaticness (C). Chromaticness is the color that is more predominant in the selected hue [51].

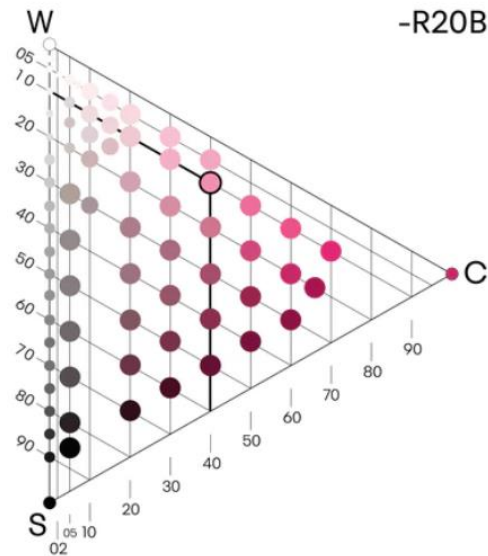


Figure 21 - Triangle used to illustrate nuance. Adapted from [47].

For any sample that is represented, the sum of S, W, and C must be 100 [1].

With all the elements above it is possible to describe a color using the NCS notation, an example of that is the following color NCS S 1040-R20B, this color has 10% of blackness, 40% of chromaticness, and given the sum mentioned above it has 50% is whiteness [51].

### **3. LITERATURE REVIEW: COLOR PREFERENCE**

Beautiful is used to describe something that is considered aesthetically pleasing but what is considered beautiful to one observer might not be to another [52], [53]. A work of art can be appreciated for reasons like emotional impact, place of the viewing, artist status, and others, all while not finding it beautiful [54].

The process of aesthetic preference was first studied by Gustave Fechner [55] since then scientific studies have varied from psychology to neuroaesthetics.

Various neuroaesthetics studies found that when observers are presented with paintings, the ones considered beautiful induce a pattern of activity in the brain different from the pattern produced when observers did not find the paintings appealing. Researchers concluded that using fMRI [56], [57]. The reason why this occurs is still unclear. One possibility is that the aesthetic value of paintings depends on the extent to which they mimic natural image statistics [58], [59]. Although paintings sometimes do not obey the laws of physics and the range of luminance is limited, paintings seem to share spatial statistical regularities with natural scenes [59].

Color preference for single colors has been intensively investigated [60]. Humphrey proposed that color sends a signal that can be an approach signal or an avoid signal [61]. He also suggested that the colors of modern artifacts like a car do not have significant signals but can be influenced by natural color signals [61]. Hurlbert and Ling [62] proposed that color preference is wired in the human visual system and based this on the cone-opponent neural responses that suffer modifications from evolutionary selection in other words this theory suggests color preference evolved to improve the performance in important tasks. They also studied their preference in the LM-axis and S-axis and found that both preferred more violet colors for the S-axis, for the LM-axis they found that females preferred redder colors and males preferred more blue-green colors the reason given for this result was that women had a visual system more specialized for finding ripe fruit, but no reasons were provided for the other results found. Ou et al. [63], [64] proposed a theory that linked preferred colors to positive emotions being produced in the observer reasons why this happens were not given.

In a more recent study (Figure 22) the ecological valence theory was created for this theory color preference is associated with affective responses to objects of certain colors.

Results show a strong preference for blues associated with blue skies and clean water and browns associated with rotten food being the less preferred colors. These results support the theory. Aspects like fashion trends, social circumstances, and others are pointed to inevitably influence color preference [65].

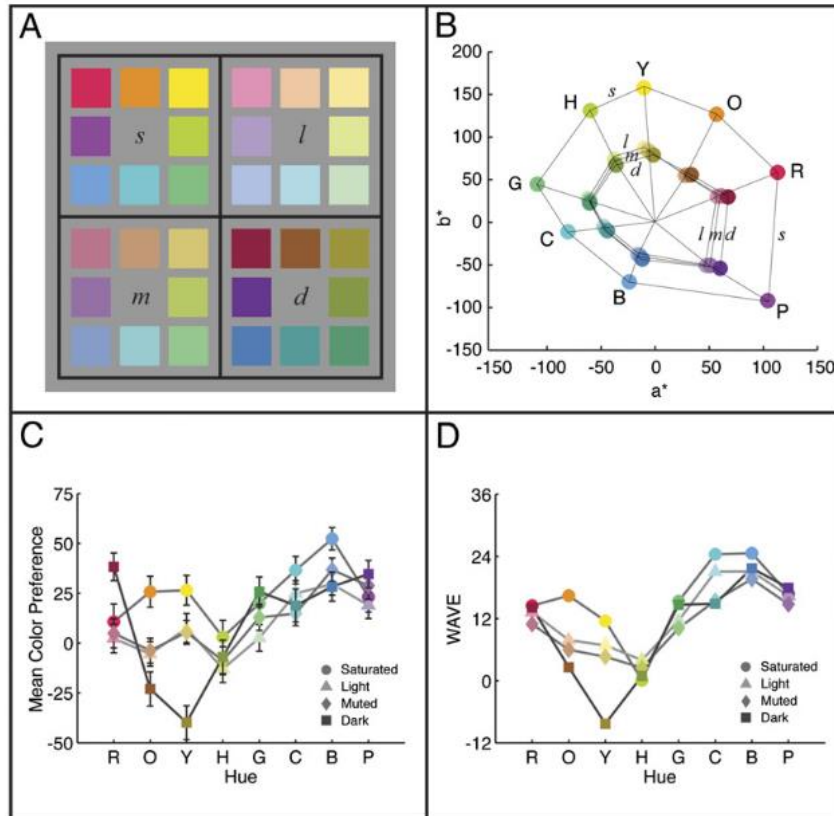


Figure 22 - (A) The 32 chromatic colors (B) The projections of the 32 colors onto an isoluminant plane in CIE LAB color space. (C) Color preferences of all 48 participants (D) WAVEs for the 32 chromatic colors. Adapted from [65].

Color is a property that researchers point out as potentially affecting our preferences although how exactly this works is not yet clear. Regarding color, paintings even the abstract type share some chromatic statistical regularities with natural scenes [54], [66].

When comparing data from hyperspectral images of 50 natural scenes and 42 abstract paintings researchers found that painters tend to use more saturated reddish colors, they reached this conclusion because the color gamut represented in the CIE LAB color space, using only two dimensions ( $a^*$ ,  $b^*$ ) was tilted to red, they also found the color gamuts were elongated in the yellow-blue direction for both natural and abstract paintings. They pointed out that this could happen because of limitations related to the pigments and dyes used in paintings, even though



they found the gamut provided by the pigments to be very uniform along the color space, they do not rule out this as an explanation to the findings. Another suggestion given was that it could be only an option made for aesthetic reasons [67].

To study color preference stimuli manipulation is common. This gives valuable information as to which factors are involved in the aesthetic appreciation of works of art. Chromatic preference according to the existing data, which uses a limited number of observers and paintings, suggests that the chromatic composition preferred is the closest to the original one [54], [66].

Concerning isolated colors studies, report a general preference for blue and green depending on factors like culture and gender. Individual color preference for each observer affects what is preferred for pairs of colors. These kinds of findings cannot help end existing doubts about complex paintings as they don't apply in their case. For colors inserted in complex scenes, studies suggest that a specific configuration of color is what allows the perception of pleasing images [54], [66].

In a study, six abstract paintings and four paintings with realistic elements were used. Out of those 10 paintings seven of them were painted by Amadeo de Souza Cardoso. Observers used in this study were divided into one naïve group, one with art experts and another with Amadeo experts. Using a hyperspectral imaging system, the data of the paintings were collected, and then for each pixel, the corresponding CIELAB coordinates were calculated using the standard D65 illuminant all these coordinates together form the color gamut. Participants could rotate the color gamut and as a consequence, the chromatic composition of the painting changed. When asked to select the preferred chromatic composition observers selected the one very close to the original this occurred for all paintings, but slight changes were found between naïve and expert observers when the paintings had realistic elements like skin, the explanation given was that people most likely try to match the skin color that is familiar to them and not the one in the original painting. Researchers suggested that certain color combinations are perceived as more pleasant than others [66].

Another study was done trying to build on the conclusions previously found. The hyperspectral data of the selected abstract paintings was once again converted into CIELAB coordinates. This time to test if preference depends on the spatial configuration found in paintings three types of stimuli were used those being the original paintings, paintings with spatial composition scrambled but chromatic composition preserved and paintings with spatial and chromatic composition scrambled. For original and spatial scramble stimuli the angles around the

original color distribution were preferred but for spatial and chromatic scramble stimuli the curves of preference found suggest that all angles were equally preferred. The results suggest that color can contribute to the aesthetic experience of abstract paintings regardless of the spatial configuration [54].

Another study analyzed the relationship between the perception of naturalness in the colors of an image and the aesthetic preference of each observer. The images displayed to observers were manipulated, they were divided into scrambled or unscrambled images after that, observers selected the image they preferred. Researchers concluded that natural colors present in complex images are perceived as the most natural ones, even when the hue composition of natural scenes is manipulated the participants still selected the original composition as the most natural one. Another important finding was that preferred color compositions tend to be the colors perceived as most natural. These two findings support the idea that naturalness and preference are related to the perception of color in images and that both are possibly driven by similar mechanisms [68].

Studies done using the hyperspectral data of inscriptions on walls or nowadays street art on walls otherwise known as graffiti. Two hundred twenty-eight graffiti were used the colors of each pixel were represented in the CIELAB color space researchers found that graffiti has color gamuts with the same elongation in the yellow-blue direction this suggests that colors used in graffiti are also like those in the natural world. A difference found was that graffiti have a larger color gamut and more saturated colors this is explained by the existence of new synthetic pigments that enlarge the possibilities of colors available [69].

In the case of preference differences between genders, multiple studies can be discussed only some will be mentioned in this Chapter. In a study, where participants from the United Kingdom and China were forced to pick between two color samples displayed on a CRT monitor, the hue preference was plotted for both populations and sex (Figure 23). They found that the hue preference curves differ according to the sex and country of the observer but do not differ significantly according to lightness and saturation levels. Women's preference peaks in the reddish-purpleish region but male preference peaks in the blue-green region. Evolutionary factors like the task division of males as hunters and females as caregivers and collectors of ripped fruit were given as the reasons why preferences have these patterns. Chinese participants show a more significant

preference for reddish colors than the United Kingdom participants, a hypothesis presented for this is that in China red is a color related to good luck [62].

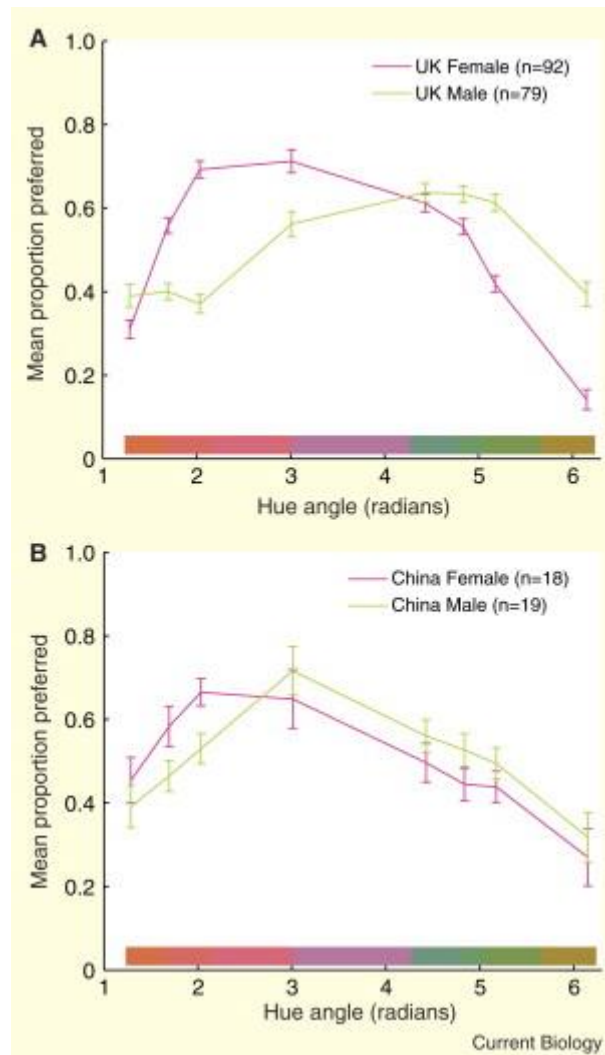


Figure 23 - Mean hue preference curves. (A) British subjects. (B) Chinese subjects. Adapted from [62].

Absolute color preference was studied for adults and children in an experiment that used a color picker with no restrictions. The analysis carried out revealed sex to be a predictor of preference of the pink/purple, red, and other (all hues that are not red, blue, and pink) hue categories but not the blue. Both sexes preferred blue hues as their favorite followed by pink/purple hues for the girls and red or other for the boys. They explained these results based on gender-related norms, saying boys avoid pink as is seen as girly. When it comes to adults, the analysis revealed sex to be a predictor of preference for the red and other hue categories but not for pink/purple or blue. For the least favorite color asked only to adults, sex was not a predictor of preference for any hue category, this means men and women pick the same hue as their least

favorite, which is the yellow hue. As for their favorite women chose blue and red hue categories followed by other and men chose blue and other hue categories as their favorite. According to these authors in adulthood, the pink stigma seems to continue leading both sexes to drift away from it, causing women to shift to red hues and men to reinforce their childhood tendencies [70].

Even though plenty of work has been done regarding color preference and many theories have emerged and some very well credited and supported by the newer studies discussed in this Chapter, this topic is still an ongoing subject of study given that no theory was proven capable of answering all the questions.

The goal of this work is to investigate the properties of the color combinations we like. This will be carried out by developing a vision test where participants select a set of colored samples from a collection of standard colors to make compositions they like. We also will analyze the mean ratings of observers for the same collection of standard colors. The test was implemented in adults with and without artistic education. Data was analyzed quantitatively with colorimetry to understand which are the regularities in the color compositions and ratings from a large set of participants.

## **4. GENERAL METHODS**

### **4.1. Selection of the samples and illumination**

The color samples used were a selection from the NCS Original color system which represents reasonably well the colors of natural scenes [50]. The full-color system has 1950 samples but only 1943 samples were used since the laboratory did not have the remaining seven their reflectances were measured using the PR-650 SpectraScan® (SpectraColourimeter, PR-650, Photo Research Inc., Chatsworth, California).

The first step was to select a reasonable collection of samples that could represent the colors we perceive without being too many to handle in the experiment.

The spectrum of theoretical daylight illuminants was computed using the tabled x coordinate (Appendix I) of eight different color-correlated temperatures (CCT). The radiance was obtained using these values.

The tristimulus values were computed for the NCS colors and the illumination. With these, the CIECAM02-UCS coordinates were calculated. The  $J'$  coordinate in this color space is equivalent to the  $L^*$ , it describes lightness.

Three ranges of values of lightness were used, one ranged from 35 to 45 where 10 color samples were selected, the other from 54 to 65 where 10 color samples were selected, and the last from 75 to 85 where 10 color samples were selected. Three more color samples were selected from a range of lightness values between 75 to 85, and 10 from a range of lightness between 54 to 65 but with higher saturation values. The neutral color samples were also selected in three levels of lightness, they were the black, white, and gray color samples.

In total, the final number of samples used in the experiment was 46. A computational representation of the samples is shown in Figure 24 obtained using the RGB coordinates of each sample.

In the first row of Figure 24 are the 10 samples with lightness ranging from 75 to 85, in the second row are the three samples with the same lightness but higher saturation levels, in the third row are the 10 samples with lightness ranging from 54 to 65, in the fourth row are the 10 samples with the same lightness but higher saturation levels, in the fifth row are the 10 samples with lightness ranging from 35 to 45, and in the sixth row are the three achromatic samples.

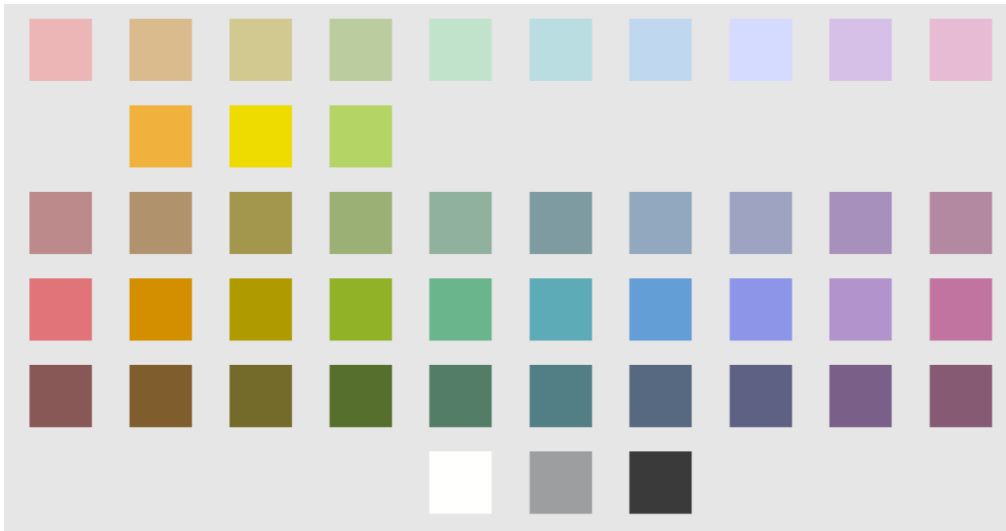


*Figure 24 - sRGB representation of the selected NCS samples illuminated by the Solux lamp with the diffuser used.*

With the 46 samples, the same calculations were applied but this time to understand the impact of varying the illuminant in each NCS color sample, the  $\Delta E$  was calculated using Equation 16.

The next step was to compare the theoretical daylight illuminants with the two options of lamps available, those were a Solux lamp (Tailored Lighting, Inc., Rochester, NY) and a D65 lamp. The spectrum of the lamps was measured with a telespectroradiometer PR-650 SpectraScan®. This was done to understand if the lamps available produced colors similar to the ones produced by daylight.

The Solux lamp was compared with the illuminants of 4500, 4600, and 4700 K of CCT. This was done because the Solux lamp is produced with a CCT of 4700 K according to the manufacturer [71].

The D65 lamp was compared with the illuminants of 6500 and 7500 K of CCT.

The mean, standard deviation, maximum, and minimum of the  $\Delta E$  for the Solux lamp without a diffuser are expressed in Table 1.

*Table 1 - Values of mean, standard deviation, maximum, and minimum  $\Delta E$  for the Solux lamp without a diffuser.*

Comparison	Mean	Standard deviation	Maximum	Minimum
Solux//4500K	1.40	0.55	2.64	0.15
Solux//4600K	1.39	0.52	2.49	0.14
Solux//4700K	1.40	0.49	2.37	0.16

The mean, standard deviation, maximum, and minimum of the  $\Delta E$  for the D65 lamp without a diffuser are expressed in Table 2.

*Table 2 - Values of mean, standard deviation, maximum, and minimum  $\Delta E$  for the D65 lamp without a diffuser.*

Comparison	Mean	Standard deviation	Maximum	Minimum
D65//6500K	5.33	2.03	9.05	0.30
D65//7500K	5.34	1.91	8.50	0.38

Studies [70],[71] established about 1.5 as the threshold accepted for the CIECAM02-UCS color space, the Solux lamp was chosen because it was below this value.

Chandeliers with the Solux lamp were used in the experiments. To improve the uniformity of light distribution, a diffuser (Lamp Sock Soft Diffuser 18 cm from Honoson) was used in each chandelier.

The CCT measured with the spectroradiometer (SR-2, TOPCON TECHNOHOUSE CORPORATION, Tokyo, Japan) on the solux lamp with the diffuser was 3240 K.

The spectra of two theoretical daylight illuminants with 3300 and 3400 K were calculated using Equation 17 and then compared with the CCT of the solux lamp with the diffuser because the tabled values range from 4000 to 25000 K [43]. The CCT values outside these tabled values can be calculated but have an error associated with them.

$$x_D = -4.6070 \frac{10^9}{T_c^3} + 2.9678 \frac{10^6}{T_c^2} + 0.09911 \frac{10^3}{T_c} + 0.244063 \quad \text{Equation 17}$$

The mean, standard deviation, maximum, and minimum of the  $\Delta E$  for the Solux lamp with a diffuser are expressed in Table 3.

*Table 3 - Values of mean, standard deviation, maximum, and minimum  $\Delta E$  for the Solux lamp with a diffuser.*

Comparison	Mean	Standard deviation	Maximum	Minimum
Solux//3300K	0.50	0.24	1.15	0.02
Solux//3400K	0.44	0.26	1.14	0.02

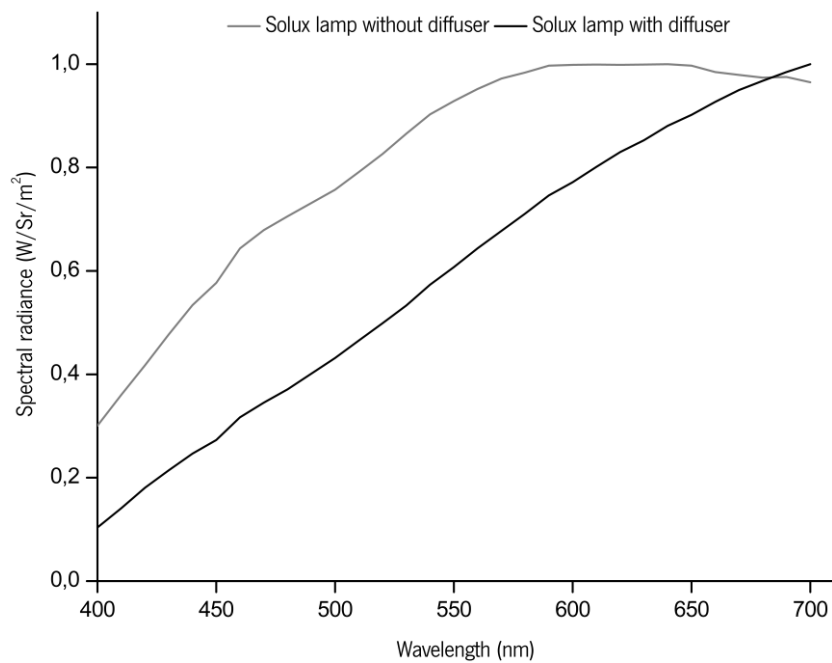


*Figure 25 - Spectra of the solux lamp with (black line) and without (gray line) diffuser.*

The spectrum radiance of the lamp was measured again with and without (Figure 25) the diffuser using a spectroradiometer.

The two-dimensional representation of the CIECAM02-UCS of the Solux lamp with the diffuser is in Figure 26. Represented with yellow dots are the three samples with lightness ranging from 75 to 85 with a higher level of saturation, with blue dots are the 10 selected samples with lightness ranging from 75 to 85, with red dots are the 10 samples with lightness ranging from 54 to 65 with higher saturation levels, with gray triangles are the 10 samples with lightness ranging from 54 to 65, with green dots are the 10 samples with lightness ranging from 35 to 45 and with gray dots the three achromatic samples used.



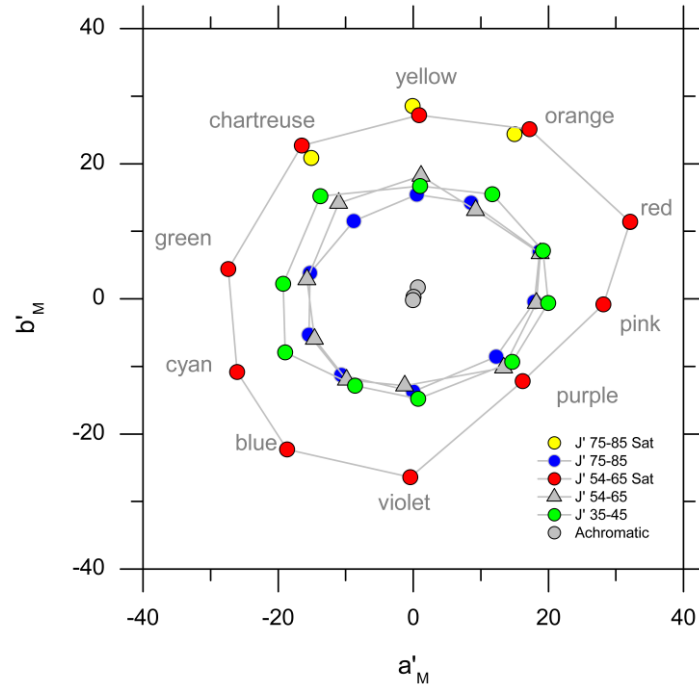


Figure 26 - Two-dimensional representation of the CIECAM02-UCS of the selected samples solux lamp divided by lightness level.

#### 4.2. Making the physical samples

After selecting the NCS colors, it was necessary to assemble the samples. Different methods were tested but the following procedure was the best.

The NCS colors were manually cut into squares of 3.5 by 3.5 cm and glued into wood squares of 3 by 3 cm (Figure 27). Once dried the excess was cut using an Exacto knife.



Figure 27 - Sample making.

To make the task of recognizing which sample was being used easier, the name was placed on the back of each sample. Also, for the samples used in the experiment where color combinations were made, symbols were used to easily identify the samples of each board.

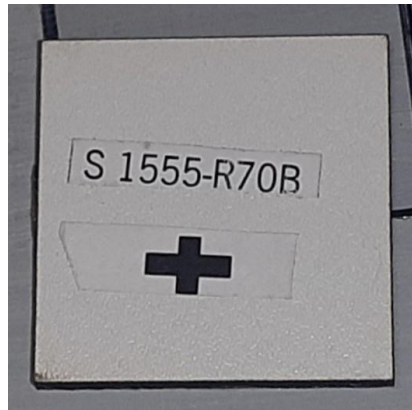


*Figure 28 - Example of sample with name and symbol.*

In total over 800 color samples were handmade in the laboratory using this method.

## **5. PILOT EXPERIMENTS**

### **5.1. Color preference for single colors without the achromatic samples**

#### **5.1.1. Objective**

The goal of this experiment was to measure the color preference ratings of samples for single colors using NCS color samples selected for this work. These results allow comparisons to be made with studies [65] where different color systems were used, like the Munsell Book of Colors, Glossy Series. This experiment uses physical samples instead of color samples reproduced in a monitor.

#### **5.1.2. Methods**

##### Participants

Fifty participants with a mean age of 22 years (ranging from 18 to 40 years) did this experiment. An equal number of females and males was used, and participants were for the most part students of the University of Minho.

All participants were tested using the Ishihara plates test (38 plates edition, Kanehara & Co., Ltd., Tokyo, Japan) to ensure they had normal color vision, none of them presented with color vision deficiencies. This procedure was carried out before starting the experiment and one chandelier with the Solux lamp served as illumination for the Ishihara plates. The data sheet used to register this information can be found in Appendix II.

Informed consent (Appendix III and Appendix IV) was given to all participants and the experiment protocol respected the Declaration of Helsinki (1964, World Medical Association) and was approved by the Comissão de Ética para a Investigação em Ciências da Vida e da Saúde (CEICVS 052/2021) of the University of Minho.

##### Samples

Forty-three out of the 46 samples available were used, the three excluded were the achromatic color samples. A complete description of the selection and manufacturing process of the NCS color samples can be found in Chapter 4.

##### Procedure

To display the samples a board of wood with 52.5 cm of width and 60 cm of length was used.

The board was painted using the Munsell N7 paint from VeriVide Limited, Quartz Close, Warrens Business Park, Enderby, Leicester LE19 4SG United Kingdom. The paint used was a standard neutral gray that dries completely matt and has neutral saturation these properties make this paint ideal for color matching and visual assessment tasks because it will not influence color perception [74].

The light source used was one chandelier with a Solux lamp and the diffuser previously described in Chapter 4. It was placed 30 cm from the standard gray board and luminance was measured with PR-650 SpectraScan® on Barium sulfate (BaSO4) for a square of 15 by 15 cm, using Equation 18 [43] and considering that  $\varepsilon_D$  is the angle with the perpendicular to the measuring surface and  $\cos \varepsilon_D = 1$  the illuminance was obtained, results can be found in Table 4.

$$L_D = \frac{E_n \cos \varepsilon_D}{\pi} \quad \text{Equation 18}$$

Table 4 - Luminance and illuminance result for 15 by 15 cm square.

Position	Luminance (cd/m <sup>2</sup> )	Illuminance (lux)
Top left corner	376	1181
Top right corner	333	1046
Middle	419	1316
Bottom left corner	392	1231
Bottom right corner	293	920

$$\text{Variation} = \frac{\text{Middle value} - \text{smallest value}}{\text{Middle luminance}} \quad \text{Equation 19}$$

The luminance variation obtained using Equation 19 on the top was 20.5% and on the bottom was 30% compared to the middle value. The participant sat on a stool, and the visual angle ( $\theta$ ) was obtained using Equation 20 where the d was the width of the board was 52.5 cm, and the

height (h) from the board to the eye, in this case, was 52 cm making a visual angle of 45.3 degrees. The visual angle for the sample of 3 cm is about 3.3 degrees in these viewing conditions.

A visual representation of the visual angle calculated is illustrated in Figure 29.

$$\gamma = \tan^{-1} \left( \frac{h}{d} \right)$$

*Equation 20*

$$\theta = 180 - 90 - \gamma$$

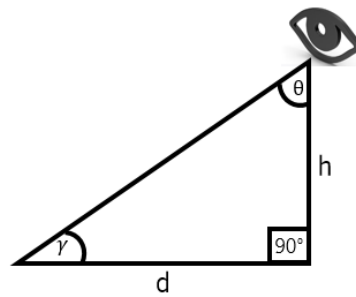


*Figure 29 - Visual angle representation.*

To rank color preference a scale from -10 to 10 was used, where 10 was liking the color sample zero was neutral, and -10 disliking the color sample. The procedure is similar to Palmer et al. [65] where a scale appeared on the monitor and using the cursor observers clicked on it to lock in their answers.

One color sample at the time was placed on the gray board always in the same position (the center), and the distance between the sample and the scale was always 20 cm as shown in Figure 30.



*Figure 30 - Experiment setup.*

Participants were presented with the 43 color samples one by one in a random order. The color was taken out of a box at random by the investigator such that both parties never knew what color would be placed on the board. Once the color sample was on the board participants could take as much time as they needed to rank it. To rank, the color of the sample all they had to do was point on the scale. After being ranked the sample was placed in an open box preserving the order that it was viewed by the observer. This way by the end of the experiment information about the order was also photographed. The data sheet used to register this information can be found in Appendix V and Appendix VI.

Participants took an average of 9.3 minutes with a standard deviation of  $\pm 1.6$  minutes to complete this procedure, 14 minutes was the maximum time that a participant took, and seven minutes was the minimum.

### **5.1.3. Results and conclusions**

Figure 31 represents the average preference ratings across all 50 participants, the x-axis represents the hues tested and the y-axis represents the mean ratings, the error bars represent the standard error of the mean. On the left are the mean results of the rating for the samples with lightness levels ranging from 54 to 65, 75 to 85, and 35 to 45. On the right are the mean results of the rating for the samples with lightness levels ranging from 54 to 65, and 75 to 85 but with higher saturation levels.

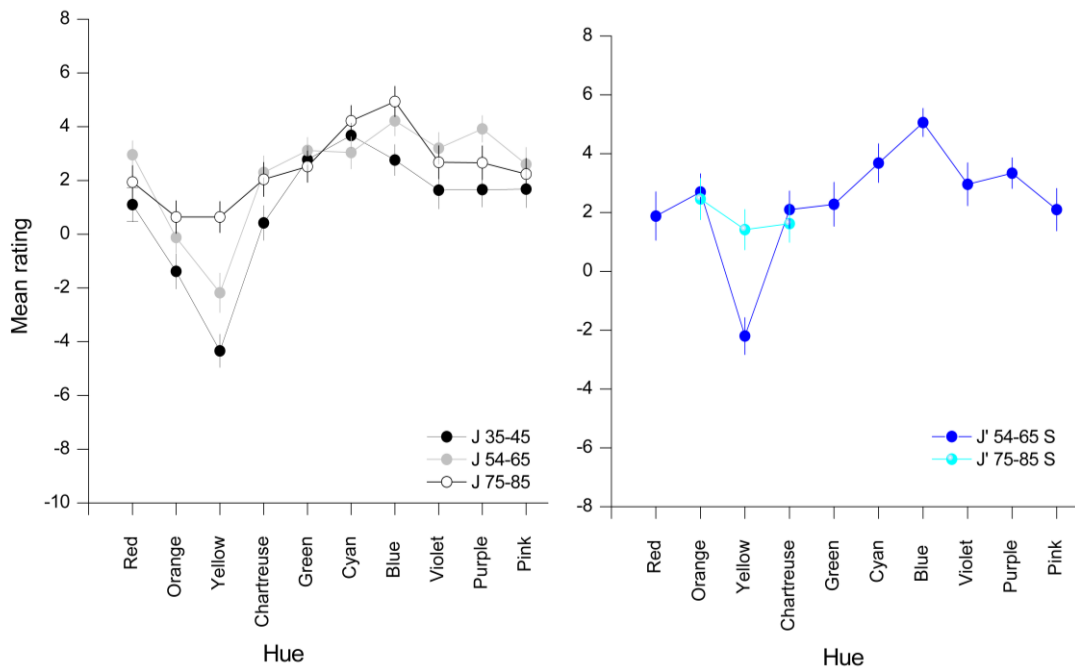


Figure 31 - Mean ratings across all participants.

The peaks of this figure can be associated with highest-rated hues and depressions can be associated with the lowest-rated hues. This also occurs in the more saturated lightness levels. Blue hues are the highest rated by observers and yellow, in particular, dark yellows are the lowest rated.

Variations across hues for the different lightness levels and saturation levels exist but the overall profile of the curve is very similar for the different levels.



Figure 32 - sRGB computational representation of samples S 6030-Y (lowest rated) on the left and S 2050-B (highest rated) on the right.

Figure 32 is the computational representation of the colors with the lowest mean rating on the left and the highest mean rating on the right. Sample S 6030-Y has a mean rating of -4.34 and is the sample with the lowest mean rating. Sample S 2050-B has a mean rating of 5.06 and is the sample with the highest mean rating.

To test if the mean ratings are different between males and females (Figure 33), statistical analysis was conducted and, in some samples, statistical significant differences were found, the full statistical analysis can be seen in Appendix IX.

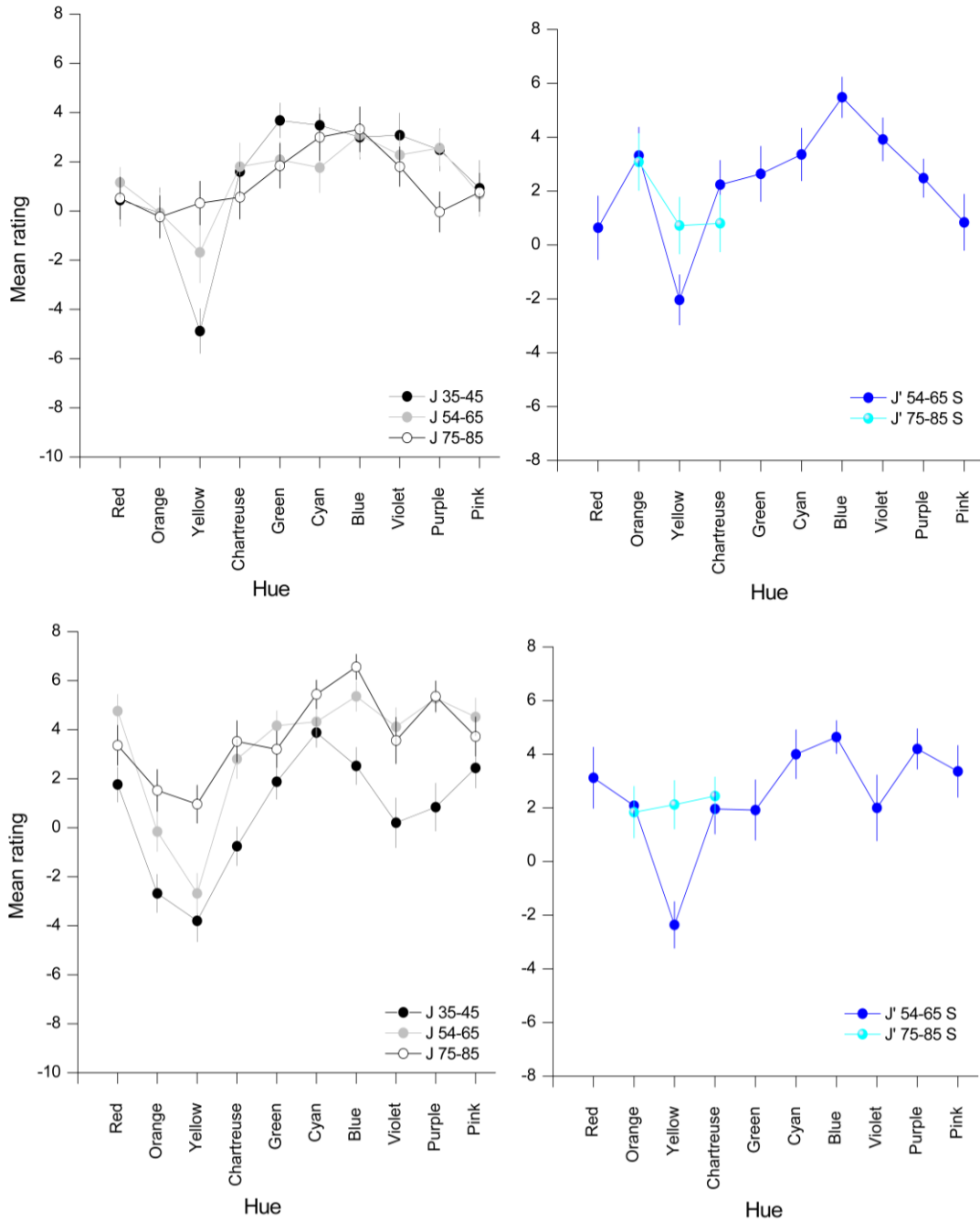


Figure 33 - Mean ratings across males (on the top); Mean ratings across females (on the bottom).

In six out of 10 samples with a lightness range of 75 to 85, statistical significant differences were found, those samples are S 1030-R, S 2020-G40Y, S 1020-B50G, S 1020-B, S 1030-R50B, S 1030-R30B and represent red, chartreuse, cyan, blue, purple, and pink hues respectively they are illustrated in Figure 34. Females have higher ratings than males for these samples.





*Figure 34 - sRGB computational representation of samples S 1030-R, S 2020-G40Y, S 1020-B50G, S 1020-B, S 1030-R50B, and S 1030-R30B (from left to right).*

In four out of 10 samples with a lightness range of 54 to 65 statistical significant differences were found, those samples are S 3030-R, S 3020-G, S 3030-R50B, and S 3030-R30B and represent red, green, purple, and pink hues respectively they are illustrated in Figure 35. Higher mean ratings in females than males in these samples.



*Figure 35 - sRGB computational representation of samples S 3030-R, S 3020-G, S 3030-R50B, and S 3030-R30B (from left to right).*

In two out of 10 samples with a lightness range of 35 to 45 statistical significant differences were found, those samples are S 5540-G40Y and S 6020-R70B and represent chartreuse and violet hues respectively they are illustrated in Figure 36. For these samples higher mean ratings were found in males than in females.



*Figure 36 - sRGB computational representation of samples S 5540-G40Y, and S 6020-R70B (from left to right).*

#### **5.1.4. Discussion**

Results indicate higher rating values were given to blue hues and lower rating values were given to yellow hues.

The blue hue sample (S 2050-B), is on average the favorite of observers it has a lightness ranging from 75 to 85 as for the least favorite the yellow hue sample (S 6030-Y) has a lightness level ranging from 35 to 45. When comparing the mean ratings from this experiment with the

results in Figure 22C one common and important conclusion is that the same blue hues are preferred. Different techniques were used in Palmer et al. study 32 samples were displayed on a monitor placed 70 cm away with a gray background one at a time randomly, and in this study samples and scale were physical. This study tested two extra hues named violet and pink making the total samples tested 43 [65].

One difference is apparent in the curves obtained in this study, the chartreuse hue does not have depression like the one in the Palmer et al. study. Other slight changes are noticeable in the curves this is likely to happen due to the different techniques used.

To complete the analysis of this data a comparison between males and females was conducted, resulting in significant statistical differences being found in some samples illustrated in Figure 34, Figure 35, and Figure 36 where they are divided by lightness levels and saturation levels. These results seem to indicate that differences in ratings between males and females exist especially in the lightness level ranging from 75 to 85.

Overall the results obtained are similar to the ones already described in literature some of these mentioned in Chapter 3.

## **5.2. Color preference for color combinations without repetition**

### **5.2.1. Objective**

The goal of this experiment is to study the properties of color combinations preferred without repeated color samples, i.e., there is only one set of 43 color samples.

### **5.2.2. Methods**

#### Participants

Fifty participants with a mean age of 22 (ranging from 18 to 40) did this experiment. An equal number of females and males was used, and participants were for the most part students of the University of Minho.

Forty-one (25 females and 16 males) participants had already done the color preference experiment described in Chapter 5.1, those who did not were tested using the Ishihara plates test to ensure they had normal color vision, and none of them presented with color vision deficiencies. This procedure happened before starting the experiment and one chandelier with the solux lamp

served has illumination for the Ishihara plates. The data sheet used to register this information can be found in Appendix II.

Inform consent (Appendix III and Appendix IV) was given to all participants and the experiment protocol respected the Declaration of Helsinki (1964, World Medical Association) and was approved by the Comissão de Ética para a Investigação em Ciências da Vida e da Saúde (CEICVS 052/2021) of the University of Minho.

### Samples

The same samples used in Section 5.1 were used in this experiment.

### Procedure

The same board of wood described in Section 5.1 was used, and in addition, a box lid with 34 cm of length, 24.5 cm of width, and 3 cm of height was painted gray with the Munsell N7 paint [74]. The box lid was used to place the set of 43 samples from which participants could select (Figure 38).

The same solux lamp was placed 30 cm from the standard gray board and luminance was measured with PR-650 SpectraScan® on Barium sulfate (BaSO<sub>4</sub>) for a square of 12 by 12 cm, using Equation 18 [43] and [43] and considering that  $\varepsilon_D$  is the angle with the perpendicular to the measuring surface and  $\cos \varepsilon_D = 1$  the illuminance was obtained, and results can be found in Table 5.

*Table 5 - Luminance and illuminance result for the 12 by 12 cm square.*

Position	Luminance (cd/m <sup>2</sup> )	Illuminance (lux)
Top left corner	405	1272
Top right corner	399	1253
Middle	502	1577
Bottom left corner	445	1398
Bottom right corner	438	137

The luminance variation obtained using Equation 19 on the top was 20.5% and on the bottom was 12.7% compared to the middle value.

The same procedure was repeated for another solux lamp placed 30 cm away from the box lid.

*Table 6 - Luminance and illuminance result for the box lid.*

Position	Luminance (cd/m <sup>2</sup> )	Illuminance (lux)
Top left corner	249	782
Top right corner	260	817
Middle	422	1326
Bottom left corner	176	553
Bottom right corner	216	678

The luminance variation obtained using Equation 19 on the top was 41% and on the bottom was 58.3% compared to the middle value.

All participants sat on a stool, the visual angle was the same as previously mentioned. Five grids were made so that participants knew how many samples to combine and where to place them this is possible to visualize in Figure 37. These grids were placed one at a time on the center of the board.

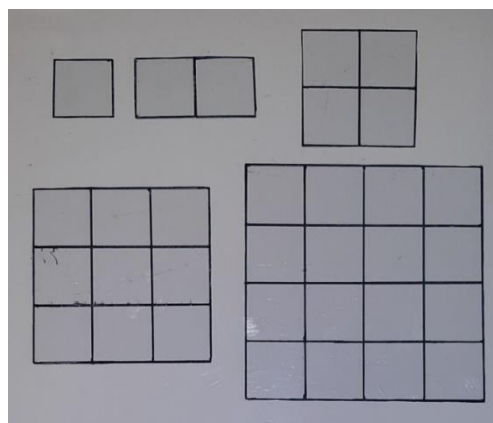


*Figure 37 - Grids used.*

The first grid was only one (1x1) square, and the task of the participant was to select out of the 43 samples the one they liked the most. The second grid had two squares (2x1) side by side and participants had to pick a combination of two colors they liked to see together. The third grid was a two-by-two (2x2) square and in total participants had to pick four samples that they liked to see combined. The fourth grid was a three-by-three (3x3) square and in total participants had to pick nine samples that they liked combined. The fifth grid was a four-by-four (4x4) square and in total participants had to pick 16 samples that they enjoyed seeing combined. To make it easier the first, second, third, fourth, and fifth grids will be referred 1x1, 2x1, 2x2, 3x3, and 4x4 grids respectively.

Participants were instructed to make combinations of colors and place them on top of each grid. They were given full liberty to start to fill the grid from where they wanted and to change samples as much as they needed to reach something they truly liked. After picking the samples for each grid participants had to respond to the following question: From 1 to 10 how satisfied they were with their decisions, where 1 was not satisfied and 10 was fully satisfied. This question was a way to measure satisfaction with their final selection. The data sheet used to register this information can be found in Appendix VII and Appendix VIII.

Figure 38 shows how all the material used was assembled.

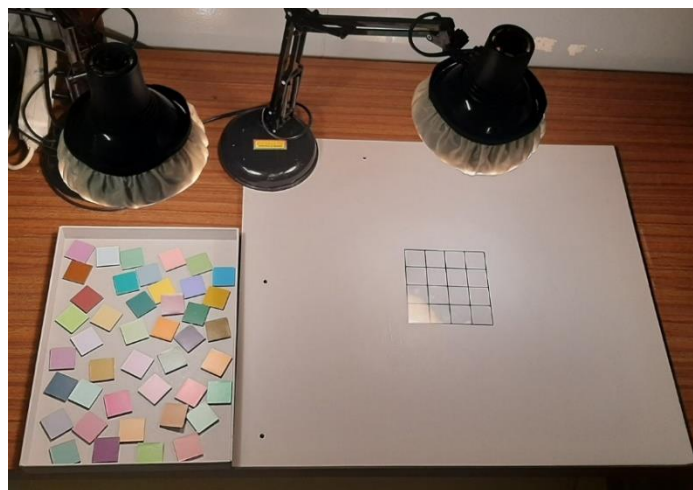


*Figure 38 - Setup used.*

Participants took an average of 8.37 minutes with a standard deviation of  $\pm 3.6$  minutes to complete this procedure, 25 minutes was the maximum time that a participant took, and four minutes was the minimum.

### 5.2.3. Results and conclusions

Two models were created using MATLAB (MathWorks, Natick, MA 01760-2098, USA) the scripts were developed in-house to analyze the colors selected by the observers. One was the randomly generated data (represented using blue and named Random) this data simulated what would happen if participants made their combinations by selecting the samples at random. The other was the randomly generated data based on ratings from the experiment with single colors (represented using green and named Single color preference). It was generated to simulate the answers of 50000 participants.

The experimental data (represented using red and named Experimental) are the results obtained by the combinations made by the 50 observers.

This script was created and ellipses (Figure 39) were adjusted to the data points. Three variables of the ellipses were analyzed: The angle corresponds to the angle defined by the direction of larger color variation, the area corresponds to the area of the ellipse, and the axis ratio is the result of the ratio of the shorter and longer axis length.

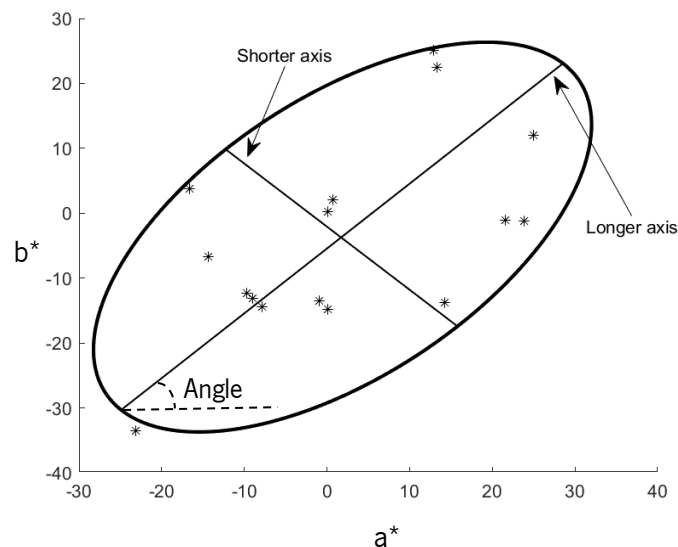


Figure 39 - Example of ellipse.

- **1x1 grid**

To analyze if observers when asked to pick their favorite color sample would pick the one they rated higher in the experiment described in Section 5.1 the plot in Figure 40 was produced. This plot does not include the 9 participants who did not do the color preference for single colors experiment because comparisons would be impossible to make.

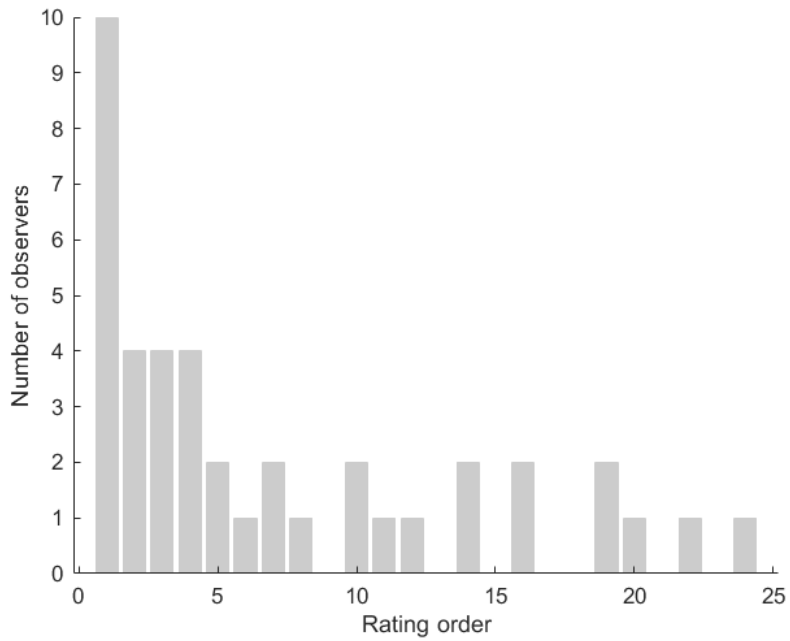


Figure 40 - Plot of the number of observers for the rating order.

The data in this plot demonstrates that 10 out of the 41 observers, select the color sample that they rated higher when asked to pick their favorite.

The second, third, and fourth highest-rated color samples were picked by four observers each as their favorite.

- **2x1 grid**

To analyze the 2x1 grid the  $\Delta E$  between the two colors samples picked was calculated using Equation 16.

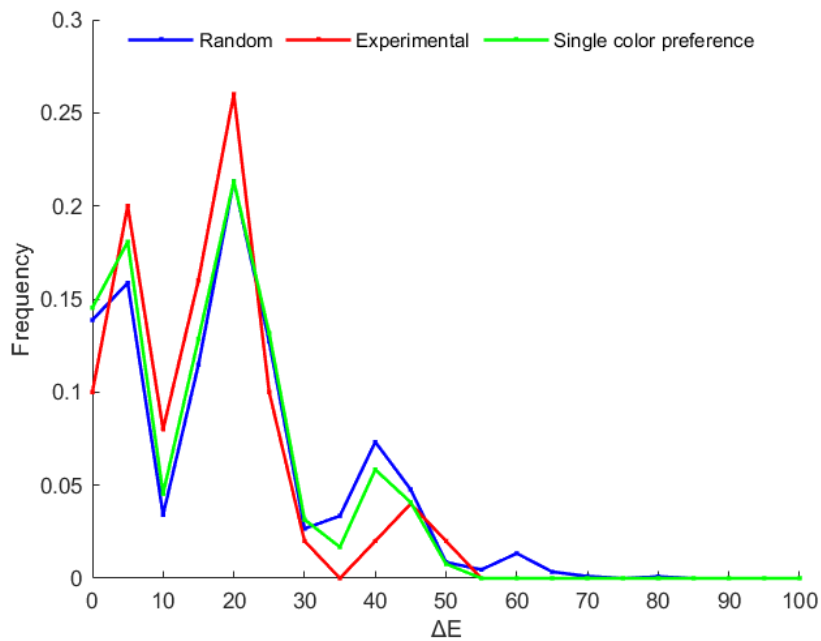


Figure 41 - Difference of color for the lightness axis.

Figure 41 represents the  $\Delta E$  of the J' axis for all three types of data on the x-axis and the frequency on the y-axis. The peak of  $\Delta E$  for the combinations occurs at around 20.

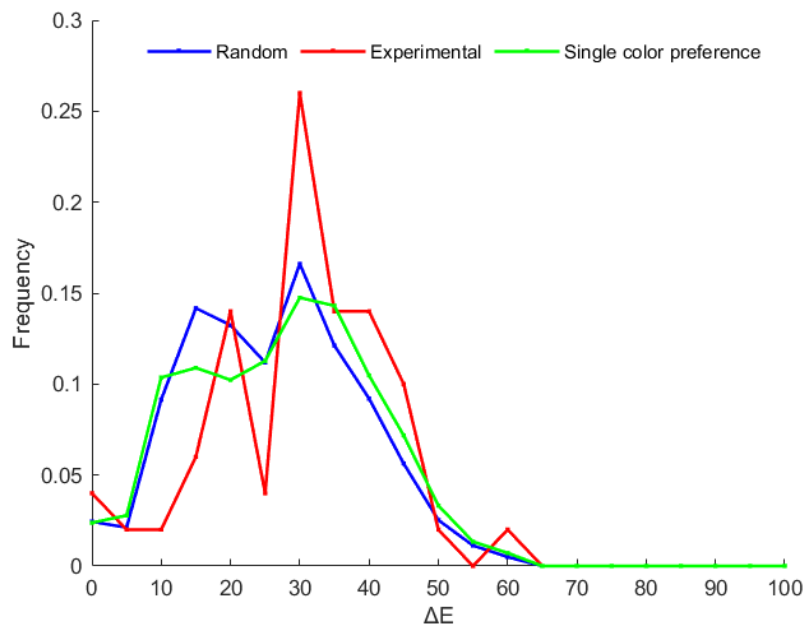


Figure 42 - Difference of color for the chromatic axis.

Figure 42 represents the  $\Delta E$  for the  $a'_M$  and  $b'_M$  axis for all three types of data on the x-axis and the frequency on the y-axis. The peak of  $\Delta E$  for the combinations occurs at around 35.

- **2x2 grid**

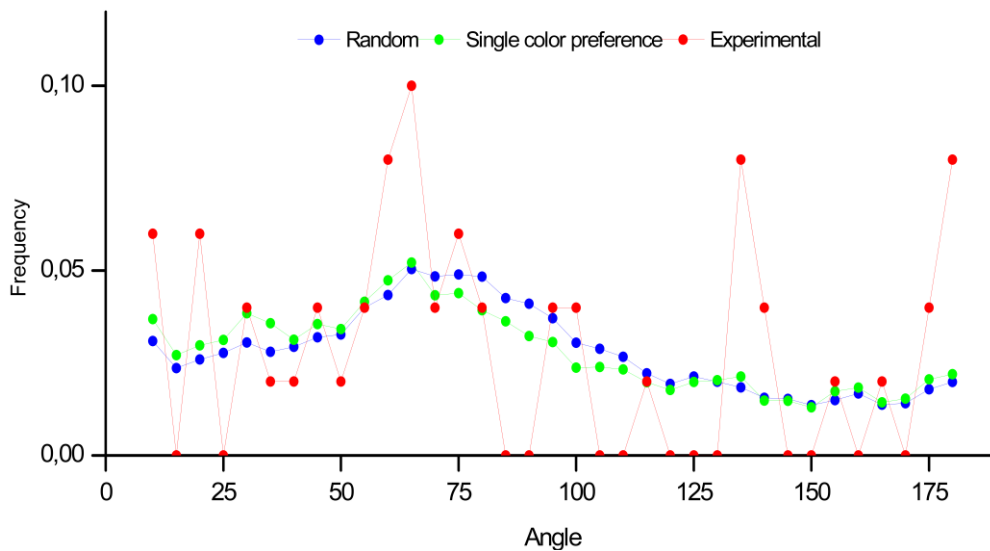


Figure 43 - Angle results for the 2x2 grid.

The average angle for the experimental data is 80 degrees, for the random data is 79 degrees, and for random data based on the results of the single color preference experiment is 77 degrees.



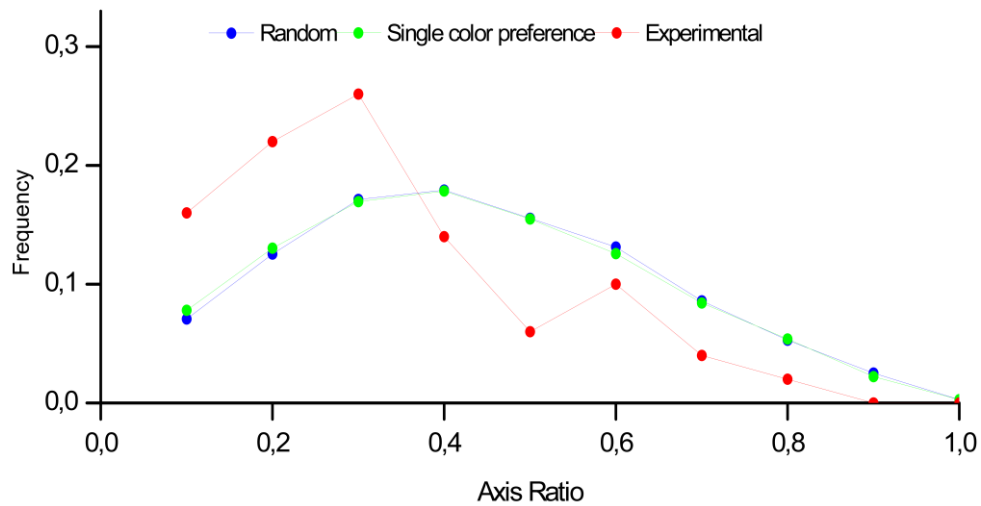


Figure 44 - Axis ratio results for the 2x2 grid.

The average axis ratio for the experimental data is 0.32, for the random data is 0.44, and for the random data based on the results of the single color preference experiment is 0.43.

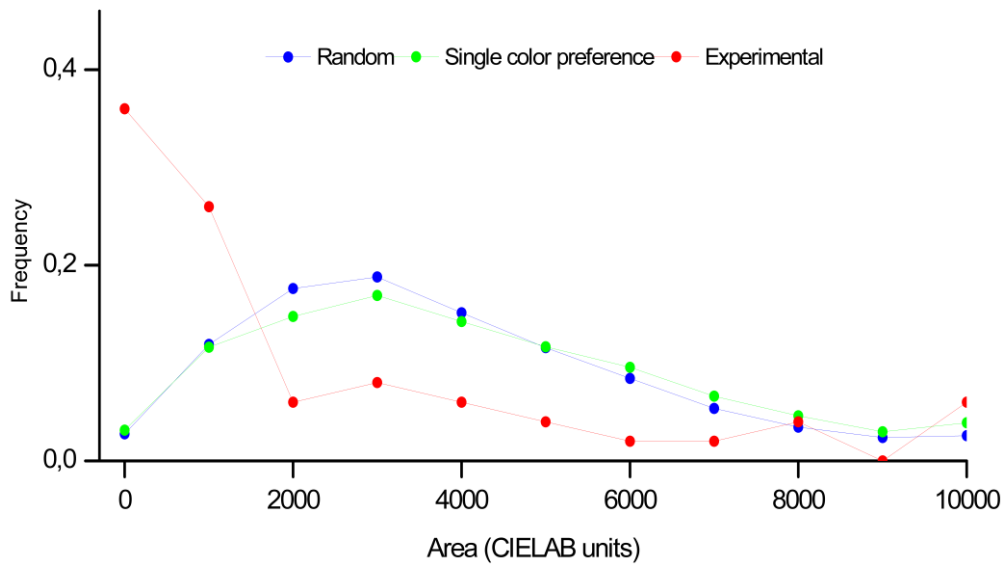


Figure 45 - Area results for the 2x2 grid.

The average area of the fitted ellipses for the experimental data is 2388 CIELAB units, for the random data is 3877 CIELAB units, and for the random data based on the results of the single color preference experiment is 4173 CIELAB units.

- **3x3 grid**

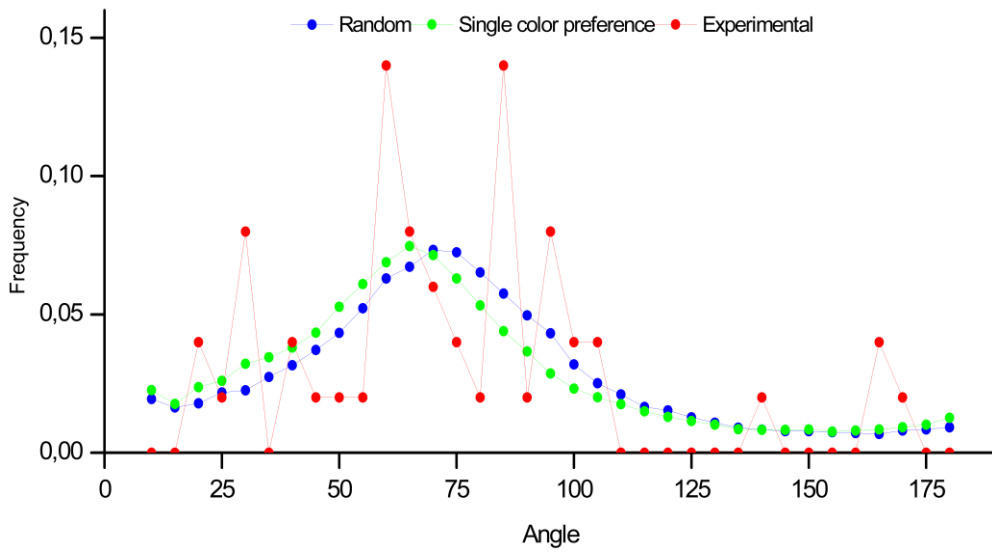


Figure 46 - Angle results for the 3x3 grid.

The average angle for the experimental data is 72 degrees, for the random data is 72 degrees, and for the random data based on the results of the single color preference experiment is 69 degrees.

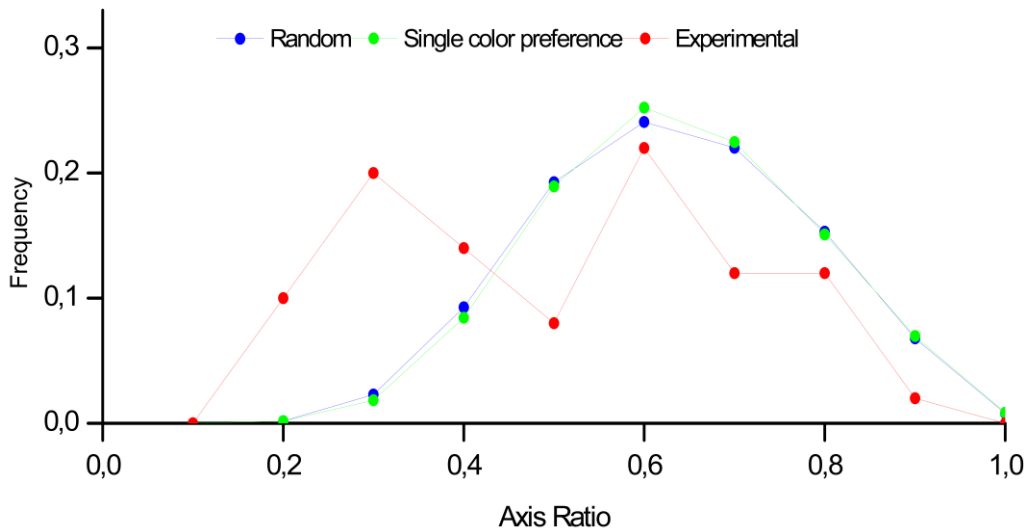


Figure 47 - Axis ratio results for the 3x3 grid.

The average axis ratio for the experimental data is 0.50, for the random data is 0.63, and for the random data based on the results of the single color preference experiment is 0.63.

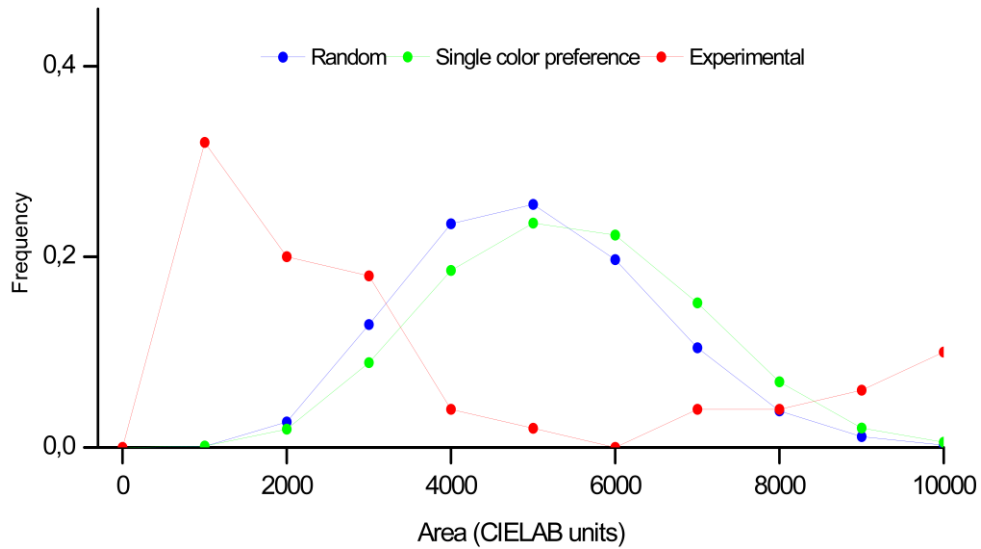


Figure 48 - Area results for the 3x3 grid.

The average area of fitted ellipses for the experimental data is 3677 CIELAB units, for the random data is 4999 CIELAB units, and for the random data based on the results of the single color preference experiment is 5414 CIELAB units.

● **4x4 grid**

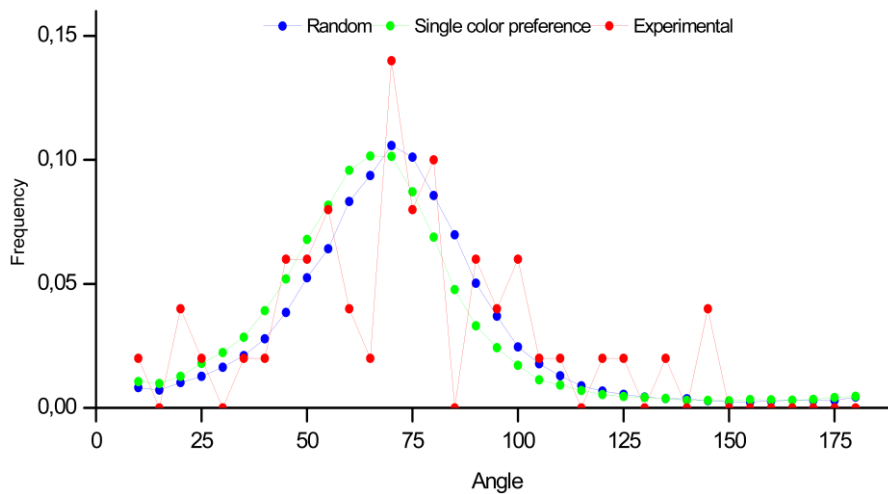


Figure 49 - Angle results for the 4x4 grid.

The average angle for the experimental data is 69 degrees, for the random data is 67 degrees, and for the random data based on the results of the single color preference experiment is 63 degrees.

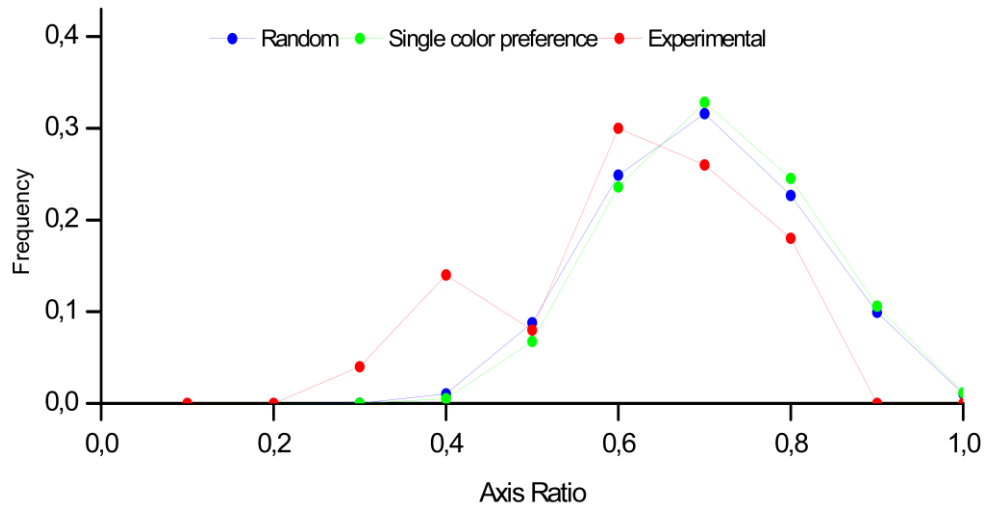


Figure 50 - Axis ratio results for the 4x4 grid.

The average axis ratio for the experimental data is 0.61, for the random data is 0.70, and for the random data based on the results of the single color preference experiment is 0.71.

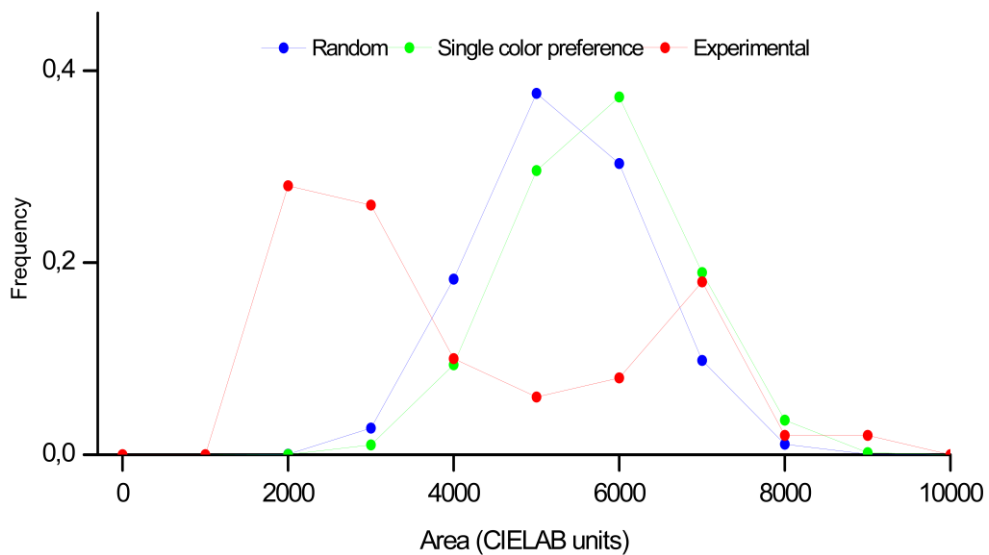


Figure 51 - Area results for the 4x4 grid.

The average area of fitted ellipses for the experimental data is 4131 CIELAB units, for the random data is 5294 CIELAB units, and for the random data based on the results of the single color preference experiment is 5752 CIELAB units.

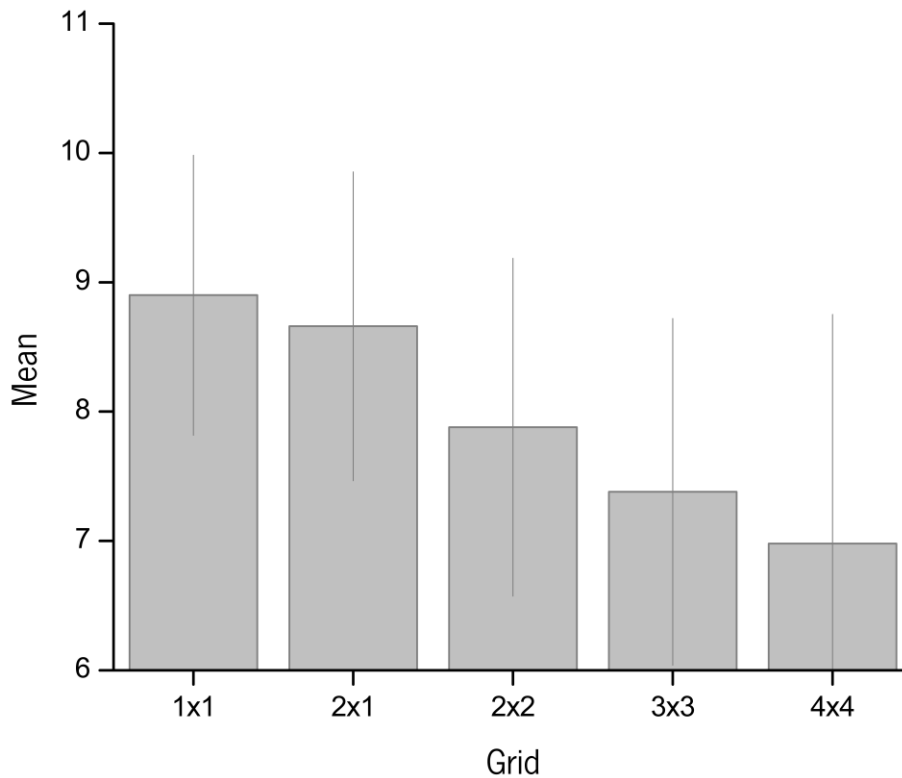


Figure 52 - Mean satisfaction for each grid.

Figure 52 shows the mean satisfaction for each grid and the error bars are the standard deviation, the y-axis scale range was defined from six to eight to improve data visualization but satisfaction was measured on a scale from one to 10. The average satisfaction for the 1x1 grid for the 50 observers was 8.9 with a standard deviation of  $\pm 1.1$ , for the 2x1 grid was 8.7 with a standard deviation of  $\pm 1.2$ , for the 2x2 grid was 7.9 with a standard deviation of  $\pm 1.3$ , for the 3x3 grid was 7.4 with a standard deviation of  $\pm 1.3$ , and for the 4x4 grid was 7 with a standard deviation of  $\pm 1.8$ .

#### 5.2.4. Discussion

For the 1x1 grid results show that most participants when asked to pick their favorite color choose the ones rated the highest in the experiment of single colors. These experiments were conducted on different days possibly if they were executed one after the other this would increase the number of participants who picked the highest-rated color sample.

The 2x1 grid combinations seem to differ in lightness and chromaticity.

The ellipses are a technique commonly used in studies [66], [67] to analyze the distribution of data points but it is not perfect. Ellipses are roughly adjusted to the data points and sometimes points are left outside the ellipses so some information is lost.

The points fitted in the ellipses of the 2x2 grid occupied an average of 100% for all three types of data. The 3x3 grid occupied an average of 93% for all three types of data, and the 4x4 grid occupied an average of 91.1% when the experimental data was used, 89.5% when the randomly generated data was used, and 90.4% when the randomly generated based on the results of the single color preference experiment data was used.

Montagner et al. found average angles of  $92^\circ$  for natural scenes,  $66^\circ$  for paintings ( $72^\circ$  for figurative and  $58^\circ$  for abstract paintings) [67]. When comparing the results of the three types of data of all grids they are closer to the ones of paintings, especially the figurative paintings.

Montagner et al. found an average axis ratio of 0.51 for natural scenes, 0.58 for paintings (0.56 for figurative and 0.6 for abstract paintings) [67]. When comparing these results to the ones of the 2x2 grid they are closer to the ones of natural scenes for all three types of data, for the 4x4 grid they are closer to the ones of paintings especially abstract paintings for all three types of data, for 3x3 grid they are closer to the ones of paintings especially abstract paintings except in the experimental data where they are closer to natural scenes.

Montagner et al. found an average area of fitted ellipses of 1226 CIELAB units (range from 210 to 6613 CIELAB units) for natural scenes, 1338 CIELAB units (range from 124 to 5610 CIELAB units) for paintings [67]. When comparing the results of the three types of data of all grids they are closer to the ones of paintings.

The mean satisfaction of the combinations made is expressed in Figure 52 and it decreases as the complexity of the combination increases.

Both models fail to predict the combinations made by participants on some occasions results are similar but never truly close. This indicates that observers do not make combinations randomly and they do not use only individual color preferences to build their combinations.

Although individual color preference seems to partially affect the color combinations made it does not fully explain the results obtained.

There appear to be different aspects that affect color combinations that are not yet known.

## **6. COLOR PREFERENCE FOR SINGLE COLORS**

### **6.1. Objective**

The goal of this experiment is the same as the one reported in Chapter 5 (Section 5.1).

The difference is that this time the achromatic color samples were used and adjustments in the lights were made to improve light distribution across the board. Also, an anchoring technique was used.

### **6.2. Methods**

#### Participants

Fifty participants with a mean age of 22 years (ranging from 18 to 33 years) did this experiment. An equal number of females and males was used and participants were for the most part students of the University of Minho.

All participants were tested using the Ishihara plates to ensure they had normal color vision, none of them presented with color deficiencies. This procedure happened before starting the experiment and one chandelier with the solux lamp served as illumination for the Ishihara plates. The data sheet used to register this information can be found in Appendix II.

Informed consent (Appendix III and Appendix IV) was given to all participants and the experiment protocol respected the Declaration of Helsinki (1964, World Medical Association) and was approved by the Comissão de Ética para a Investigação em Ciências da Vida e da Saúde (CEICVS 052/2021) of the University of Minho.

#### Samples

Forty-six samples were used. A complete description of the selection and making process of the color samples is described in Chapter 4.

#### Procedure

To display the samples a board with 27.8 cm of width and 39.7 cm of length was used, this board was changed to make transportation easier. The board was painted using the Munsell N7 (Figure 53).

The light source was one chandelier with a solux lamp it was placed 40 cm from the standard gray board and luminance was measured with PR-650 SpectraScan® on Barium sulfate (BaSO<sub>4</sub>) for a square of 12 by 12 cm, using Equation 18 [43] [43] and considering that  $\varepsilon_D$  is the angle with

the perpendicular to the measuring surface and  $\cos \varepsilon_D = 1$  the illuminance was obtained, results can be found in Table 7

*Table 7 - Luminance and illuminance result for 12 by 12 cm square.*

Position	Luminance (cd/m <sup>2</sup> )	Illuminance (lux)
Top left corner	246	773
Top right corner	255	801
Middle	268	842
Bottom left corner	264	829
Bottom right corner	255	801

The luminance variation obtained using Equation 19 on the top was 8.2% and on the bottom was 4.8% compared to the middle value.

The luminance variation was smaller with the chandelier placed 40 cm away from the board instead of the previous 30 cm, this improvement in light distribution was the reason it was changed.

Using Equation 20 the  $\theta$  obtained was 28.1 degrees in this case d was 27.8 cm and h was 52 cm. The visual angle of the samples was the same as previously reported.

The same procedure described in Chapter 5 (Section 5.1) was used this time around with the only difference being that before starting the experiment participants saw all 46 samples and picked their favorite and their least favorite. This technique is called anchoring and was used in similar studies [75].

After they chose, it was explained to them that their favorite color sample symbolized a 10 and their least favorite a -10 this was done so they could better understand the scale in front of them.



Figure 53 shows the setup used.



Figure 53 - Experiment setup.

Participants took an average of 9.08 minutes with a standard deviation of  $\pm 1.37$  minutes to complete this procedure, 13 minutes was the maximum time that a participant took, and seven minutes was the minimum.

### 6.3. Results and conclusions

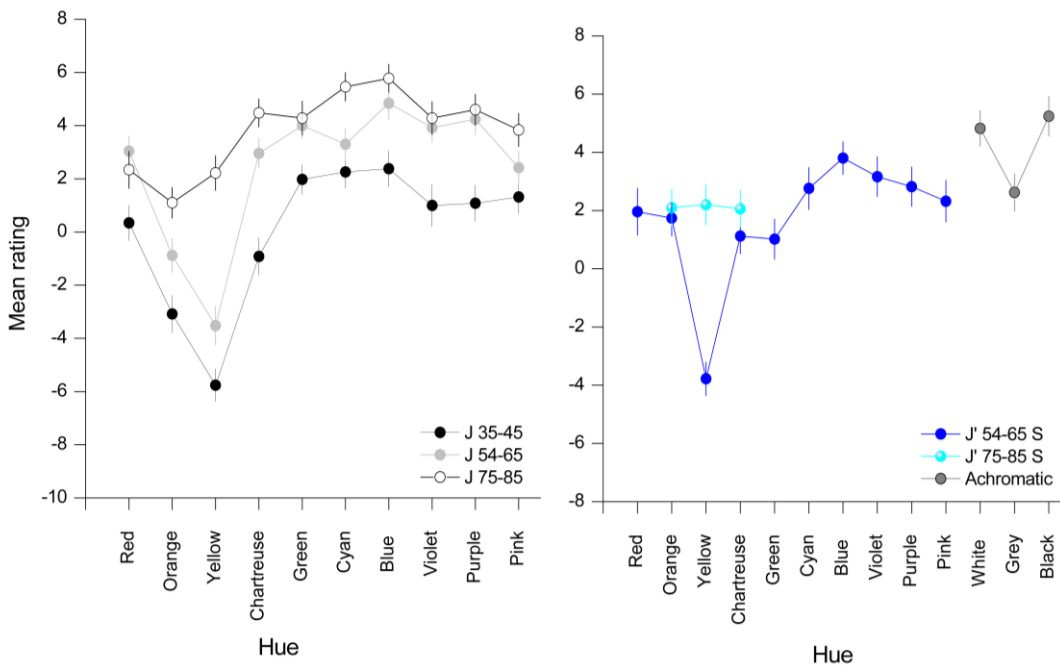


Figure 54 - Mean rating across all observers.

Figure 54 represents the mean ratings of different levels of lightness for the tested hues, on the right are the different saturation levels and the achromatic samples, and the error bars represent the standard error of the mean.

The peaks of this figure can be associated with highest-rated hues and depressions can be associated with the lowest-rated hues. Blue hues are the highest rated by observers and yellow, in particular, dark yellows are the lowest rated.

The samples with the highest rating and lowest are the same as the ones in Chapter 5 (Section 5.1) represented in Figure 32. The color sample S 6030-Y has the lowest rating of -5.76 and the color sample S 1020-B has the highest rating of 5.78.

Just like in Chapter 5 (Section 5.1) an attempt to verify if there were any differences between the ratings of males and females (Figure 55) was made. Statistical analysis was done, the full statistical analysis can be seen in Appendix X

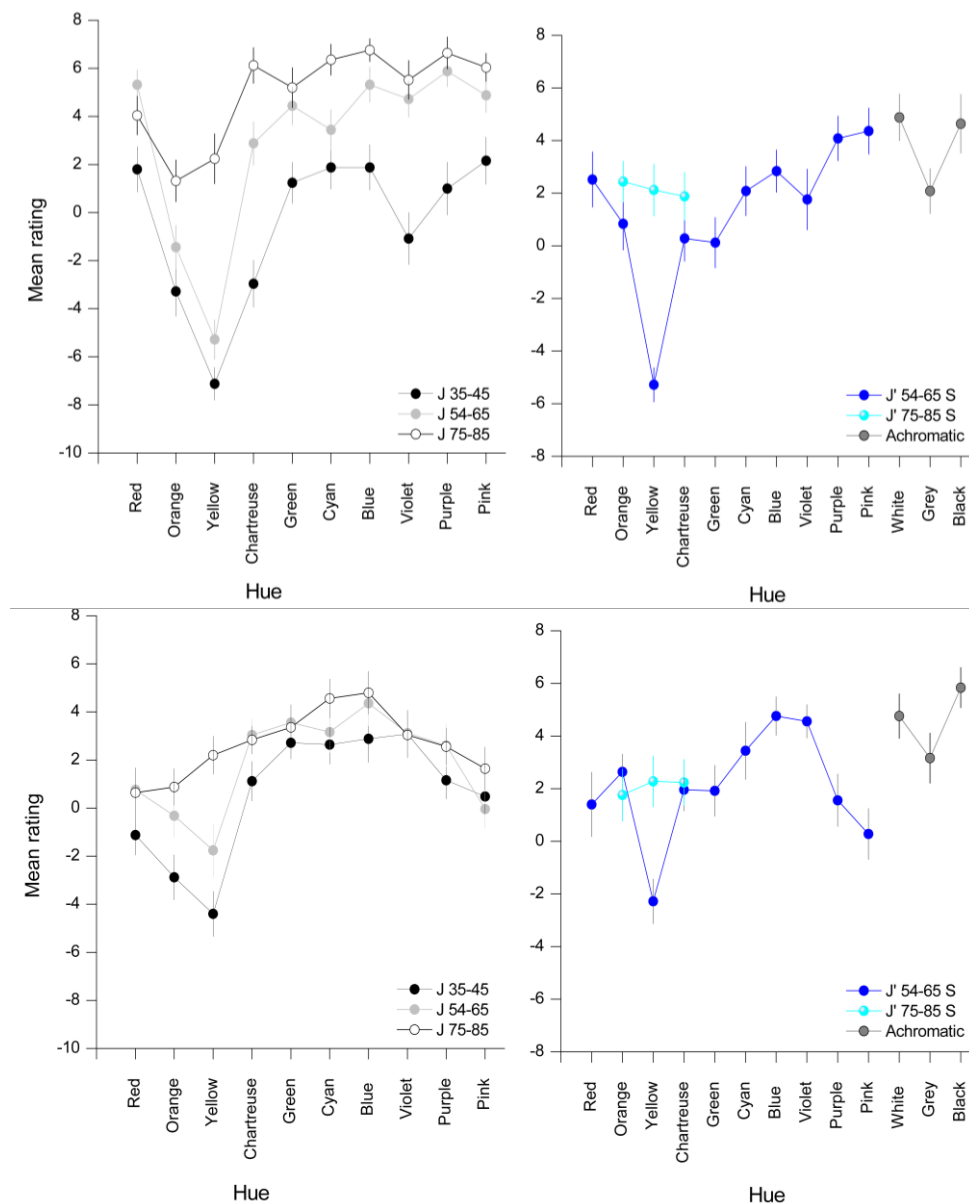


Figure 55 - Mean ratings across females (on the top); Mean ratings across males (on the bottom).

In five out of 10 samples with a lightness range of 75 to 85, statistical significant differences were found, those samples are S 1030-R, S 1030-R50B, S 1030-R30B, S 2020-G40Y, and S0525-R70B and represent red, purple, pink, chartreuse, and violet hues respectively they are illustrated in Figure 56. Females give higher mean ratings than males for these samples.



*Figure 56 - sRGB computational representation of samples S 1030-R, S 1030-R50B, S 1030-R30B, S 2020-G40Y, and S0525-R70B (from left to right).*

In four out of 10 samples with a lightness range of 54 to 65 statistical significant differences were found, those samples are S 3030-R, S 4030-Y, S 3030-R50B, and S 3030-R30B and represent red, yellow, purple, and pink hues respectively they are illustrated in Figure 57.

Higher ratings were given by females than by males for these samples, except for the yellow one.



*Figure 57 - sRGB computational representation of samples S 3030-R, S 4030-Y, S 3030-R50B, and S 3030-R30B (from left to right).*

In two out of 10 samples with a lightness range of 54 to 65 saturated, statistical significant differences were found, those samples are S 3060-Y and S 2050-R30B and represent yellow and pink hues respectively they are illustrated in Figure 58. For these samples, females give higher ratings for the pink hue sample and the opposite happens for the yellow hue sample.



*Figure 58 - sRGB computational representation of samples S 3060-Y and S 2050-R30B (from left to right).*

In four out of 10 samples with a lightness range of 35 to 45 statistical significant differences were found, those samples are S 5030-R, S 6030-Y, S 5540-G40Y, and S 6020-R70B and represent red, yellow, chartreuse, and violet hues respectively they are illustrated in Figure 59. For these samples, males give higher ratings, except for the red hue sample.



*Figure 59 - sRGB computational representation of samples S 5030-R, S 6030-Y, S 5540-G40Y, and S 6020-R70B (from left to right).*

#### **6.4. Discussion**

Higher ratings were found for blue hues and lower ratings for yellow hues. It is possible to make this conclusion because of the peaks and depressions that fall on these areas in Figure 54. The samples with the highest and the lowest rating values can be seen in Figure 32 and are the same as the ones even though slight differences in the methodology of this experiment were implemented. One important difference was the use of the anchoring technique which seemed to not influence participants' responses.

The blue hue color sample (S 2050-B) is on average the favorite of observers it has a lightness ranging from 75 to 85 as for the least favorite the yellow hue color sample (S 6030-Y) has a lightness level ranging from 35 to 45. When comparing the mean ratings from this experiment with the results in Figure 22C one common conclusion is that the same hues are preferred. Different techniques were used in Palmer et al. study 32 samples were displayed on a monitor placed 70 cm away with a gray background one at a time randomly, and in this study samples and scale were physical. This study tested two extra hues violet and pink. Also, the achromatic color samples were part of this experiment, making the total samples tested 46 [65].

Results show high mean rating values for the achromatic samples. Black is the preferred achromatic color sample followed by white and then gray.

To complete the analysis of this data a comparison between males and females was done significant statistical difference was found in some samples illustrated in Figure 56, Figure 57, Figure 58, and Figure 59 where they are divided by lightness and saturation levels, these results seem to indicate that different preferences between males and females exist in some samples.

No difference between males and females was found for the achromatic samples.

The results obtained in this experiment were similar to the ones in research papers about the topic previously mentioned in Chapter 3.

## 7. COLOR PREFERENCE FOR COLOR COMBINATIONS

### 7.1. Objective

The goal of this experiment is the same as the one in Chapter 5 (Section 5.2). Only this time it was possible to repeat samples when making the combinations.

### 7.2. Methods

#### Participants

The same participants who did the experiment described in Chapter 6 did this one.

#### Samples

This time multiple sets of samples were needed so that repetition of samples could be achieved. In total, 16 sets of 46 samples were made. The achromatic samples were included in this experiment.

A complete description of the selection and making process of the color samples is described in Chapter 3.

#### Procedure

The same board described in Chapter 6 was used and the center of the board was marked as a displaying reference.

Using black cardboard nine pieces in total with 38.5 cm of length, 28.3 cm of width, and 0.5 cm of height were made, 8 of them carried 2 sets of 46 samples each the extra one was used on top to secure the samples in place when transportation was necessary (Figure 60).

Four plastic lids with 39.7 cm of length, 29 cm of width, and 2.7 cm of height were used 2 cardboard pieces were placed in each lid, allowing transportation to be much easier (Figure 60).



Figure 60 - Lids and black cardboard used.

The same solux lamp was placed 40 cm from the standard gray board and luminance was measured with PR-650 SpectraScan® on Barium sulfate ( $\text{BaSO}_4$ ) for a square of 12 by 12 cm (Figure 37) using Equation 18 [43] and [43] and considering that  $\varepsilon_D$  is the angle with the perpendicular to the measuring surface and  $\cos \varepsilon_D = 1$  the illuminance was obtained, results can be found in Table 7. Another solux lamp was placed 40 cm from the cardboard with the samples.

The participant sat on a stool during the experiment. The  $\theta$  was the same as the one in Chapter 6.

The grids were presented in the same conditions described in Chapter 5 (Section 5.2) and were the same as shown in Figure 37. All participants ranked their choices of combination just like in the experiment mentioned.

Figure 61 shows how all the material used was assembled.

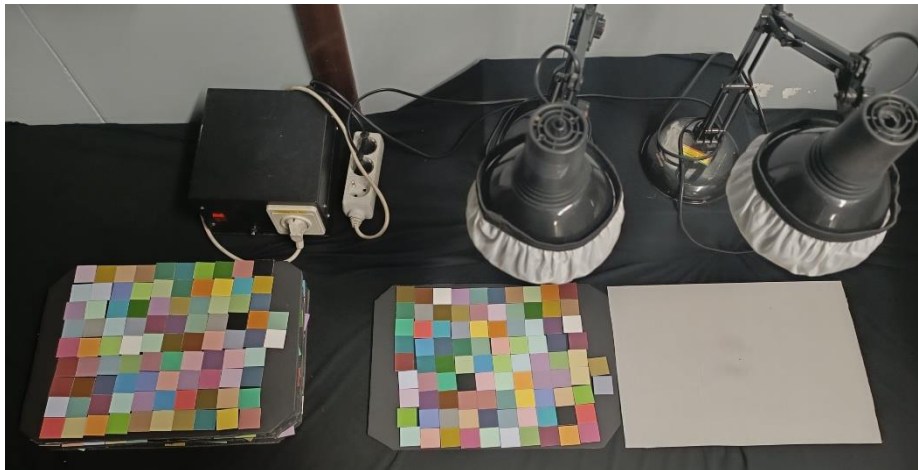


Figure 61 - Setup used.

Participants took an average of 8.64 minutes with a standard deviation of  $\pm 2.94$  minutes to complete this procedure, 20 minutes was the maximum time that a participant took, and four minutes was the minimum.

### 7.3. Results and conclusions

The same analysis described in Chapter 5 (Section 5.2) was done in this experiment.

- **1x1 grid**

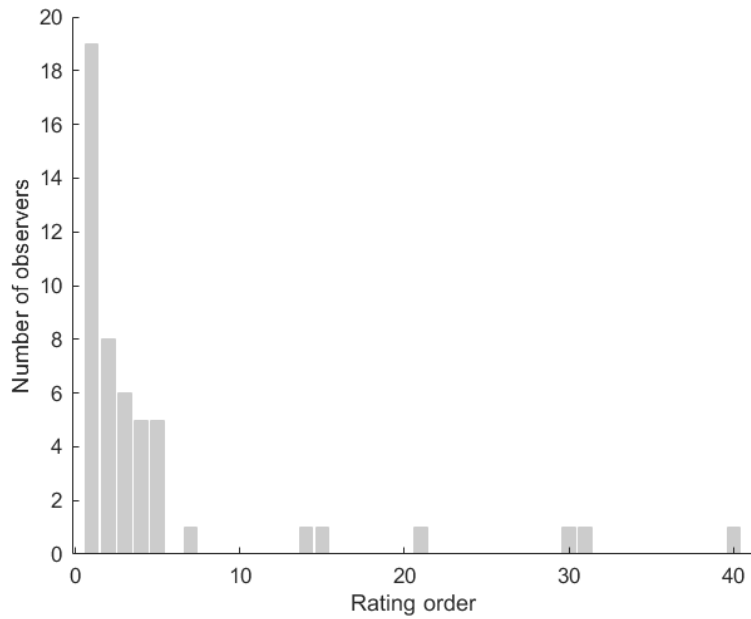


Figure 62 - Plot of the number of observers for the rating order.

Nineteen observers picked the color sample they rated the highest in the experiment described in Chapter 6. Eight, six, and five observers picked the second, third, fourth, and fifth highest-rated color respectively.

- **2x1 grid**

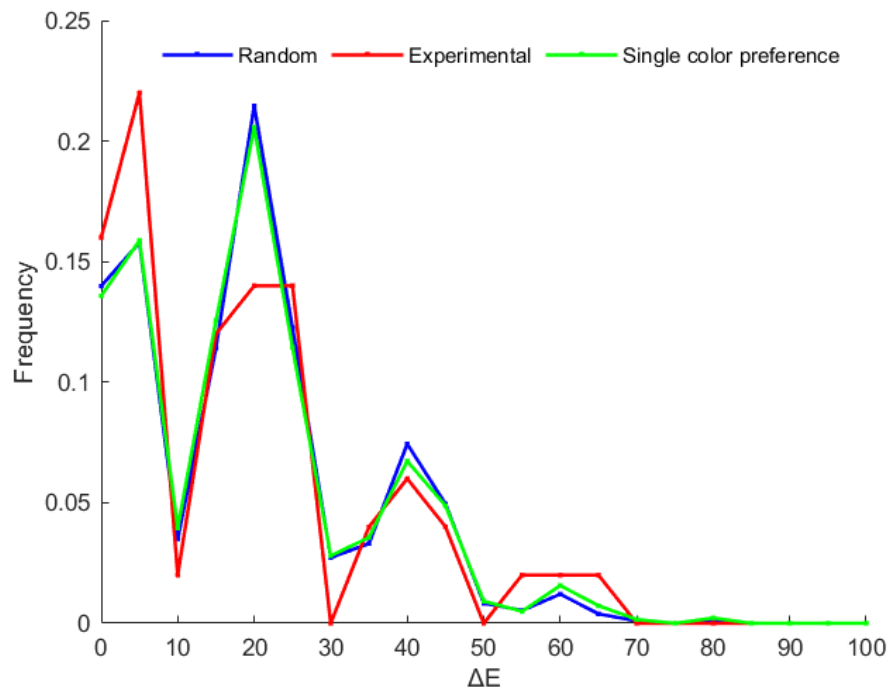


Figure 63 - Difference of color for the lightness axis.



Figure 63 represents the  $\Delta E$  of the J' axis for all three types of data on the x-axis and the frequency on the y-axis.

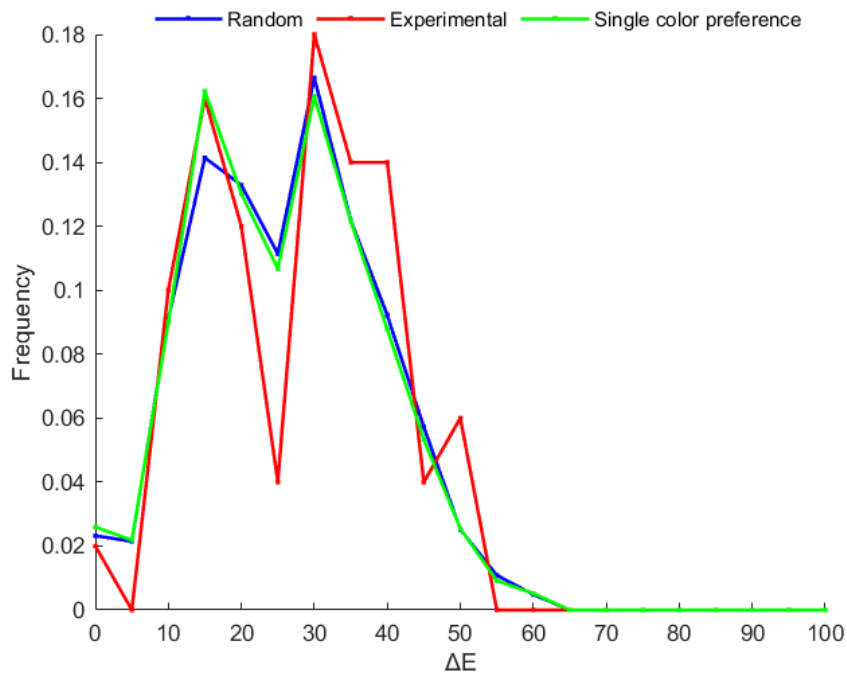


Figure 64 - Difference of color for the chromatic axis.

Figure 64 represents the  $\Delta E$  for the  $a'_M$  and  $b'_M$  for all three types of data on the x-axis and the frequency on the y-axis.

• **2x2 grid**

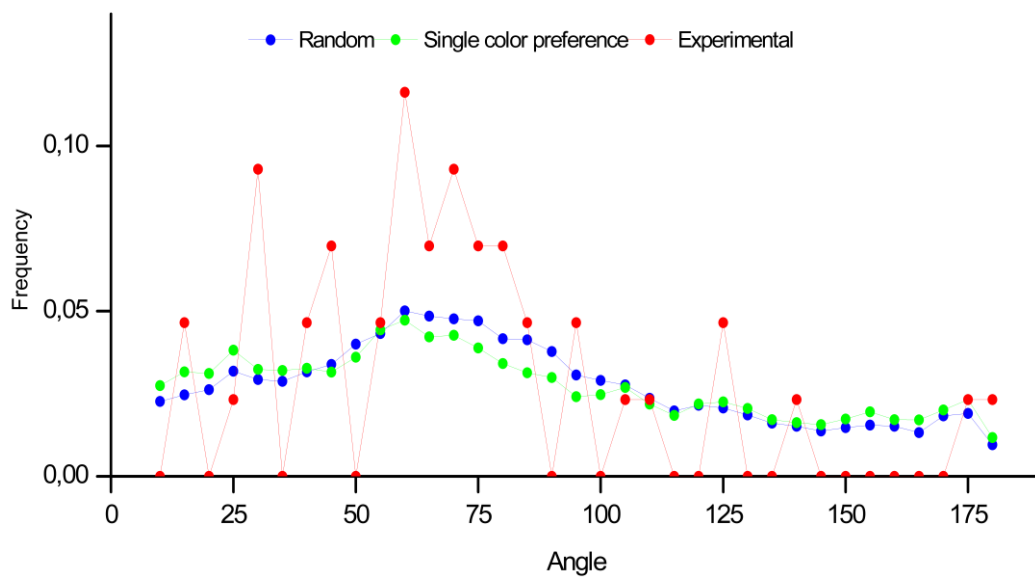


Figure 65 - Angle results for the 2x2 grid.

The average angle for the experimental data is 71 degrees, for the random data is 79 degrees, and for the random data based on the results of the single color preference experiment is 79 degrees.

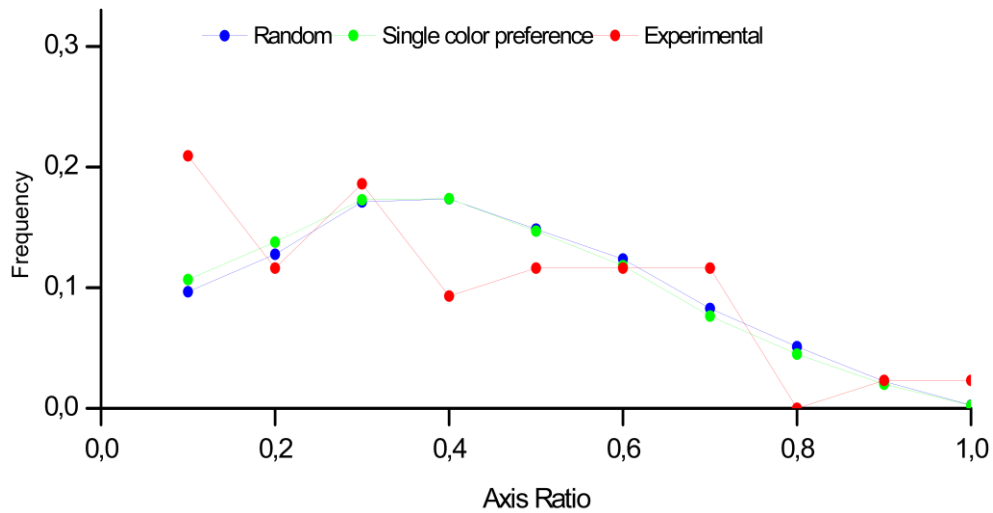


Figure 66 - Axis ratio results for the 2x2 grid.

The average axis ratio for the experimental data is 0.38, for the random data is 0.42, and for the random data based on the results of the single color preference experiment is 0.41.

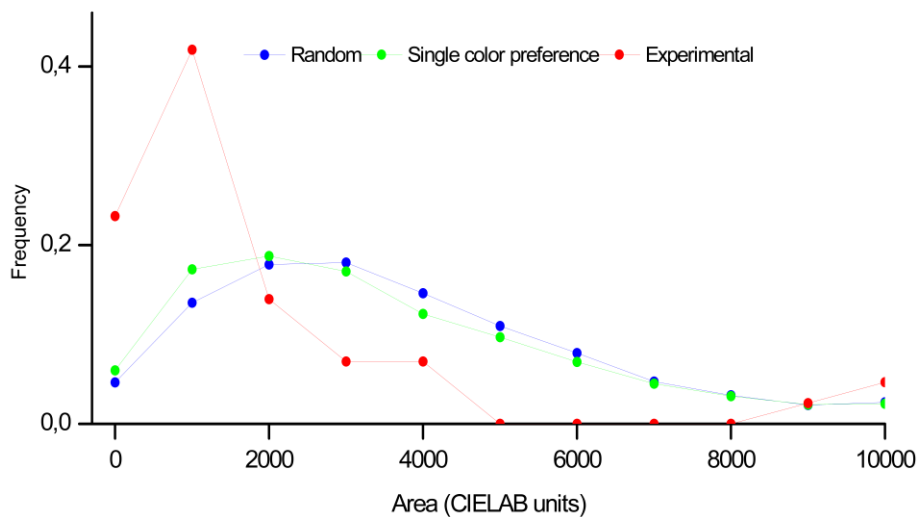


Figure 67 - Area results for the 2x2 grid.

The average area of the fitted ellipses for the experimental data is 1953 CIELAB units, for the random data is 3688 CIELAB units, and for the random data based on the results of the single color preference experiment is 3463 CIELAB units.

• **3x3 grid**

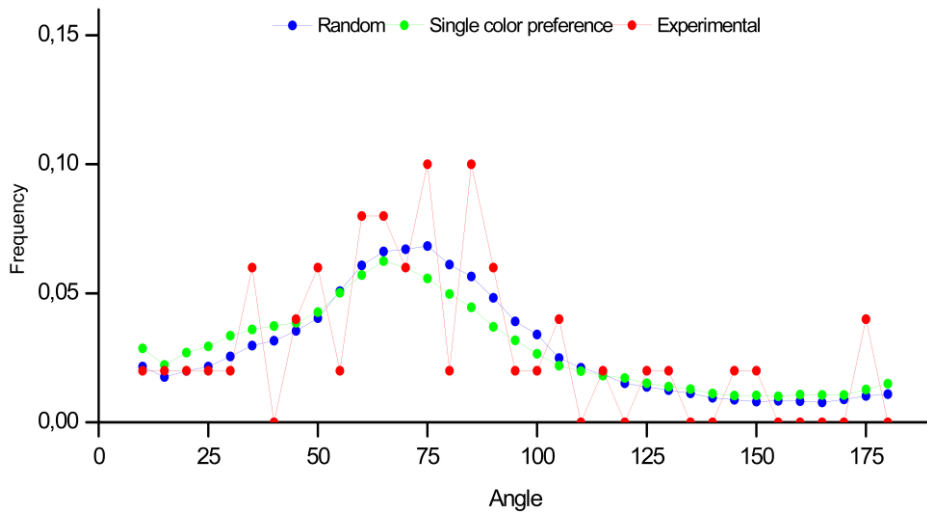


Figure 68 - Angle results for the 3x3 grid.

The average angle for the experimental data is 70 degrees, for the random data is 73 degrees, and for the random data based on the results of the single color preference experiment is 72 degrees.

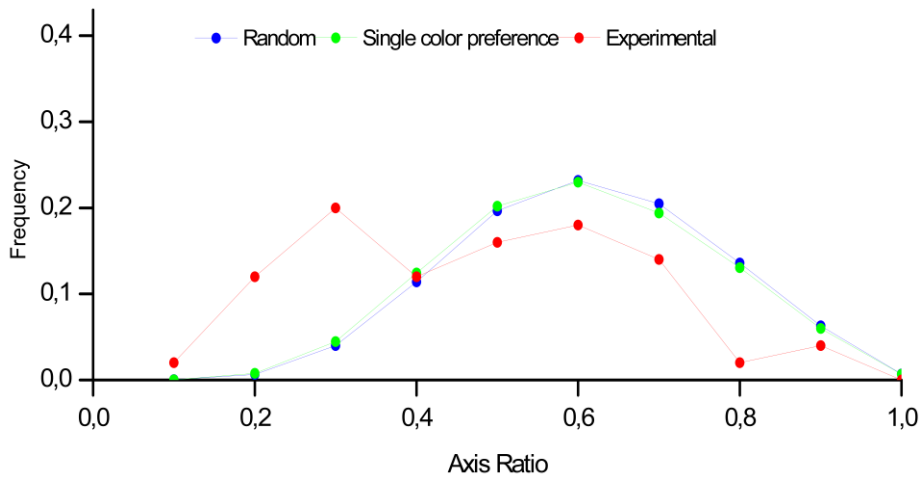


Figure 69 - Axis ratio results for the 3x3 grid.

The average axis ratio for the experimental data is 0.47, for the random data is 0.61, and for the random data based on the results of the single color preference experiment is 0.60.

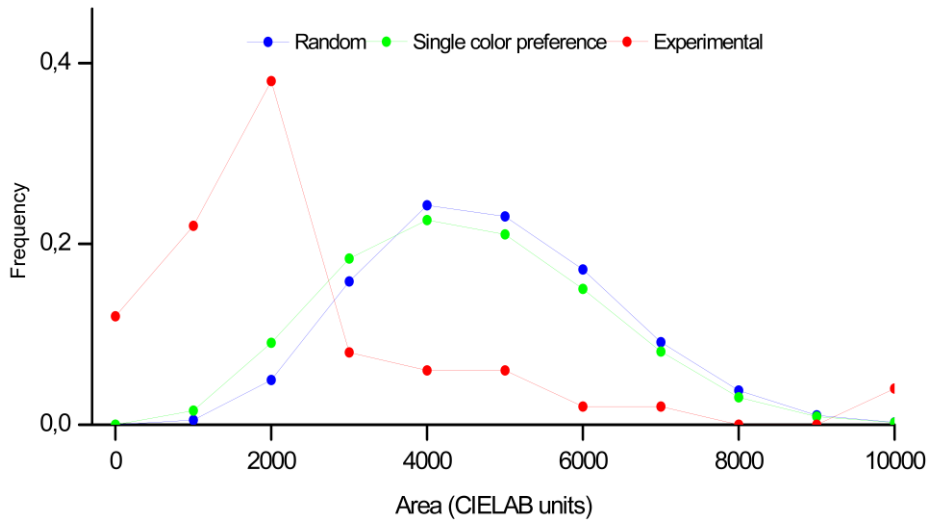


Figure 70 - Area results for the 3x3 grid.

The average area of the fitted ellipses for the experimental data is 2488 CIELAB units, for the random data is 4795 CIELAB units, and for the random data based on the results of the single color preference experiment is 4522 CIELAB units.

• **4x4 grid**

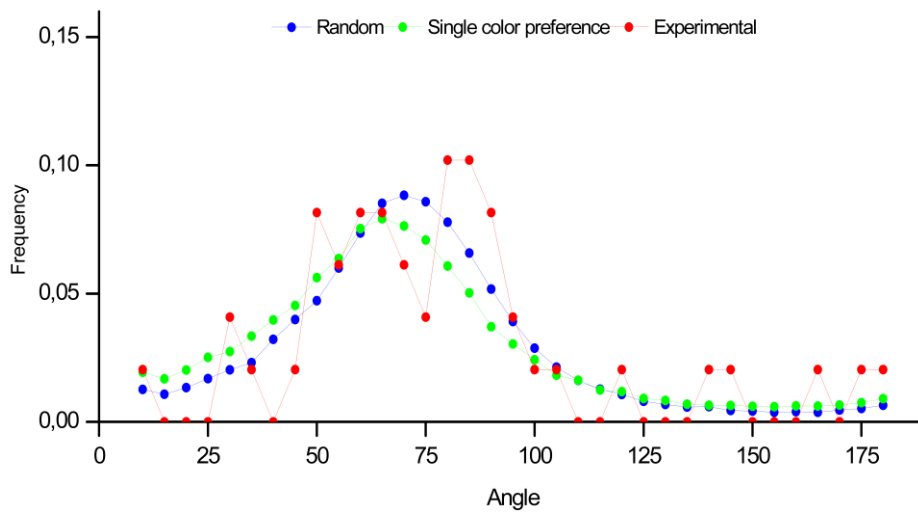


Figure 71 - Angle results for the 4x4 grid.

The average angle for the experimental data is 74 degrees, for the random data is 69 degrees, and for the random data based on the results of the single color preference experiment is 67 degrees.

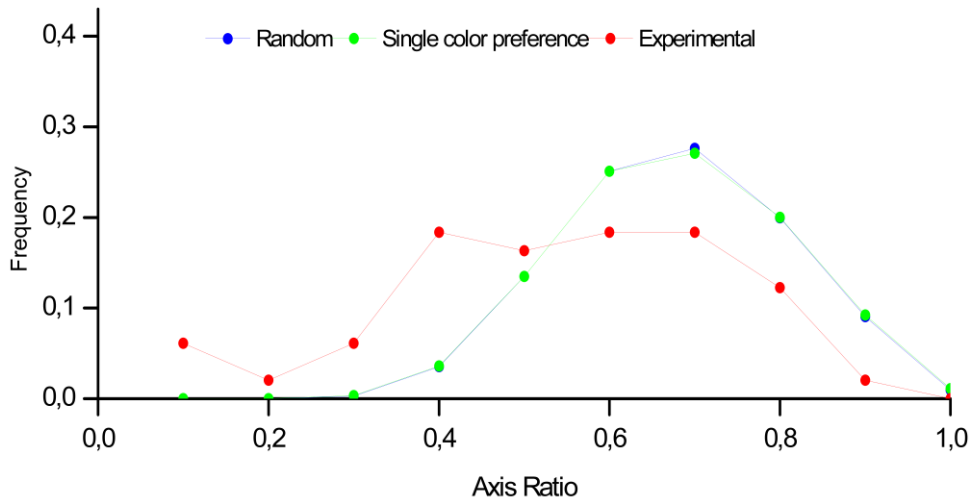


Figure 72 - Axis ratio results for the 4x4 grid.

The average axis ratio for the experimental data is 0.54, for the random data is 0.68, and for the random data based on the results of the single color preference experiment is 0.68.

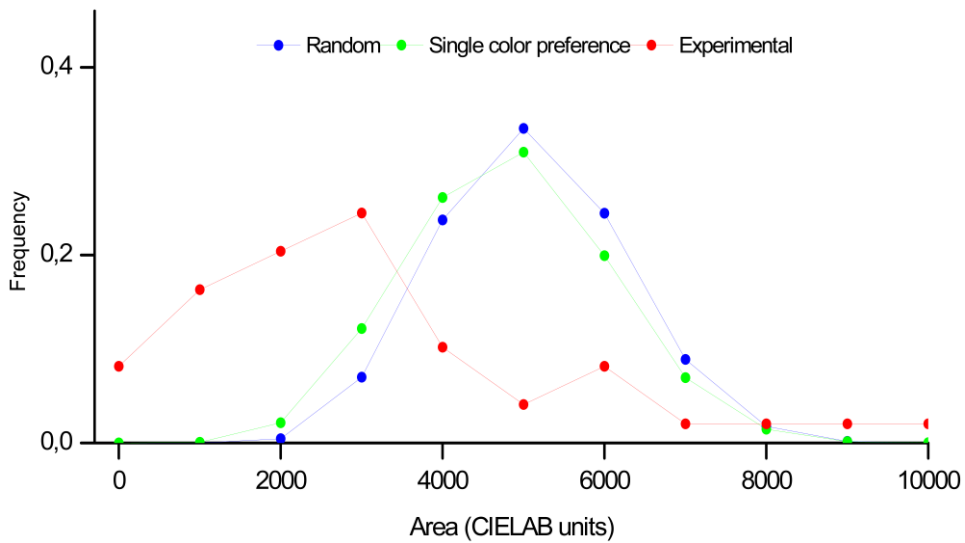
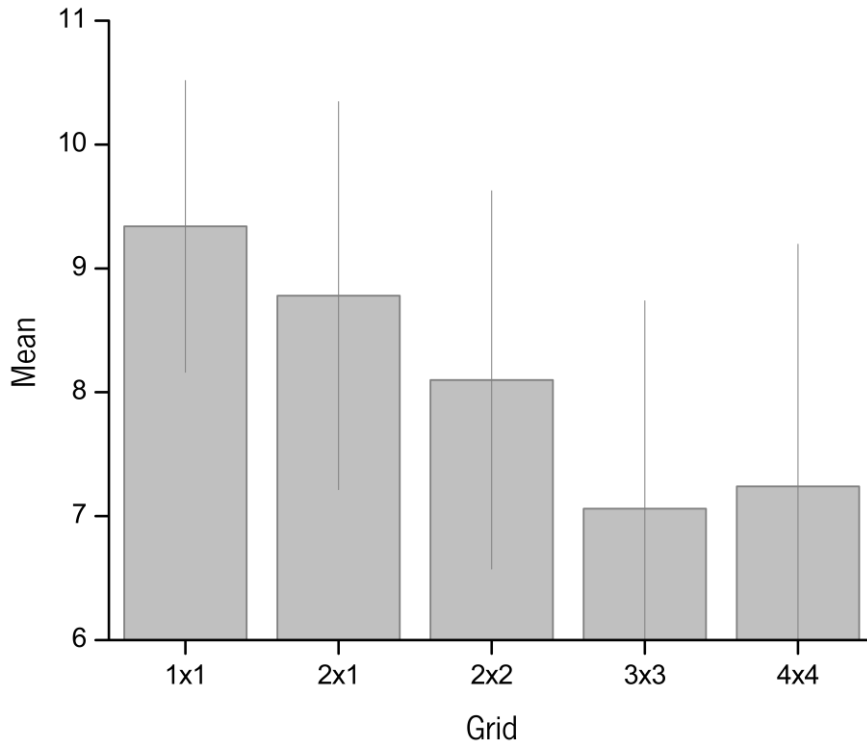


Figure 73 - Area results for the 4x4 grid.

The average area of the fitted ellipses for the experimental data is 3416 CIELAB units, for the random data is 5092 CIELAB units, and for the random data based on the results of the single color preference experiment is 4816 CIELAB units.



*Figure 74 - Mean satisfaction for each grid.*

Figure 74 shows the mean satisfaction for each grid and the error bars are the standard deviation, the y-axis scale range was defined from six to eight to improve data visualization but satisfaction was measured on a scale from one to 10. The average satisfaction for the 1x1 grid was 9.3 with a standard deviation of  $\pm 1.2$ , for the 2x1 grid was 8.3 with a standard deviation of  $\pm 1.6$ , for the 2x2 grid was 8.1 with a standard deviation of  $\pm 1.5$ , for the 3x3 grid was 7.1 with a standard deviation of  $\pm 1.7$ , and for the 4x4 grid was 7.2 with a standard deviation of  $\pm 2.0$ .

#### **7.4. Discussion**

The 1x1 grid results expressed in Figure 62 show that most participants when asked to pick their favorite color chose the ones rated the highest in the experiment of single colors preference experiment. In this case up to the fifth highest-rated color sample. This experiment was conducted on the same day that the color preference for single colors possibly this is a reason for the increase in the number of participants who picked the highest-rated color sample.

The 2x1 grid combinations seem to differ in lightness and chromaticity when analyzing the  $\Delta E$  expressed in Figure 63 and Figure 64.

The ellipses were calculated using the same scripts mentioned in Chapter 5 (Section 5.2) with some adjustments. The points fitted in the ellipses of the 2x2 grid occupied an average of 100% for all three types of data. The 3x3 grid occupied an average of 93.5% when the experimental data was used, 92.8% when randomly generated data was used, and 91.3% when randomly generated data based on the results of the single color preference experiment was used. The 4x4 grid occupied an average of 92% when the experimental data was used, 90.2% when randomly generated data was used, and 88.8% when randomly generated data based on the results of the single color preference experiment.

Montagner et al. found average angles of  $92^\circ$  for natural scenes,  $66^\circ$  for paintings ( $72^\circ$  for figurative and  $58^\circ$  for abstract paintings) [67]. When comparing the results of the three types of data of all grids they are closer to the ones of paintings, especially the figurative paintings.

Montagner et al. found an average axis ratio of 0.51 for natural scenes, 0.58 for paintings (0.56 for figurative and 0.6 for abstract paintings) [67]. When comparing these results to the one of the 2x2 grid they are closer to the ones of natural scenes for all three types of data, for the 4x4 grid they are closer to the ones of paintings especially abstract paintings for all three types of data, for 3x3 grid they are closer to the ones of paintings especially abstract paintings except in the experimental data where they are closer to natural scenes.

Montagner et al. found an average area of fitted ellipses of 1226 CIELAB units (range from 210 to 6613 CIELAB units) for natural scenes, 1338 CIELAB units (range from 124 to 5610 CIELAB units) for paintings [67]. When comparing the results of the three types of data of all grids they are closer to the ones of paintings.

The mean satisfaction of the combinations made is expressed in Figure 74. It decreases as the complexity of the combination increases, except for the 4x4 grid where the mean satisfaction slightly increases.

Both models fail to predict the combinations made by participants on some occasions results are similar but never truly close. This indicates that observers do not make combinations randomly and they do not use only individual color preferences to build their combinations.

Although individual color preference seems to affect in part the color combinations made it does not fully explain the results obtained.

There appear to be different aspects that affect color combinations that are not yet known.

## **8. EFFECTS OF ARTISTIC EDUCATION ON COLOR PREFERENCE FOR SINGLE COLORS**

### **8.1. Objective**

The goal of this experiment is to obtain the mean preference ratings of observers who have artistic education. These results will allow comparisons to be made with the results obtained in Chapter 6.

### **8.2. Methods**

#### Participants

Fifty observers, five males and 45 females, with a mean age of 24 (ranging from 18 to 52) did the experiment. They were for the most part students of the Faculty of Fine Arts of the University of Lisbon doing their bachelor's in painting, drawing, and design, also they were master's students of conservation of modern and contemporary art and a few Ph.D. students. Professors and attendees of a conference at the Faculty of Fine Arts of the University of Lisbon did these experiments most of their focus was on the conservation and restoration of works of art.

Informed consent (Appendix III and Appendix IV) was given to all participants and the experiment protocol respected the Declaration of Helsinki (1964, World Medical Association) and was approved by the Comissão de Ética para a Investigação em Ciências da Vida e da Saúde (CEICVS 052/2021) of the University of Minho.

All participants were tested using the Ishihara plates to ensure they had normal color vision, none of them presented with color deficiencies. This procedure happened before starting the experiment and one chandelier with the solux lamp served as illumination for the Ishihara plates. The data sheet used to register this information can be found in Appendix II.

#### Samples

This experiment used the same samples mentioned in Chapter 6.

#### Procedure

This experiment used the procedure described in Chapter 6.

Even though the experiment was done at the Faculty of Fine Arts of the University of Lisbon the setup was assembled so conditions were the same as the ones mentioned in Chapter 6.



Participants took an average of 9.23 minutes with a standard deviation of  $\pm 1.14$  minutes to complete this procedure, 13 minutes was the maximum time that a participant took, and seven minutes was the minimum.

### 8.3. Results and conclusion

Figure 75 represents the mean ratings of different levels of lightness for the tested hues, on the right are the different saturation levels and the achromatic samples, and the error bars represent the standard error of the mean.

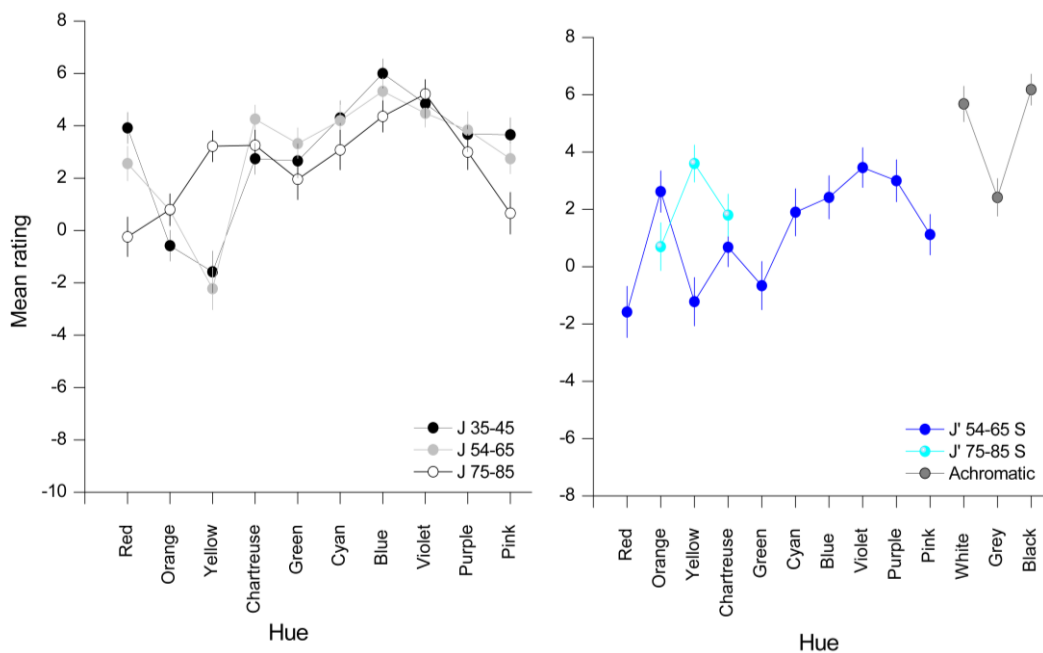


Figure 75 - Mean rating across all participants.

The black color sample, S 9000-N, is the highest rated by observers and S 4030-Y is the yellow color sample with the lowest rating. Figure 76 illustrates on the right the highest-rated sample with a mean rating of 6.18, and on the left is the lowest-rated sample with a mean rating of -2.22.



Figure 76 - sRGB computational representation of samples S 4030-Y (lowest rated) on the left and S 9000-N (highest rated) on the right.

An attempt to test if there were any differences between the ratings of observers with or without artistic education by comparing these results with the ones in Chapter 6. Statistical analysis was done, the full statistical analysis can be seen in Appendix XI.

In four out of 10 samples with a lightness range of 75 to 85 statistical significant differences were found, those samples are S 1030-R, S 1020-G, S 1020-B50G, S 1030-R30B and represent red, green, cyan, and pink hues respectively they are illustrated in Figure 77. Observers without artistic education have higher ratings than the ones with artistic education for these samples.



*Figure 77 - sRGB computational representation of samples S 1030-R, S 1020-G, S 1020-B50G, S1030-R30B (from left to right).*

In one out of 10 samples with a lightness range of 54 to 65 statistical significant difference was found, for the S 3030-G40Y sample, which corresponds to a chartreuse hue illustrated in Figure 78. Observers with artistic education have higher ratings than the ones without artistic education for this sample.



*Figure 78 - sRGB computational representation of sample S 3030-G40Y.*

In two out of 10 samples with a lightness range of 54 to 65 saturated statistical significant differences were found, those samples are S 1060-R and S 3060-Y and represent red and yellow hues respectively they are illustrated in Figure 79. Observers without artistic education have higher ratings for the red hue sample and the opposite happens for the yellow hue sample.



*Figure 79 - sRGB computational representation of samples S 1060-R, S 3060-Y (from left to right).*

In eight out of 10 samples with a lightness range of 35 to 45 statistical significant differences were found, those samples are S 5030-R and S 6030-Y40R, S 6030-Y, S 5540-G40Y, S 5030-B50G, S 6020-R70B and S 5030-R50B, S5030-R30B and represent red, orange, yellow, chartreuse, cyan, violet, purple and pink hues respectively they are illustrated in Figure 80. Observers with artistic education have higher ratings than the ones without artistic education for these samples.



*Figure 80 - sRGB computational representation of samples S 5030-R and S 6030-Y40R, S 6030-Y, S 5540-G40Y, S 5030-B50G, S 6020-R70B and S 5030-R50B, S5030-R30B (from left to right).*

#### **8.4. Discussion**

Overall mean ratings of observers with artistic education give higher ratings than observers without artistic education. When comparing the results of Figure 75 and Figure 54 the patterns for the hues are similar but observers with artistic education prefer color samples with lightness levels ranging from 35 to 45, this result is verified by statistics given the fact that this lightness range is the one with the highest amount of samples that had statistical significant difference. All the samples where statistical significance difference was found are illustrated in Figure 78, Figure 77, Figure 79, and Figure 80.

The achromatic samples follow the same patterns in both types of observers with black being rated the highest followed by gray being the lowest rated.

Black is the sample rated the highest closely followed by the S 6020-B blue hue sample with an average rating of 6, for observers with artistic education. The yellow hue sample (S 4030-Y) is the lowest rated by observers with artistic education.

Observers with artistic education took on average slightly longer to complete this experiment.

Participants with artistic education said they found it hard to rate colors on the negative side of the scale this may explain why their mean ratings are higher than participants without artistic education or maybe this type of education plays a role in preference that is not yet known.

## 9. EFFECTS OF ARTISTIC EDUCATION ON COLOR PREFERENCE FOR COLOR COMBINATIONS

### 9.1. Objective

The goal of this experiment is to study the properties of color combinations preferred by observers with artistic education.

### 9.2. Methods

#### Participants

The same participants mentioned in Chapter 8 did this experiment.

#### Samples

This experiment used the same color samples mentioned in Chapter 7.

#### Procedure

This experiment used the procedure described in Chapter 7.

Participants took an average of 10.02 minutes with a standard deviation of  $\pm 3.3$  minutes to complete this procedure, 20 minutes was the maximum time that a participant took, and 5 minutes was the minimum.

### 9.3. Results and conclusion

The same analysis described in Chapter 5 (Section 5.2) was done in this experiment

- **1x1 grid**

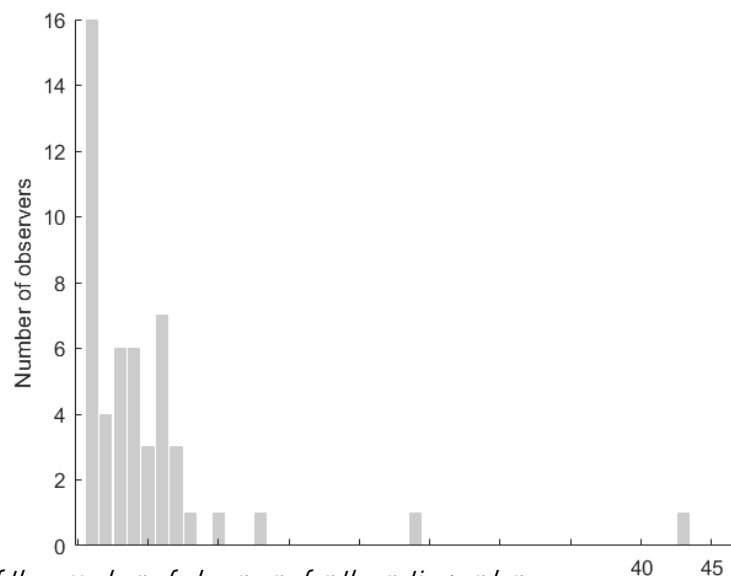


Figure 81 - Plot of the number of observers for the rating order.

Sixteen observers picked the color sample they rated the highest in the experiment described in Chapter 8.

- **2x1 grid**

To analyze the 2x1 grid the color difference between the two color samples picked was calculated using Equation 16.

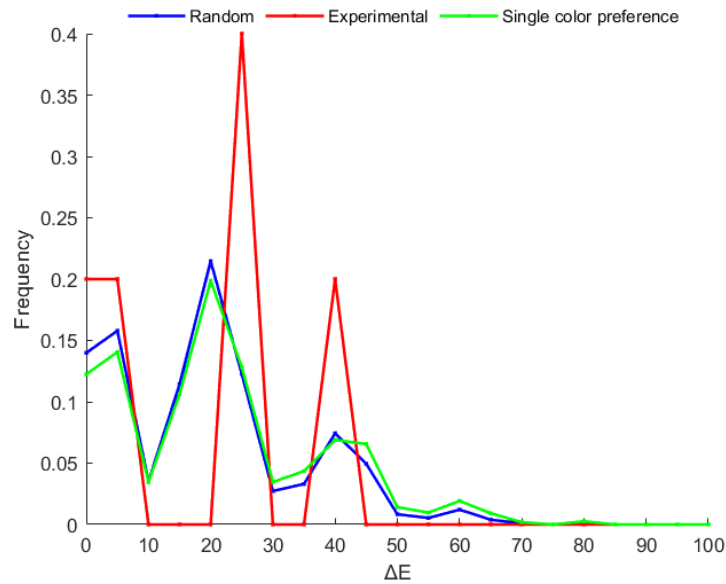


Figure 82 - Color difference for the lightness axis.

Figure 82 represents the  $\Delta E$  of the  $J'$  axis for all three types of data on the x-axis and the frequency on the y-axis. The  $\Delta E'_{J'}$  value most frequently picked is the 30 for observers with artistic education.

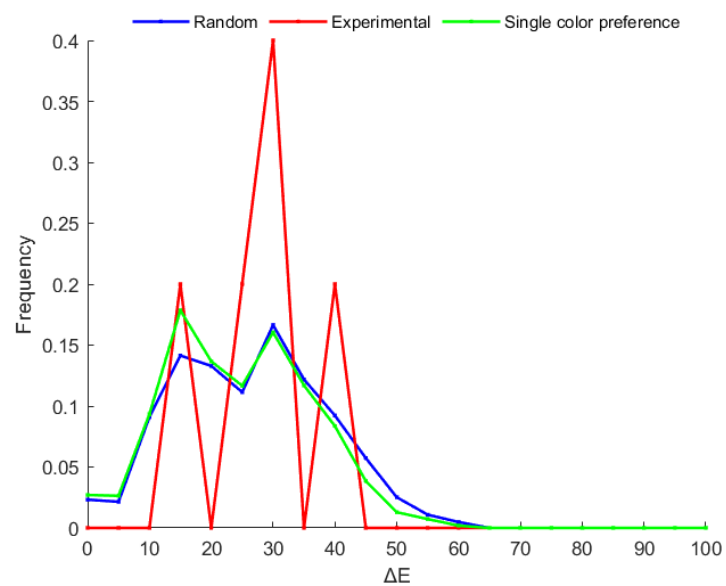


Figure 83 - Color difference for the chromatic axis.

Figure 83 represents the  $\Delta E$  for the  $a'_M$  and  $b'_M$  for all three types of data on the x-axis and the frequency on the y-axis. The  $\Delta E$  value most frequently picked is the 30 for observers with artistic education.

- **2x2 grid**

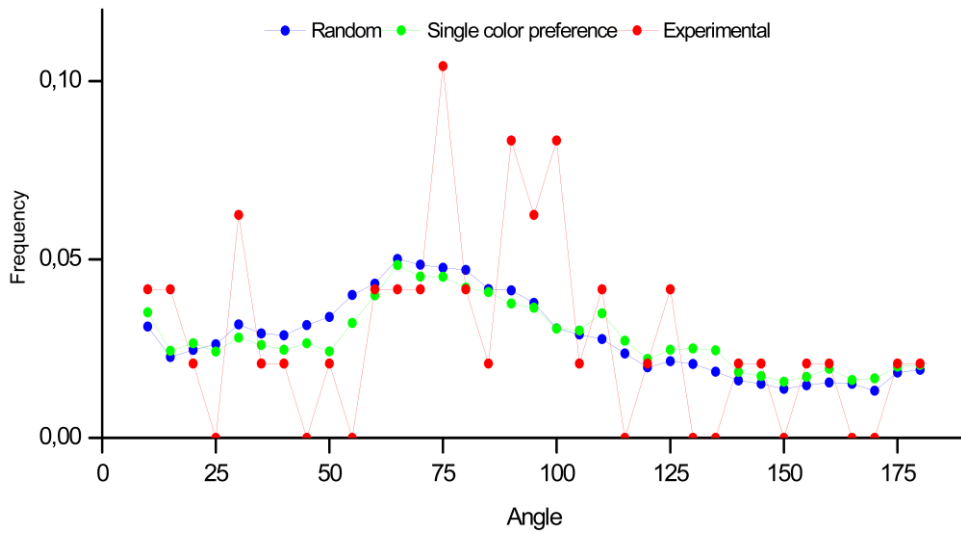


Figure 84 - Angle results for the 2x2 grid.

The average angle for the experimental data is 78 degrees, for the random data is 79 degrees, and for the random data based on the results of the single color preference experiment is 83 degrees.

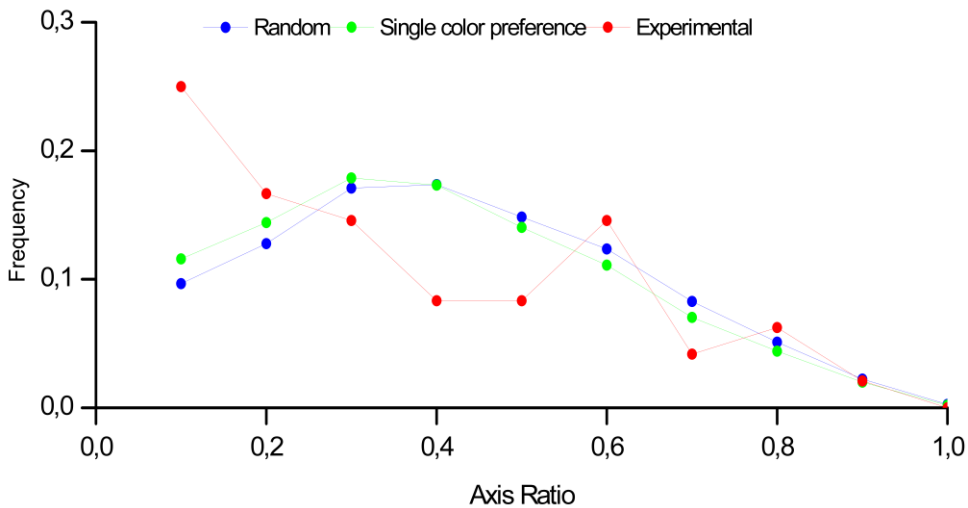


Figure 85 - Axis ratio results for the 2x2 grid.

The average axis ratio for the experimental data is 0.35, for the random data is 0.42, and for the random data based on the results of the single color preference experiment is 0.40.

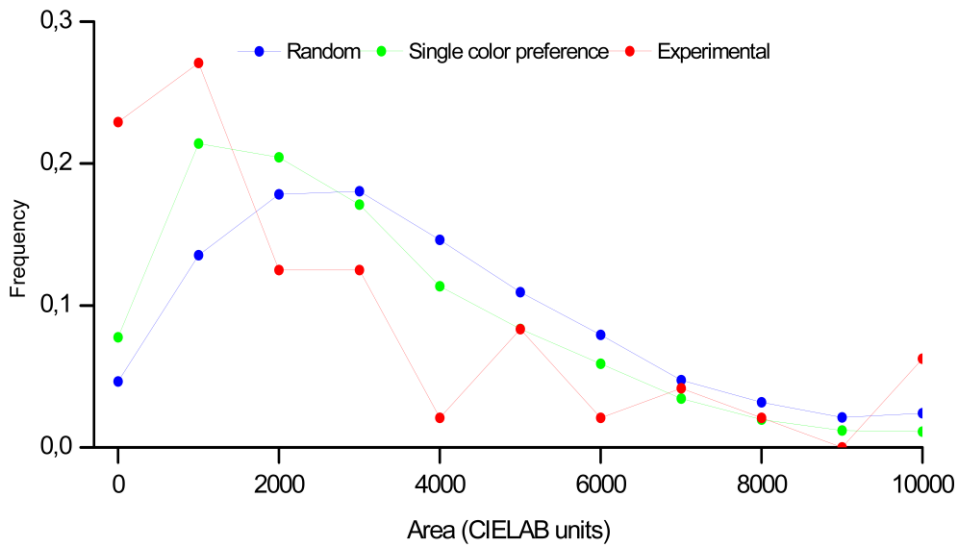


Figure 86 - Area results for the 2x2 grid.

The average area of the fitted ellipses for the experimental data is 2742 CIELAB units, for the random data is 3688 CIELAB units, and for the random data based on the results of the single color preference experiment is 2991 CIELAB units.

• **3x3 grid**

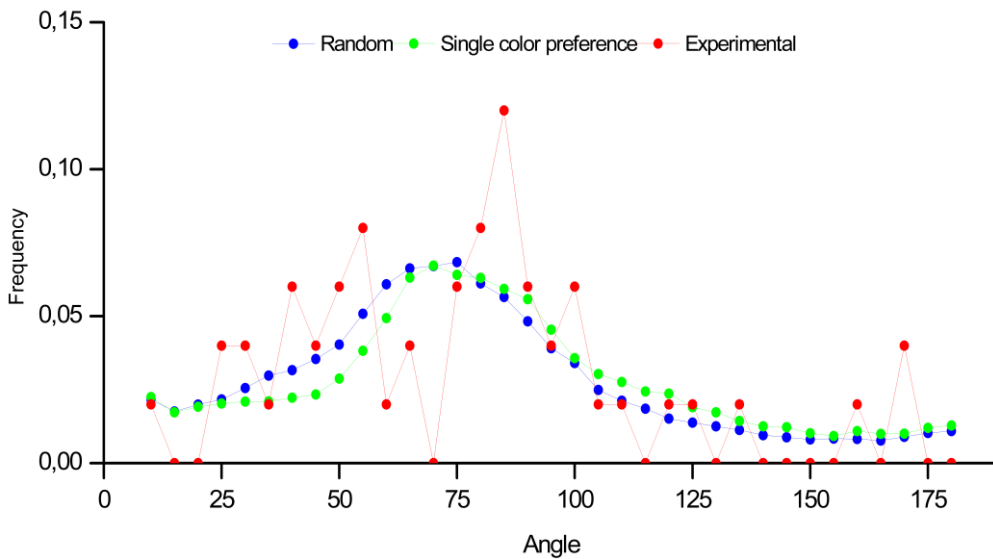


Figure 87 - Angle results 3x3 grid.

The average angle for the experimental data is 72 degrees, for the random data is 73 degrees, and for the random data based on the results of the single color preference experiment is 78 degrees.

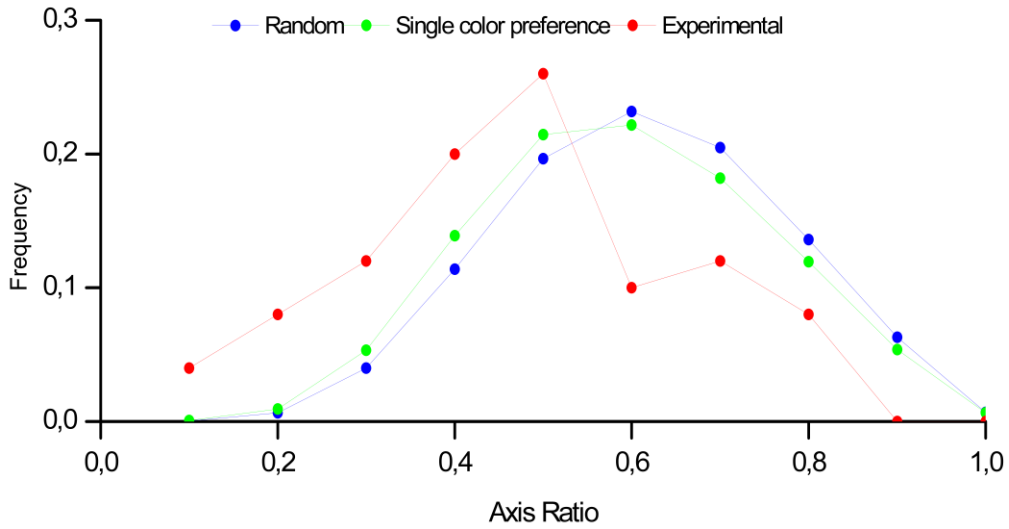


Figure 88 - Axis ratio results for the 3x3 grid.

The average axis ratio for the experimental data is 0.47, for the random data is 0.61, and for the random data based on the results of the single color preference experiment is 0.59.

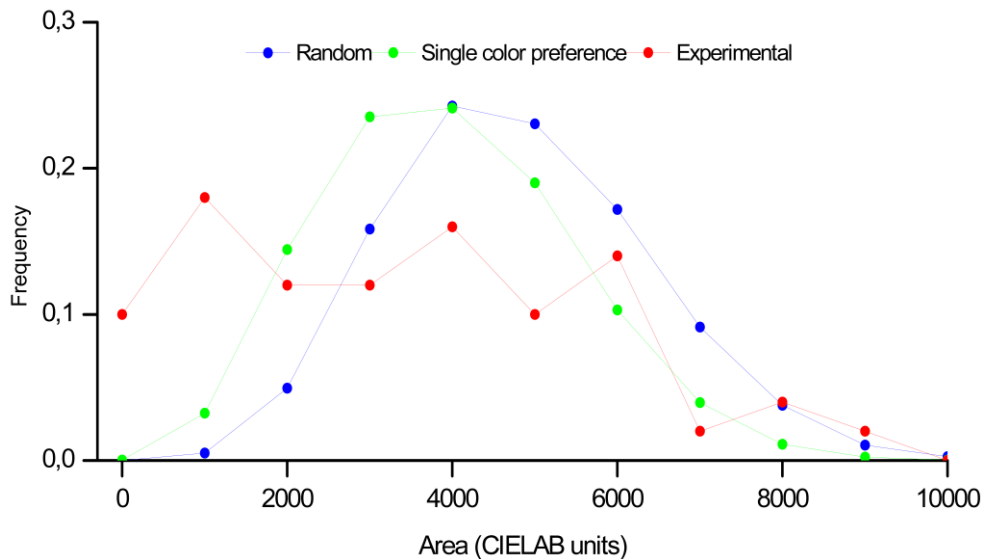


Figure 89 - Area results for the 3x3 grid.

The average area of the fitted ellipses for the experimental data is 3372 CIELAB units, for the random data is 4795 CIELAB units, and for the random data based on the results of the single color preference experiment is 3951 CIELAB units.



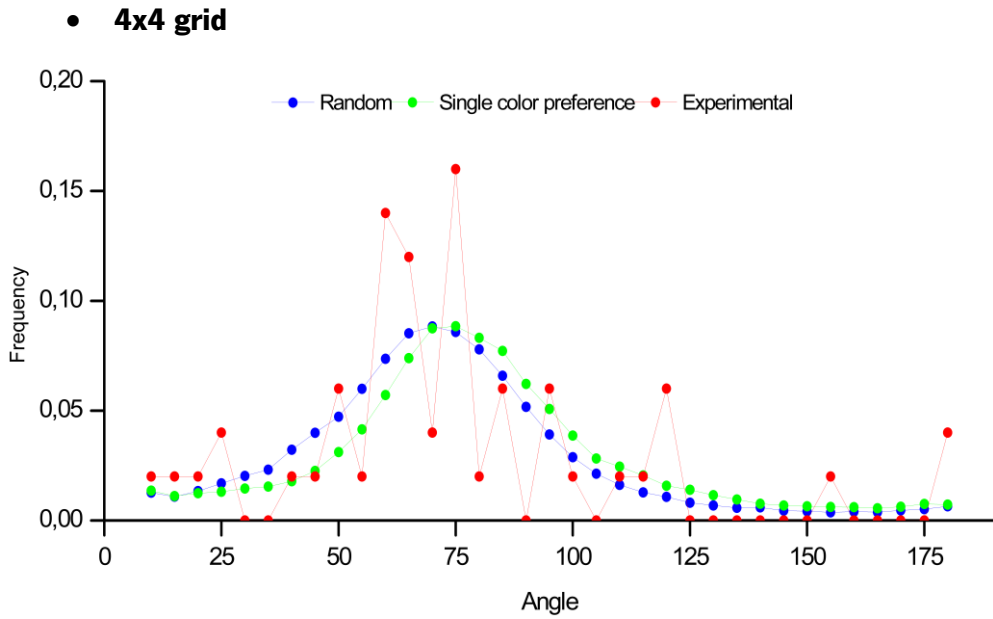


Figure 90 - Angle results for the 4x4 grid.

The average angle for the experimental data is 70 degrees, for the random data is 68 degrees, and for the random data based on the results of the single color preference experiment is 76 degrees

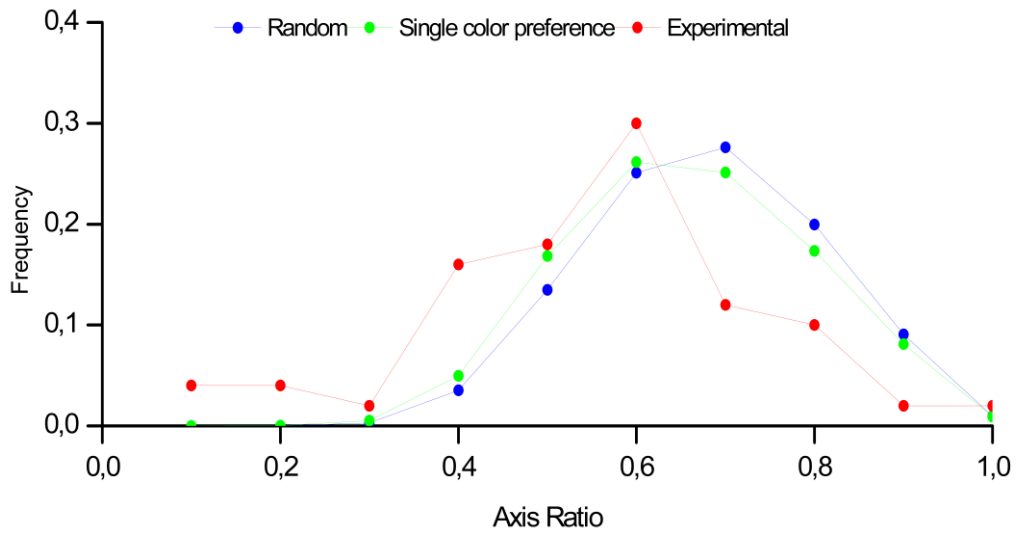


Figure 91 - Axis ratio results for the 4x4 grid.

The average axis ratio for the experimental data is 0.55, for the random data is 0.67, and for the random data based on the results of the single color preference experiment is 0.66.

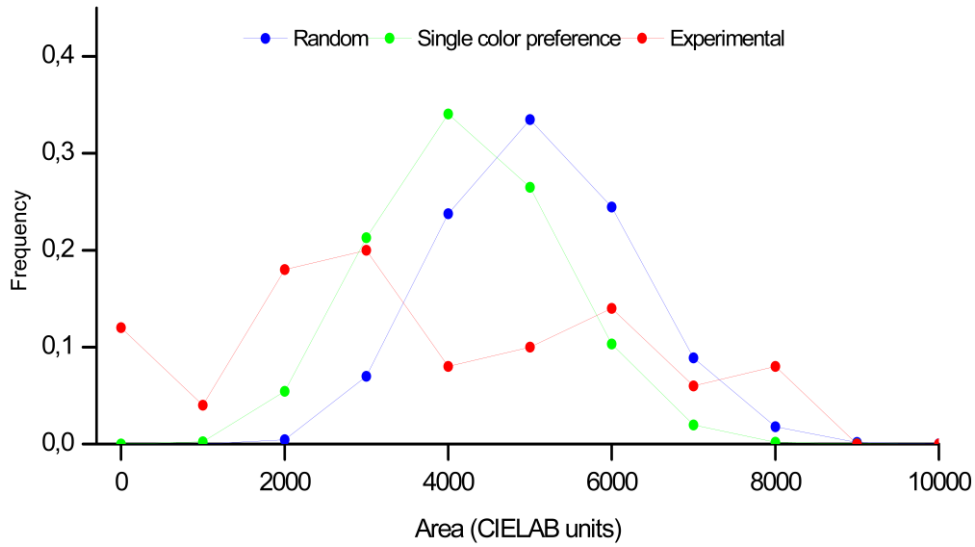


Figure 92 - Area results for the 4x4 grid.

The average area of the fitted ellipses for the experimental data is 3743 CIELAB units, for the random data is 5092 CIELAB units, and for the random data based on the results of the single color preference experiment is 4207 CIELAB units.

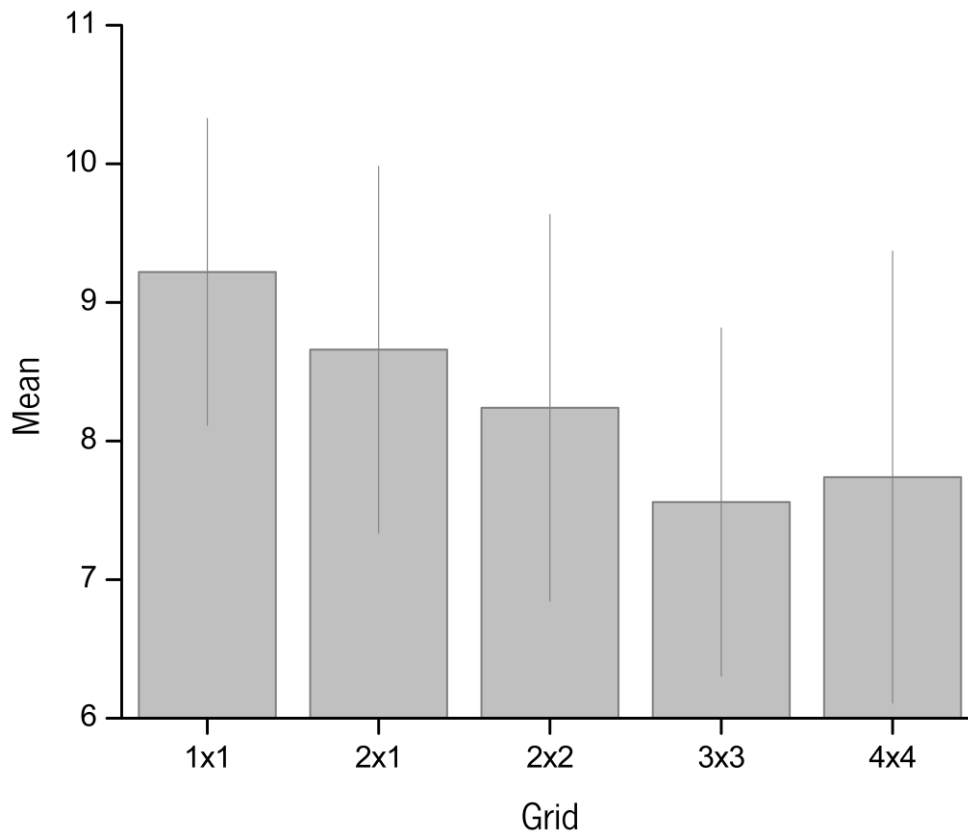


Figure 93 - Mean satisfaction for each grid.

Figure 93 shows the mean satisfaction for each grid and the error bars are the standard deviation, the y-axis scale range was defined from six to eight to improve data visualization but

satisfaction was measured on a scale from one to 10. The average satisfaction for the 1x1 grid for the 50 observers was 9.2 with a standard deviation of  $\pm 1.1$ , for the 2x1 grid for the 50 observers was 8.7 with a standard deviation of  $\pm 1.3$ , for the 2x2 grid was 8.2 with a standard deviation of  $\pm 1.4$ , for the 3x3 grid was 7.6 with a standard deviation of  $\pm 1.3$ , and for the 4x4 grid was 7.7 with a standard deviation of  $\pm 1.6$ .

#### **9.4. Discussion**

The 1x1 grid results expressed in Figure 81 show that less than half of participants when asked to pick their favorite color chose the ones rated the highest in the experiment of single colors preference.

The ellipses were calculated using the same scripts mentioned in Chapter 5 (Section 5.2) with some adjustments. The points fitted in the ellipses of the 2x2 grid occupied an average of 100% for all three types of data. The 3x3 grid occupied an average of 94% when the experimental data was used, 92.8% when randomly generated data was used, and 90.9% when randomly generated data based on the results of the results of the single color preference experiment was used. For the 4x4 grid occupied an average of 92.7% when the experimental data was used, 90.2% when randomly generated data was used, and 88.8% when randomly generated data based on the results of the single color preference experiment was used.

Montagner et al. found average angles of  $92^\circ$  for natural scenes,  $66^\circ$  for paintings ( $72^\circ$  for figurative and  $58^\circ$  for abstract paintings) [67]. When comparing the results of the three types of data of all grids they are closer to the ones of paintings, especially the figurative paintings.

Montagner et al. found an average axis ratio of 0.51 for natural scenes, 0.58 for paintings (0.56 for figurative and 0.6 for abstract paintings) [67]. When comparing these results to the ones of all grids of the experimental data they are closer to the natural scene, except for the 4x4 grid closer to figurative paintings.

Montagner et al. found an average area of fitted ellipses of 1226 CIELAB units (range from 210 to 6613 CIELAB units) for natural scenes, 1338 CIELAB units (range from 124 to 5610 CIELAB units) for paintings [67]. When comparing the results of the three types of data of all grids they are closer to the ones of paintings.

The experimental data of observers with and without artistic education present some differences. For 2x2 grid observers with artistic education have higher average angle and area

values but lower average axis ratio values. For the 3x3 grid observers with artistic education higher average values of all three variables. For the 4x4 grid observers with artistic education higher average area and axis ratio values but lower average angle values.

Participants with artistic education take longer to make all combinations a reason for that may be that they think more carefully about the choices they make.

The mean satisfaction of the combinations made is expressed in Figure 93. It decreases as the complexity of the combination increases, except for the 4x4 grid where the mean satisfaction slightly increases. This result is the same as the one of observers without artistic education (Figure 74).

Just like in the observers without artistic education mentioned in Chapter 7, both models fail to predict the combinations made by participants on some occasions results are similar but never truly close. This indicates that observers do not make combinations randomly and they do not use only individual color preferences to build their combinations.

Although individual color preference seems to affect in part the color combinations made it does not fully explain the results obtained.

There appear to be different aspects that affect color combinations that are not yet known and the type of education may be one of them.

## **10. EFFECTS OF RED-GREEN COLOR VISION DEFICIENCIES ON COLOR PREFERENCE FOR SINGLE COLORS**

### **10.1. Objective**

The goal of this experiment was to obtain the color preference ratings for color samples when using a population of dichromats.

### **10.2. Methods**

#### Participants

Five participants with a mean age of 27 (ranging from 23 to 32 years) did this experiment. Participants were dichromats previously diagnosed that are often included in experiments conducted in the Color Science Laboratory of the University of Minho. Out of them, two were deuteranopes, and three protanopes

Informed consent (Appendix III and Appendix IV) was given to all participants and the experiment protocol respected the Declaration of Helsinki (1964, World Medical Association) and was approved by the Comissão de Ética para a Investigação em Ciências da Vida e da Saúde (CEICVS 052/2021) of the University of Minho.

#### Samples

Forty-six samples were used. A complete description of the selection and making process of the color samples is described in Chapter 4.

#### Procedure

The same procedure described in Chapter 6 was used.

Participants took an average of 9.70 minutes with a standard deviation of  $\pm 2.43$  minutes to complete this procedure, 14 minutes was the maximum time that a participant took, and eight minutes was the minimum.

### **10.3. Results and conclusions**

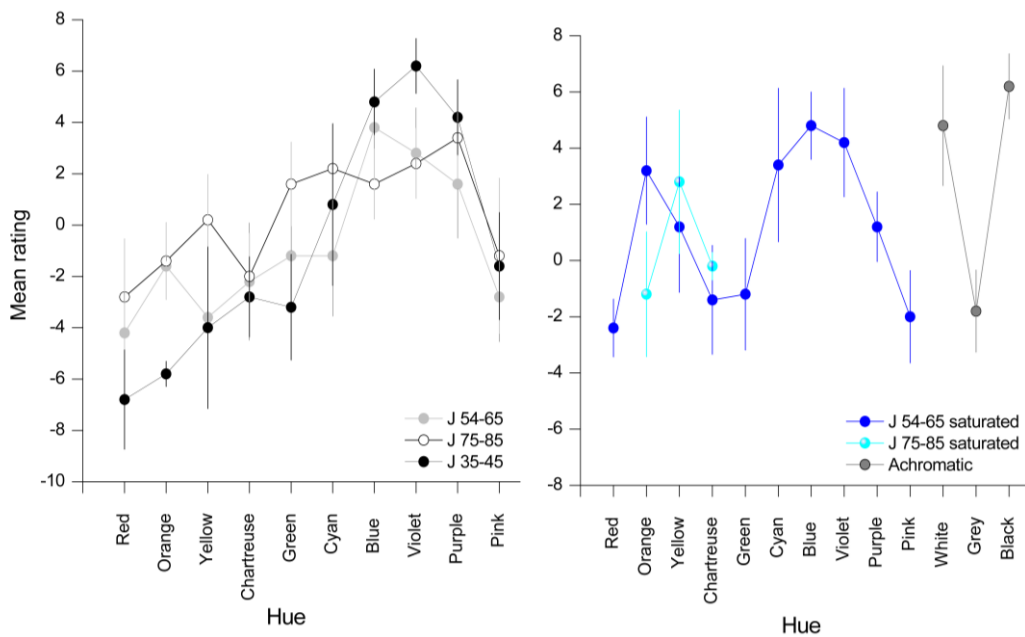


Figure 94 - Mean ratings across all dichromats.

Figure 94 represents the mean rating of the dichromats. The x-axis represents the hues tested, the y-axis represents the mean rating, and the error bars represent the standard error of the mean.

To better understand the differences between the two types of dichromats the same plot was done but for each particular case. These plots can be seen in Figure 95 where the mean rating of protanopes and deuteranopes is expressed. The x-axis represents the hues tested, the y-axis represents the mean rating, and the error bars represent the standard error of the mean.

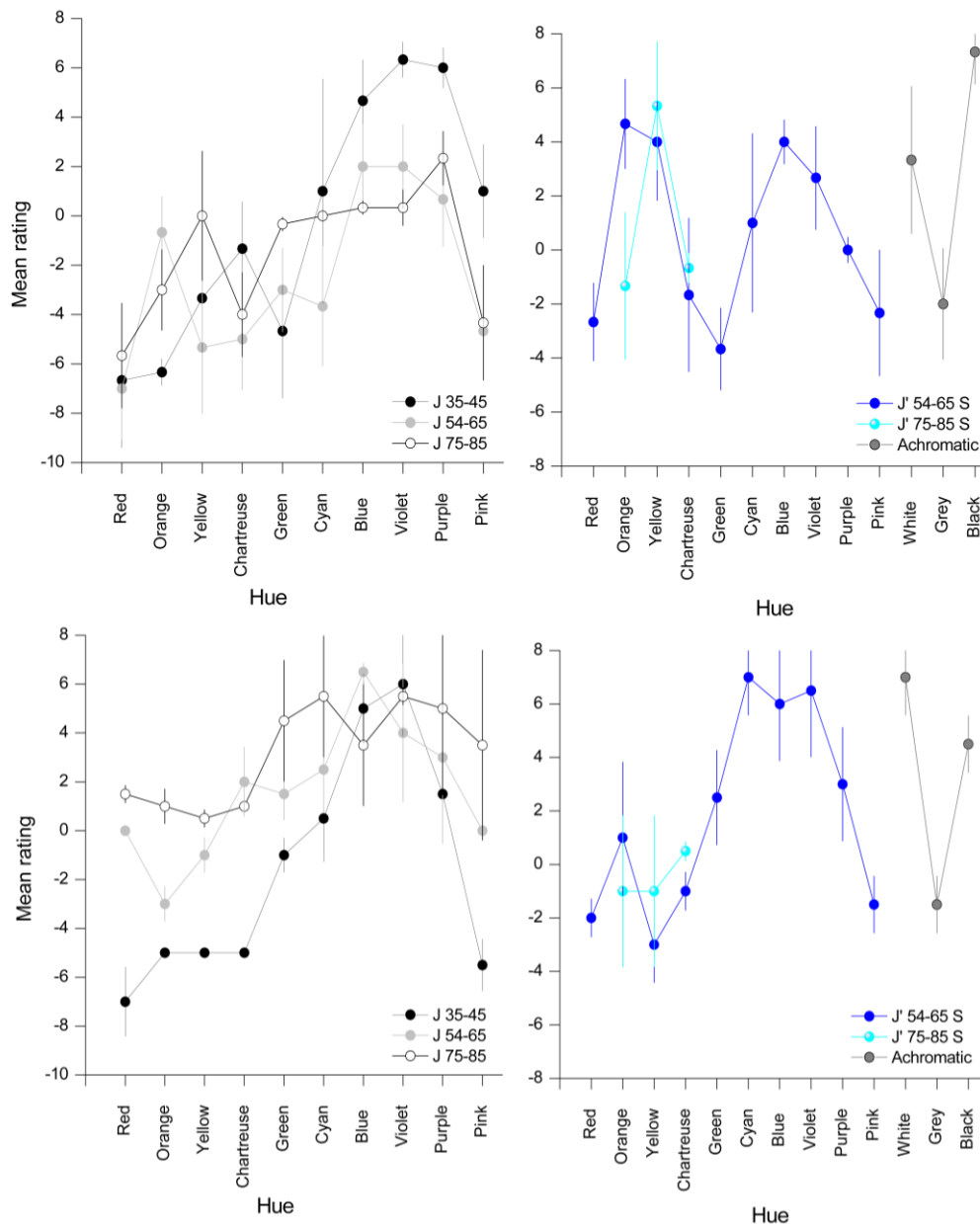


Figure 95 - Mean ratings across all protanopes (on the top); Mean ratings across all deuteranopes (on the bottom).

For protanopes black is the highest-rated color and for deuteranopes white is the highest-rated color.

#### 10.4. Discussion

Álvaro et al. [76] studied color preference in 17 deuteranopes and 15 protanopes, using color samples presented in a monitor. They found a maximum preference for yellow and a much

weaker preference for blue in dichromats than in trichromats. This study found higher ratings for black than in white for both protanopes and deuteranopes.

The results obtained are not similar to the ones reported in the Álvaro et al. paper the difference in methodology can be a reason why this occurs, but the limited number of participants is possibly the biggest reason why the patterns reported in the paper are not found in this experiment.

To truly be able to compare these results with the literature available a larger sample size had to be obtained so a clear pattern could be found eliminating the noise resulting from such small sample sizes.



## **11.EFFECTS OF RED-GREEN COLOR VISION DEFICIENCIES ON COLOR PREFERENCE FOR COLOR COMBINATIONS**

### **11.1. Objective**

The goal of this experiment is to study the properties of the color combinations preferred and quantify them in dichromats.

### **11.2. Methods**

#### Participants

The same participants did this experiment after they finished with the color preference for single colors experiment.

#### Samples

This experiment used the same samples mentioned in Chapter 7.

#### Procedure

This experiment used the procedure described in Chapter 7.

Participants took an average of 10.7 minutes with a standard deviation of  $\pm 3.4$  minutes to complete this procedure, 15 minutes was the maximum time that a participant took, and seven minutes was the minimum.

### **11.3. Results and conclusions**

- **1x1 grid**

Only one observer picked the sample they rated the highest in the single color preference experiment.

- **2x1 grid**

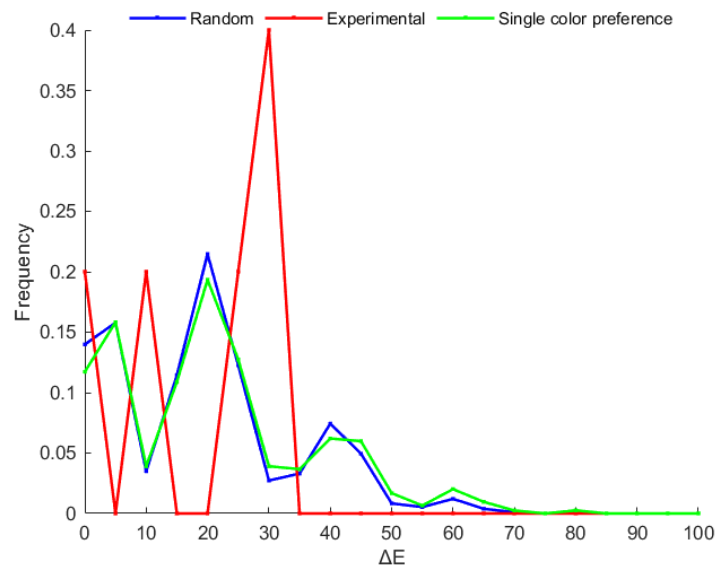


Figure 96 - Difference of color for the lightness axis.

Figure 96 represents the  $\Delta E$  of the  $J'$  axis for all three types of data on the x-axis and the frequency on the y-axis. The  $\Delta E'_{J'}$  value most frequently picked is the 30 for dichromats.

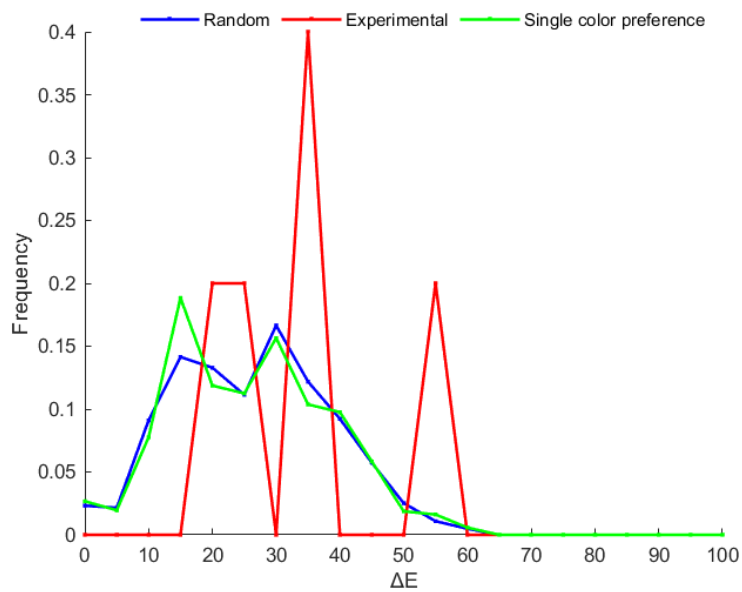


Figure 97 - Difference of color for the chromatic axis.

Figure 97 represents the  $\Delta E$  for the  $a'_M$  and  $b'_M$  for all three types of data on the x-axis and the frequency on the y-axis. The  $\Delta E$  value most frequently picked is the 35 for dichromats.

- **2x2 grid**

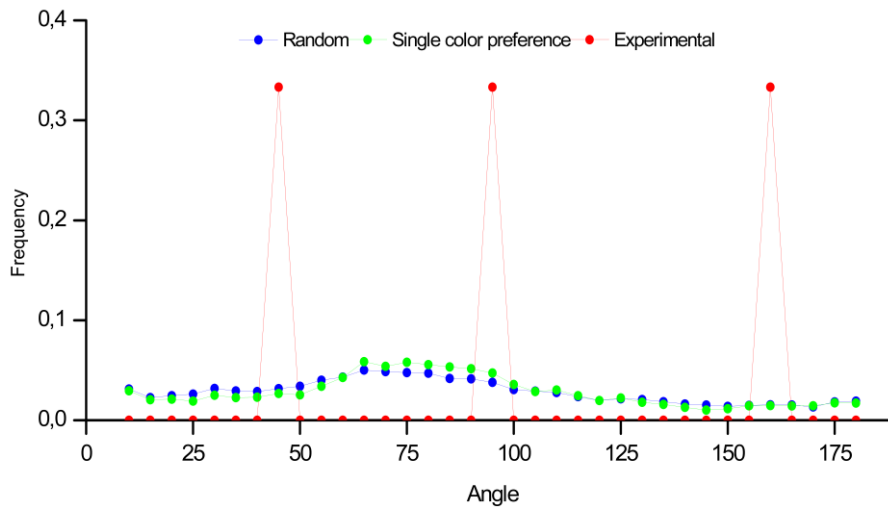


Figure 98 - Angle results for the 2x2 grid.

The average angle for the experimental data is 95 degrees, for the random data is 79 degrees, and for the random data based on the results of the single color preference experiment is 80 degrees.

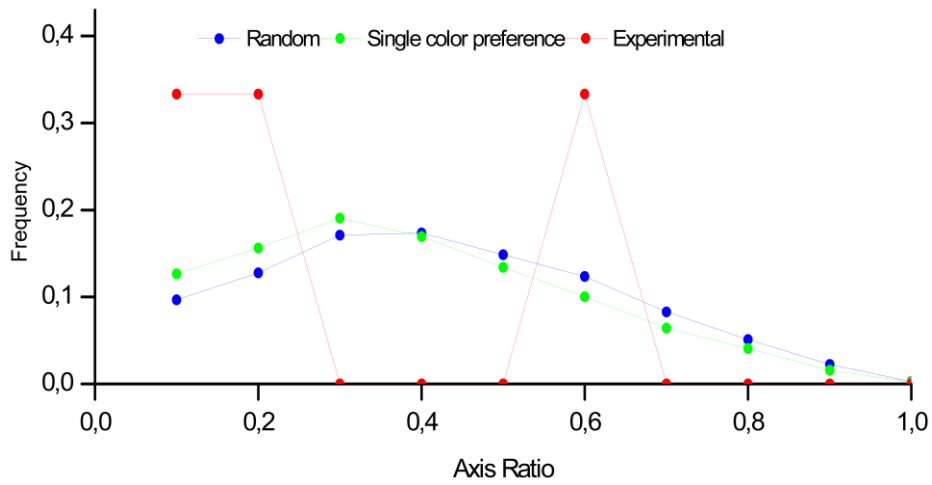


Figure 99 - Axis ratio results for the 2x2 grid.

The average axis ratio for the experimental data is 0.28, for the random data is 0.42, and for the random data based on the results of the single color preference experiment is 0.39.

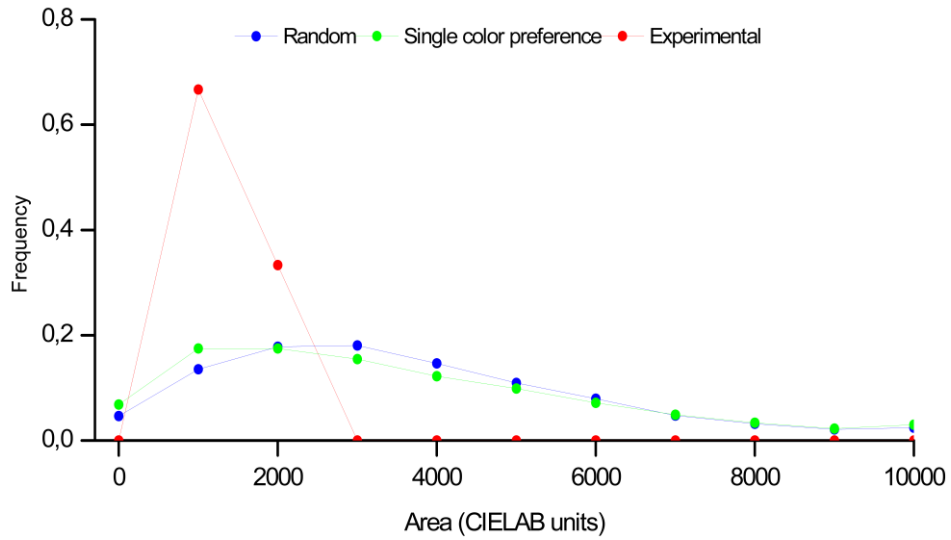


Figure 100 - Area results for the 2x2 grid.

The average area of the fitted ellipses for the experimental data is 1141 CIELAB units, for the random data is 3688 CIELAB units, and for the random data based on the results of the single color preference experiment is 3551 CIELAB units.

• **3x3 grid**

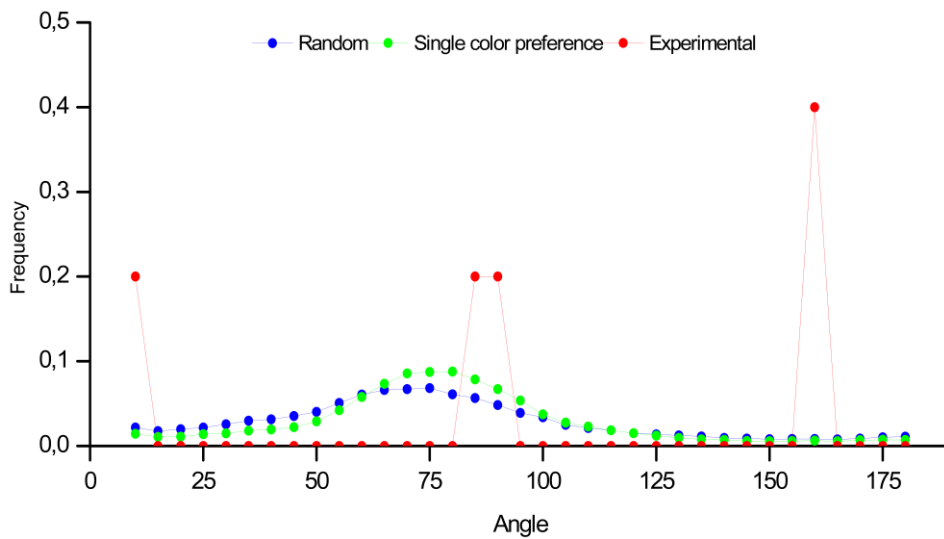


Figure 101 - Angle results for the 3x3 grid.

The average angle for the experimental data is 96 degrees, for the random data is 73 degrees, and for the random data based on the results of the single color preference experiment is 75 degrees.

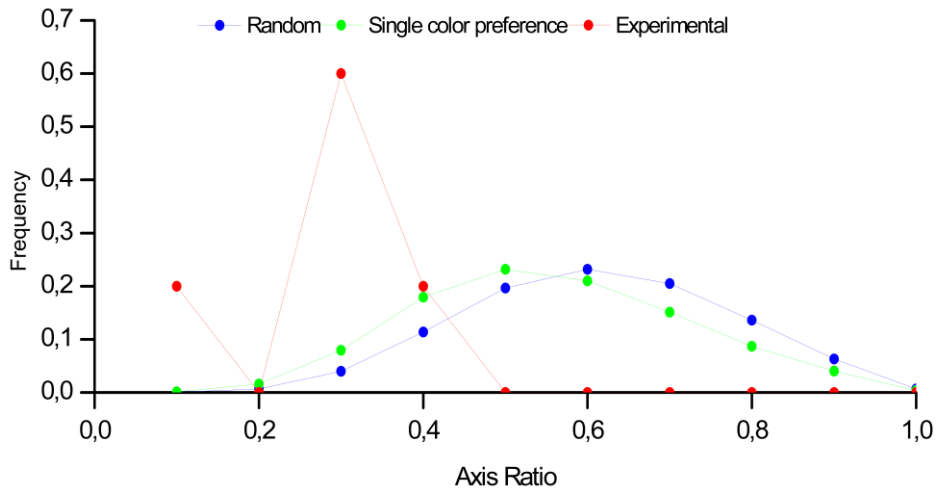


Figure 102 - Axis ratio results for the 3x3 grid.

The average axis ratio for the experimental data is 0.28, for the random data is 0.61, and for the random data based on the results of the single color preference experiment is 0.56.

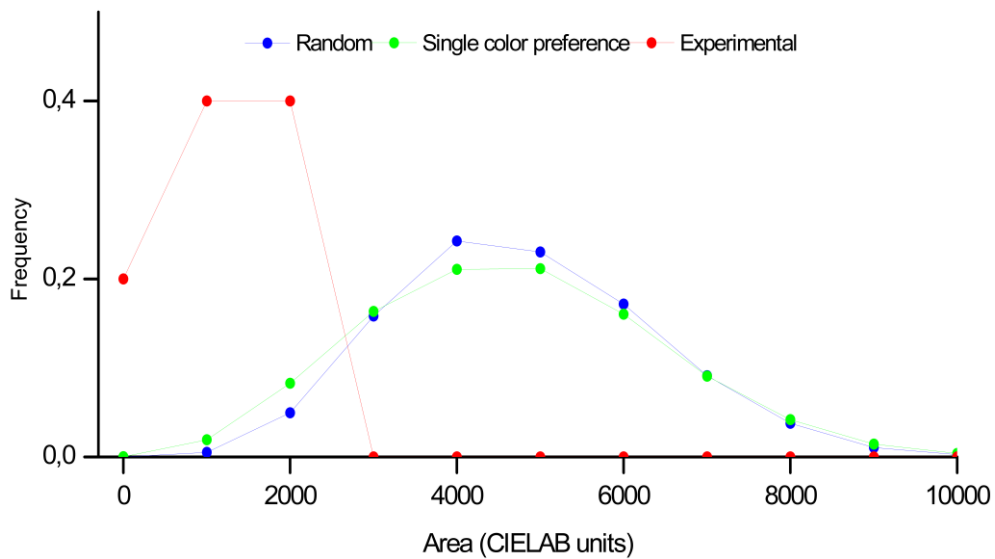


Figure 103 - Area results for the 3x3 grid.

The average area of the fitted ellipses for the experimental data is 1066 CIELAB units, for the random data is 4795 CIELAB units, and for the random data based on the results of the single color preference experiment is 4681 CIELAB units.

• **4x4 grid**

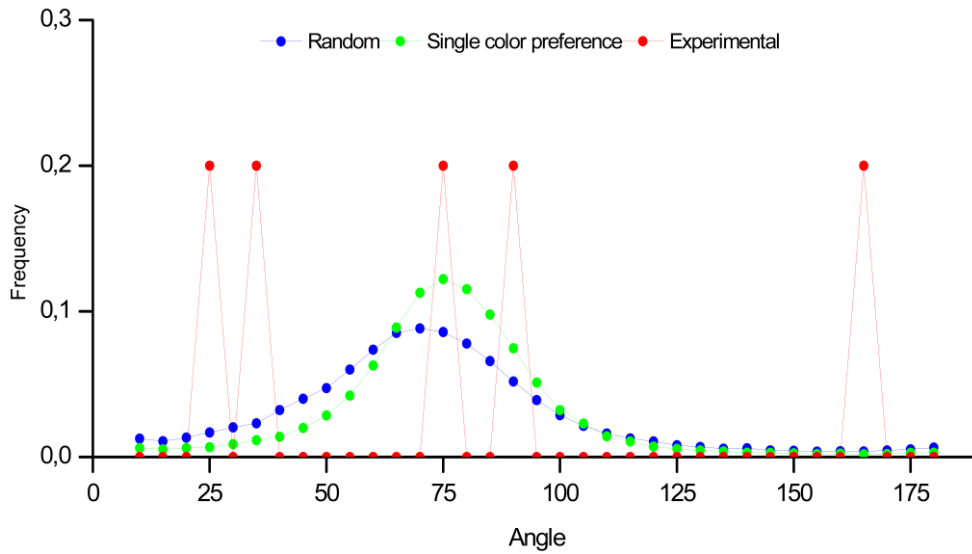


Figure 104 - Angle results for the 4x4 grid.

The average angle for the experimental data is 72 degrees, for the random data is 69 degrees, and for the random data based on the results of the single color preference experiment is 72 degrees.

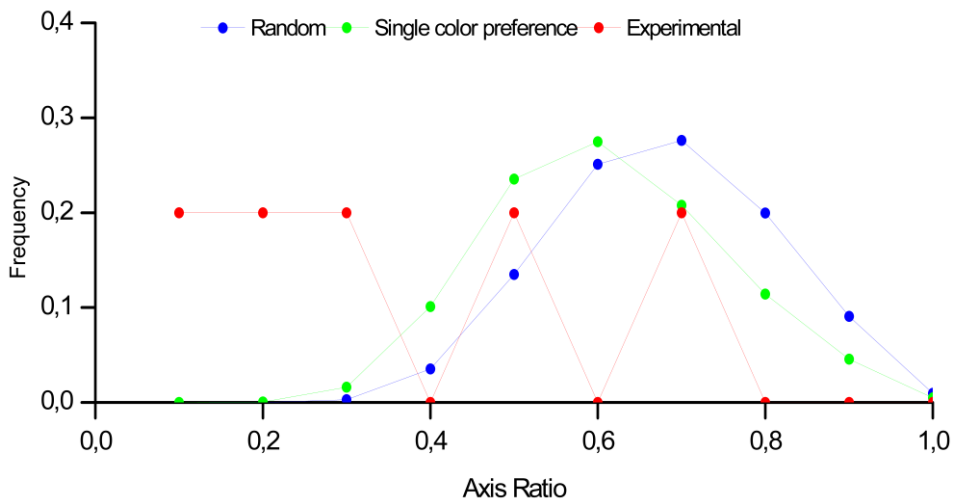


Figure 105 - Axis ratio results for the 4x4 grid.

The average axis ratio for the experimental data is 0.37, for the random data is 0.68, and for the random data based on the results of the single color preference experiment is 0.61.

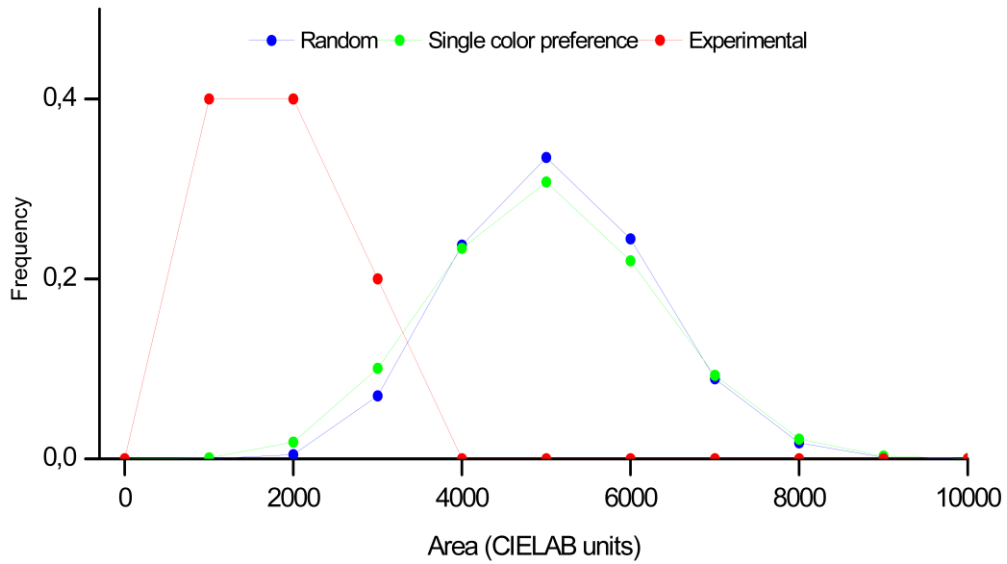


Figure 106 - Area results for the 4x4 grid.

The average area of the fitted ellipses for the experimental data is 1903 CIELAB units, for the random data is 5092 CIELAB units, and for the random data based on the results of the single color preference experiment is 4991 CIELAB units.

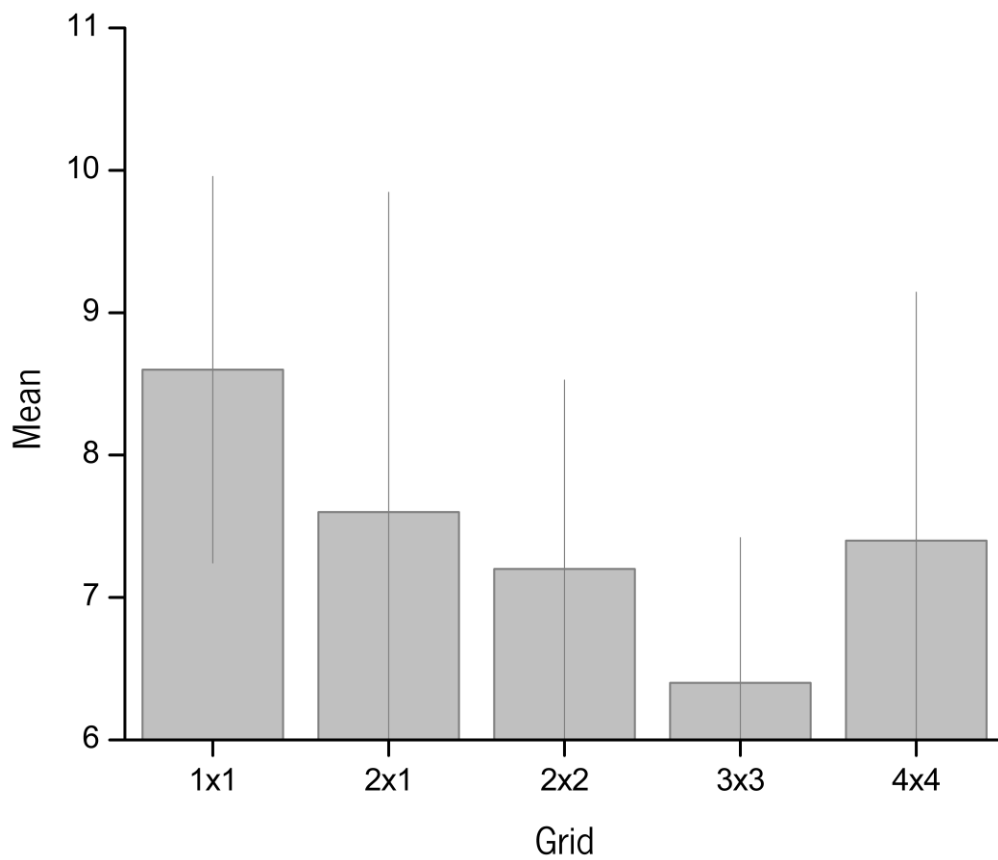


Figure 107 - Mean satisfaction for each grid.

Figure 107 shows the mean satisfaction for each grid and the error bars are the standard deviation, the y-axis scale range was defined from six to eight to improve data visualization but satisfaction was measured on a scale from one to 10. The average satisfaction for the 1x1 grid was 8.6 with a standard deviation of  $\pm 1.4$ , for the 2x1 grid was 7.6 with a standard deviation of  $\pm 2.2$ , for the 2x2 grid was 7.2 with a standard deviation of  $\pm 1.3$ , for the 3x3 grid was 6.4 with a standard deviation of  $\pm 1.0$ , and for the 4x4 grid was 7.4 with a standard deviation of  $\pm 1.7$ .

#### **11.4. Discussions**

For the 1x1 grid, only one of the dichromats picked the color sample they rated the highest in the single color preference experiment when asked to pick their favorite color sample. A possibility as to why this happens may be that colors that fall on confusion lines are seen as the same therefore some samples on the board are perceived as the same color even though they are not. This experiment was conducted on the same day that the color preference for single colors was done.

The 2x1 grid combinations seem to differ in lightness and chromaticity when analyzing the  $\Delta E$  expressed in Figure 96 and Figure 97.

The ellipses were calculated using the same scripts mentioned in Chapter 5 (Section 5.2) with some adjustments. The points fitted in the ellipses of the 2x2 grid occupied an average of 100% for all three types of data. The 3x3 grid occupied an average of 91.1% when the experimental data was used, 92.8% when randomly generated data was used, and 90.7% when randomly generated data based on the results of the single color preference experiment was used. For the 4x4 grid occupied an average of 93.7% when the experimental data was used, 90.2% when randomly generated data was used, and 88.6% when randomly generated data based on the results of the single color preference experiment was used.

A general conclusion when comparing the experimental results with the two models is that differences are evident a big reason why this happens is the difference number of observers analyzed.

Montagner et al. found average angles of  $92^\circ$  for natural scenes,  $66^\circ$  for paintings ( $72^\circ$  for figurative and  $58^\circ$  for abstract paintings) [67]. When comparing the results of the experimental data of the 2x2 and 3x3 grids they are closer to the ones of natural scenes.



Montagner et al. found an average axis ratio of 0.51 for natural scenes, 0.58 for paintings (0.56 for figurative and 0.6 for abstract paintings) [67]. When comparing the results of the three types of data of the 2x2 grid and the experimental data of the 3x3 and 4x4 grid they are closer to the ones of natural scenes.

Montagner et al. found an average area of fitted ellipses of 1226 CIELAB units (range from 210 to 6613 CIELAB units) for natural scenes, 1338 CIELAB units (range from 124 to 5610 CIELAB units) for paintings [67]. When comparing the results of the three types of data of all grids they are closer to the ones of paintings except the 2x2 and 3x3 grid of experimental data.

Comparisons with this study have to be taken with caution because they did not use dichromats.

The mean satisfaction of the combinations made is expressed in Figure 107. It decreases as the complexity of the combination increases, except for the 4x4 grid where the mean satisfaction slightly increases.

Both models fail to predict the combinations made by dichromats whether this occurs because observers do not make combinations randomly and they do not use only individual color preferences to build their combinations or because the size of the sample of observers is too small is something only possible to test when increasing the number of participants.

The number of participants is the biggest limitation of this experiment.

## **12. CONCLUSIONS AND FUTURE WORK**

The first main conclusion is that color preference for single colors is clearly influenced by artistic education. Not only the ratings for the different colors are higher than for a normal population but the relative preference for the different lightness levels is different. Although the first result might be anticipated as artists tend to like colors more, the second is more surprising and suggests that artists like more contrasting colors.

The second conclusion is that the color compositions that participants build cannot be explained by a completely random process or a random process based on their single color preference. New computational instruments need to be developed to address the analysis better and in particular the differences between populations with artistic education from populations without specific artistic education.

In the comparisons of color preference for single colors between males and females, some differences are found for the different lightness levels and hues tested.

The conclusion for the experiments with dichromats is that the small sample size analyzed does not allow a clear pattern of preference to be revealed.

Future work will be to apply the experimental paradigm developed here to different populations, Asian and South American populations. More data from color-deficient individuals is necessary to compare with the data from color normals. Finally, new and better computational instruments need to be developed to improve the analysis of the existing data.

### **13.OUTPUTS OF THIS WORK**

This work was presented at two International Conferences:

- “Color Vision and aesthetics”, Patrícia M.H. Oliveira, João M. M. Linhares, Claudia Feitosa-Santana, and Sérgio M. C. Nascimento, 7th edition of the International Meeting on Retouching of Cultural Heritage (RECH7 - 2023) at the Faculty of Fine Arts of the University of Lisbon (FBAUL), Lisbon, Portugal.
- “Color preference for simple and complex compositions”, Patrícia M.H. Oliveira, João M. M. Linhares, Claudia Feitosa-Santana, and Sérgio M. C. Nascimento, Congresso Internacional de Optometria e Ciências da Visão (CIOCV-2023) at Espaço Vita, Braga, Portugal.

## REFERENCES

- [1] M. D. Fairchild, *Color appearance models*, Third edition. in The wiley-IS&T series in imaging science and technology. Chichester, West Sussex: John Wiley & Sons, Inc, 2013.
- [2] R. S. Snell and M. A. Lemp, *Clinical Anatomy of the Eye*, 2nd ed. Somerset: Wiley, 2013.
- [3] S. Agatonovic-Kustrin, A. Evans, and R. G. Alany, "Prediction of corneal permeability using artificial neural networks," *Pharm.*, vol. 58, no. 10, pp. 725–729, Oct. 2003.
- [4] D. W. DelMonte and T. Kim, "Anatomy and physiology of the cornea," *J. Cataract Refract. Surg.*, vol. 37, no. 3, pp. 588–598, Mar. 2011, doi: 10.1016/j.jcrs.2010.12.037.
- [5] R. W. G. Hunt and M. Pointer, *Measuring colour*, 4th ed. in Wiley-IS&T series in imaging science and technology. Chichester, West Sussex, U.K: Wiley, 2011.
- [6] M. M. Bradley, L. Miccoli, M. A. Escrig, and P. J. Lang, "The pupil as a measure of emotional arousal and autonomic activation," *Psychophysiology*, vol. 45, no. 4, pp. 602–607, Jul. 2008, doi: 10.1111/j.1469-8986.2008.00654.x.
- [7] S. Dorgaleleh, K. Naghipoor, A. Barahouie, F. Dastaviz, and M. Oladnabi, "Molecular and biochemical mechanisms of human iris color: A comprehensive review," *J. Cell. Physiol.*, vol. 235, no. 12, pp. 8972–8982, Dec. 2020, doi: 10.1002/jcp.29824.
- [8] C. A. Curcio, K. R. Sloan, R. E. Kalina, and A. E. Hendrickson, "Human photoreceptor topography," *J. Comp. Neurol.*, vol. 292, no. 4, pp. 497–523, Feb. 1990, doi: 10.1002/cne.902920402.
- [9] A. Stockman and L. T. Sharpe, "The spectral sensitivities of the middle- and long-wavelength-sensitive cones derived from measurements in observers of known genotype," *Vision Res.*, vol. 40, no. 13, pp. 1711–1737, Jun. 2000, doi: 10.1016/S0042-6989(00)00021-3.
- [10] T. D. Lamb, "Photoreceptor spectral sensitivities: Common shape in the long-wavelength region," *Vision Res.*, vol. 35, no. 22, pp. 3083–3091, Nov. 1995, doi: 10.1016/0042-6989(95)00114-F.
- [11] K. P. Hofmann and T. D. Lamb, "Rhodopsin, light-sensor of vision," *Prog. Retin. Eye Res.*, vol. 93, p. 101116, Mar. 2023, doi: 10.1016/j.preteyeres.2022.101116.
- [12] L. S. Mure, "Intrinsically Photosensitive Retinal Ganglion Cells of the Human Retina," *Front. Neurol.*, vol. 12, 2021, Accessed: Sep. 06, 2023. [Online]. Available: <https://www.frontiersin.org/articles/10.3389/fneur.2021.636330>
- [13] R. G. Foster, S. Hughes, and S. N. Peirson, "Circadian Photoentrainment in Mice and Humans," *Biology*, vol. 9, no. 7, Art. no. 7, Jul. 2020, doi: 10.3390/biology9070180.
- [14] A. Bringmann *et al.*, "The primate fovea: Structure, function and development," *Prog. Retin. Eye Res.*, vol. 66, pp. 49–84, Sep. 2018, doi: 10.1016/j.preteyeres.2018.03.006.
- [15] S. Lambertus *et al.*, "Highly sensitive measurements of disease progression in rare disorders: Developing and validating a multimodal model of retinal degeneration in Stargardt disease," *PLOS ONE*, vol. 12, no. 3, p. e0174020, Mar. 2017, doi: 10.1371/journal.pone.0174020.
- [16] J. S. Werner, S. K. Donnelly, and R. Kliegl, "Aging and human macular pigment density: Appended with translations from the work of Max Schultze and Ewald Hering," *Vision Res.*, vol. 27, no. 2, pp. 257–268, Jan. 1987, doi: 10.1016/0042-6989(87)90188-X.
- [17] S. Beatty, M. Boulton, D. Henson, H. H. Koh, and I. Murray, "Macular pigment and age related macular degeneration," *Br. J. Ophthalmol.*, vol. 83, pp. 867–77, Aug. 1999, doi: 10.1136/bjo.83.7.867.
- [18] H. A. Quigley, "The Size and Shape of the Optic Disc in Normal Human Eyes," *Arch. Ophthalmol.*, vol. 108, no. 1, p. 51, Jan. 1990, doi: 10.1001/archopht.1990.01070030057028.

- [19] M. Saito, K. Miyamoto, Y. Uchiyama, and I. Murakami, "Invisible light inside the natural blind spot alters brightness at a remote location," *Sci. Rep.*, vol. 8, p. 7540, May 2018, doi: 10.1038/s41598-018-25920-9.
- [20] A. Grace and S. Mohideen, "An Economic System for Screening of Diabetic Retinopathy Using Fundus Images," *OnLine J. Biol. Sci.*, vol. 14, pp. 254–260, Apr. 2014, doi: 10.3844/ojbsci.2014.254.260.
- [21] J. Martinovic, "Magno-, Parvo-, Koniocellular Pathways," in *Encyclopedia of Color Science and Technology*, R. Luo, Ed., Berlin, Heidelberg: Springer, 2014, pp. 1–5. doi: 10.1007/978-3-642-27851-8\_278-1.
- [22] M. Livingstone and D. Hubel, "Segregation of form, color, movement, and depth: anatomy, physiology, and perception," *Science*, vol. 240, no. 4853, pp. 740–749, May 1988, doi: 10.1126/science.3283936.
- [23] E. B. Goldstein, *Sensation and perception*, 8th ed. Belmont, CA: Wadsworth, Cengage Learning, 2010.
- [24] M. M. Bannert and A. Bartels, "Human V4 Activity Patterns Predict Behavioral Performance in Imagery of Object Color," *J. Neurosci. Off. J. Soc. Neurosci.*, vol. 38, no. 15, pp. 3657–3668, Apr. 2018, doi: 10.1523/JNEUROSCI.2307-17.2018.
- [25] K. Seymour, C. W. G. Clifford, N. K. Logothetis, and A. Bartels, "Coding and binding of color and form in visual cortex," *Cereb. Cortex N. Y. N 1991*, vol. 20, no. 8, pp. 1946–1954, Aug. 2010, doi: 10.1093/cercor/bhp265.
- [26] E. Austin *et al.*, "Visible Light Part I. Properties and Cutaneous Effects of Visible Light," *J. Am. Acad. Dermatol.*, vol. 84, no. 5, pp. 1219–1231, May 2021, doi: 10.1016/j.jaad.2021.02.048.
- [27] D. H. Sliney, "What is light? The visible spectrum and beyond," *Eye*, vol. 30, no. 2, pp. 222–229, Feb. 2016, doi: 10.1038/eye.2015.252.
- [28] H. von Helmholtz, "On the theory of compound colors," *Philos. Mag.*, vol. 4, pp. 519–534, 1852.
- [29] T. Young, "On the theory of light and colours," *Philos. Trans. R. Soc. Lond.*, vol. 92, pp. 12–48, Dec. 1802.
- [30] S. H. Schwartz, *Visual perception: a clinical orientation*, 4. ed. New York: McGraw-Hill Medical, 2010.
- [31] E. Hering, "Outlines of a Theory of the Light Sense (trans. L.M. Hurvich and D. Jameson, 1964)," *Harv. Univ. Press Camb.*, 1920.
- [32] E. J. MacNichol and G. Svaetichin, "Electric Responses from the Isolated Retinas of Fishes\*," *Am. J. Ophthalmol.*, vol. 46, no. 3, Part 2, pp. 26–46, Sep. 1958, doi: 10.1016/0002-9394(58)90053-9.
- [33] R. L. De Valois, C. J. Smith, S. T. Kitai, and A. J. Karoly, "Response of Single Cells in Monkey Lateral Geniculate Nucleus to Monochromatic Light," *Science*, vol. 127, no. 3292, pp. 238–239, Jan. 1958, doi: 10.1126/science.127.3292.238.
- [34] L. M. Hurvich and D. Jameson, "Some Quantitative Aspects of an Opponent-Colors Theory II Brightness, Saturation, and Hue in Normal and Dichromatic Vision," *J. Opt. Soc. Am.*, vol. 45, no. 8, p. 602, Aug. 1955, doi: 10.1364/JOSA.45.000602.
- [35] J. Dalton, "Extraordinary facts relating to the vision of colours: with observations, 1798.," in *Readings in the history of psychology.*, W. Dennis, Ed., East Norwalk: Appleton-Century-Crofts, 1948, pp. 102–111. doi: 10.1037/11304-013.
- [36] J. Birch, "Worldwide prevalence of red-green color deficiency," *JOSA A*, vol. 29, no. 3, pp. 313–320, Mar. 2012, doi: 10.1364/JOSAA.29.000313.

- [37] M. Neitz and J. Neitz, "Intermixing the OPN1LW and OPN1MW Genes Disrupts the Exonic Splicing Code Causing an Array of Vision Disorders," *Genes*, vol. 12, no. 8, Art. no. 8, Aug. 2021, doi: 10.3390/genes12081180.
- [38] M. Simunovic, "Color vision deficiency," *Eye Lond. Engl.*, vol. 24, pp. 747–55, Nov. 2009, doi: 10.1038/eye.2009.251.
- [39] K. R. Gegenfurtner and L. T. Sharpe, Eds., *Color vision: from genes to perception*. Cambridge ; New York: Cambridge University Press, 1999.
- [40] K. E. M. Tregillus *et al.*, "Color Compensation in Anomalous Trichromats Assessed with fMRI," *Curr. Biol.*, vol. 31, no. 5, pp. 936-942.e4, Mar. 2021, doi: 10.1016/j.cub.2020.11.039.
- [41] M. P. Simunovic, "Acquired color vision deficiency," *Surv. Ophthalmol.*, vol. 61, no. 2, pp. 132–155, Mar. 2016, doi: 10.1016/j.survophthal.2015.11.004.
- [42] G. Verriest, "Further Studies on Acquired Deficiency of Color Discrimination\*," *JOSA*, vol. 53, no. 1, pp. 185–195, Jan. 1963, doi: 10.1364/JOSA.53.000185.
- [43] G. Wyszecki and W. S. Stiles, *Color science: concepts and methods, quantitative data and formulae*, 2nd ed. in The Wiley series in pure and applied optics. New York: Wiley, 1982.
- [44] S. J. Dain, "Clinical colour vision tests," *Clin. Exp. Optom.*, vol. 87, no. 4–5, pp. 276–293, Jul. 2004, doi: 10.1111/j.1444-0938.2004.tb05057.x.
- [45] W. J. Benjamin and I. M. Borish, Eds., *Borish's clinical refraction*, 2nd ed. St. Louis Mo: Butterworth Heinemann/Elsevier, 2006.
- [46] S. Thyagarajan, P. Moradi, L. Membrey, D. Alistair, and H. Laidlaw, "Technical Note: The effect of refractive blur on colour vision evaluated using the Cambridge Colour Test, the Ishihara Pseudoisochromatic Plates and the Farnsworth Munsell 100 Hue Test," *Ophthalmic Physiol. Opt.*, vol. 27, no. 3, pp. 315–319, May 2007, doi: 10.1111/j.1475-1313.2007.00469.x.
- [47] Internationale Beleuchtungskommission, Ed., *Colorimetry*, 4th edition. in Technical report, no. 15. Vienna: Commission Internationale de l'Eclairage, 2018.
- [48] W. A. Steer, "Introduction to Colour Science." Accessed: Oct. 20, 2022. [Online]. Available: <http://www.techmind.org/colour/>
- [49] B. C. K. Ly, E. B. Dyer, J. L. Feig, A. L. Chien, and S. Del Bino, "Research Techniques Made Simple: Cutaneous Colorimetry: A Reliable Technique for Objective Skin Color Measurement," *J. Invest. Dermatol.*, vol. 140, no. 1, pp. 3-12.e1, Jan. 2020, doi: 10.1016/j.jid.2019.11.003.
- [50] R. C. Pastilha, J. M. M. Linhares, A. I. C. Rodrigues, and S. M. C. Nascimento, "Describing natural colors with Munsell and NCS color systems," *Color Res. Appl.*, vol. 44, no. 3, pp. 411–418, Jun. 2019, doi: 10.1002/col.22355.
- [51] "NCS System - NCS Colour." Accessed: Nov. 29, 2022. [Online]. Available: <https://ncscolour.com/ncs/>
- [52] M. D. Augustin, J. Wagemans, and C.-C. Carbon, "All is beautiful? Generality vs. specificity of word usage in visual aesthetics," *Acta Psychol. (Amst.)*, vol. 139, no. 1, pp. 187–201, Jan. 2012, doi: 10.1016/j.actpsy.2011.10.004.
- [53] B. R. Conway and A. Rehding, "Neuroaesthetics and the Trouble with Beauty," *PLoS Biol.*, vol. 11, no. 3, p. e1001504, Mar. 2013, doi: 10.1371/journal.pbio.1001504.
- [54] A. M. Albers, K. R. Gegenfurtner, and S. M. C. Nascimento, "An independent contribution of colour to the aesthetic preference for paintings," *Vision Res.*, vol. 177, pp. 109–117, Dec. 2020, doi: 10.1016/j.visres.2020.08.005.
- [55] G. T. Fechner, *Vorschule der Aesthetik*, 1st ed. Cambridge University Press, 2013. doi: 10.1017/CBO9781139854580.

- [56] T. Ishizu and S. Zeki, "Toward A Brain-Based Theory of Beauty," *PLoS ONE*, vol. 6, no. 7, p. e21852, Jul. 2011, doi: 10.1371/journal.pone.0021852.
- [57] H. Kawabata and S. Zeki, "Neural Correlates of Beauty," *J. Neurophysiol.*, vol. 91, no. 4, pp. 1699–1705, Apr. 2004, doi: 10.1152/jn.00696.2003.
- [58] D. Fernandez and A. J. Wilkins, "Uncomfortable Images in Art and Nature," *Perception*, vol. 37, no. 7, pp. 1098–1113, Jul. 2008, doi: 10.1068/p5814.
- [59] D. J. Graham and C. Redies, "Statistical regularities in art: Relations with visual coding and perception," *Vision Res.*, vol. 50, no. 16, pp. 1503–1509, Jul. 2010, doi: 10.1016/j.visres.2010.05.002.
- [60] A. J. Elliot, "A Historically Based Review of Empirical Work on Color and Psychological Functioning: Content, Methods, and Recommendations for Future Research," *Rev. Gen. Psychol.*, vol. 23, no. 2, pp. 177–200, Jun. 2019, doi: 10.1037/gpr0000170.
- [61] N. Humphrey, "The Colour Currency of Nature," 1976, pp. 95–98. doi: 10.4324/9781315881379-3.
- [62] A. C. Hurlbert and Y. Ling, "Biological components of sex differences in color preference," *Curr. Biol.*, vol. 17, no. 16, pp. R623–R625, Aug. 2007, doi: 10.1016/j.cub.2007.06.022.
- [63] L.-C. Ou, M. R. Luo, A. Woodcock, and A. Wright, "A study of colour emotion and colour preference. Part I: Colour emotions for single colours," *Color Res. Appl.*, vol. 29, no. 3, pp. 232–240, Jun. 2004, doi: 10.1002/col.20010.
- [64] L.-C. Ou, M. R. Luo, A. Woodcock, and A. Wright, "A study of colour emotion and colour preference. Part III: Colour preference modeling," *Color Res. Appl.*, vol. 29, no. 5, pp. 381–389, Oct. 2004, doi: 10.1002/col.20047.
- [65] S. E. Palmer and K. B. Schloss, "An ecological valence theory of human color preference," *Proc. Natl. Acad. Sci.*, vol. 107, no. 19, pp. 8877–8882, May 2010, doi: 10.1073/pnas.0906172107.
- [66] S. M. C. Nascimento *et al.*, "The colors of paintings and viewers' preferences," *Vision Res.*, vol. 130, pp. 76–84, Jan. 2017, doi: 10.1016/j.visres.2016.11.006.
- [67] C. Montagner, J. M. M. Linhares, M. Vilarigues, and S. M. C. Nascimento, "Statistics of colors in paintings and natural scenes," *J. Opt. Soc. Am. A*, vol. 33, no. 3, p. A170, Mar. 2016, doi: 10.1364/JOSAA.33.00A170.
- [68] S. M. C. Nascimento, A. Marit Albers, and K. R. Gegenfurtner, "Naturalness and aesthetics of colors – Preference for color compositions perceived as natural," *Vision Res.*, vol. 185, pp. 98–110, Aug. 2021, doi: 10.1016/j.visres.2021.03.010.
- [69] C. Feitosa-Santana, C. M. Gaddi, A. E. Gomes, and S. M. C. Nascimento, "Art through the Colors of Graffiti: From the Perspective of the Chromatic Structure," *Sensors*, vol. 20, no. 9, p. 2531, Apr. 2020, doi: 10.3390/s20092531.
- [70] D. Jonauskaitė *et al.*, "Pink for Girls, Red for Boys, and Blue for Both Genders: Colour Preferences in Children and Adults," *Sex Roles*, vol. 80, no. 9–10, pp. 630–642, May 2019, doi: 10.1007/s11199-018-0955-z.
- [71] Tailored Lighting, Inc., Accessed: Oct. 20, 2022. [Online]. Available: <https://www.solux.net/cgi-bin/tlistore/infopages/4700k.html>
- [72] M. A. Aldaba, J. M. M. Linhares, P. D. Pinto, S. M. C. Nascimento, K. Amano, and D. H. Foster, "Visual sensitivity to color errors in images of natural scenes," *Vis. Neurosci.*, vol. 23, no. 3–4, pp. 555–559, May 2006, doi: 10.1017/S0952523806233467.
- [73] D. H. Foster and A. Reeves, "Colour constancy failures expected in colourful environments," *Proc. R. Soc. B Biol. Sci.*, vol. 289, no. 1967, p. 20212483, Jan. 2022, doi: 10.1098/rspb.2021.2483.

- [74] "Paints - VeriVide." Accessed: Nov. 29, 2022. [Online]. Available: <https://www.verivide.com/product/paints/>
- [75] K. B. Schloss, D. Hawthorne-Madell, and S. E. Palmer, "Ecological influences on individual differences in color preference," *Atten. Percept. Psychophys.*, vol. 77, no. 8, pp. 2803–2816, Nov. 2015, doi: 10.3758/s13414-015-0954-x.
- [76] L. Álvaro, H. Moreira, J. Lillo, and A. Franklin, "Color preference in red–green dichromats," *Proc. Natl. Acad. Sci.*, vol. 112, no. 30, pp. 9316–9321, Jul. 2015, doi: 10.1073/pnas.1502104112.



## APPENDIX

Appendix I - The chromaticity coordinates of daylight of different color-correlated temperatures. Adapted from [43].

**Table IV(3.3.4) CIE 1931 ( $x_D, y_D$ )-Chromaticity Coordinates and Scalar Multipliers  $M_1, M_2$  of Daylight of Different Correlated Color Temperatures  $T_C$  (Planck's Constant  $c_2 = 1.4388 \times 10^{-2} \text{ m} \cdot \text{K}$ ); (CIE, 1971)**

$T_c$	$x_D$	$y_D$	$M_1$	$M_2$
4,000	0.3823	0.3838	-1.505	2.827
4,100	0.3779	0.3812	-1.464	2.460
4,200	0.3737	0.3786	-1.422	2.127
4,300	0.3697	0.3760	-1.378	1.825
4,400	0.3658	0.3734	-1.333	1.550
4,500	0.3621	0.3709	-1.286	1.302
4,600	0.3585	0.3684	-1.238	1.076
4,700	0.3551	0.3659	-1.190	0.871
4,800	0.3519	0.3634	-1.140	0.686
4,900	0.3487	0.3610	-1.090	0.518
5,000	0.3457	0.3587	-1.040	0.367
5,100	0.3429	0.3564	-0.989	0.230
5,200	0.3401	0.3541	-0.939	0.106
5,300	0.3375	0.3519	-0.888	-0.005
5,400	0.3349	0.3497	-0.837	-0.105
5,500	0.3325	0.3476	-0.786	-0.195
5,600	0.3302	0.3455	-0.736	-0.276
5,700	0.3279	0.3435	-0.685	-0.348
5,800	0.3258	0.3416	-0.635	-0.412
5,900	0.3237	0.3397	-0.586	-0.469
6,000	0.3217	0.3378	-0.536	-0.519
6,100	0.3198	0.3360	-0.487	-0.563
6,200	0.3179	0.3342	-0.439	-0.602
6,300	0.3161	0.3325	-0.391	-0.635
6,400	0.3144	0.3308	-0.343	-0.664
6,500	0.3128	0.3292	-0.296	-0.688
6,600	0.3112	0.3276	-0.250	-0.709
6,700	0.3097	0.3260	-0.204	-0.726
6,800	0.3082	0.3245	-0.159	-0.739
6,900	0.3067	0.3231	-0.114	-0.749
7,000	0.3054	0.3216	-0.070	-0.757
7,100	0.3040	0.3202	-0.026	-0.762
7,200	0.3027	0.3189	0.017	-0.765
7,300	0.3015	0.3176	0.060	-0.765
7,400	0.3003	0.3163	0.102	-0.763
7,500	0.2991	0.3150	0.144	-0.760
7,600	0.2980	0.3138	0.184	-0.755
7,700	0.2969	0.3126	0.225	-0.748
7,800	0.2958	0.3115	0.264	-0.740
7,900	0.2948	0.3103	0.303	-0.730
8,000	0.2938	0.3092	0.342	-0.720
8,100	0.2928	0.3081	0.380	-0.708
8,200	0.2919	0.3071	0.417	-0.695
8,300	0.2910	0.3061	0.454	-0.682
8,400	0.2901	0.3051	0.490	-0.667
8,500	0.2892	0.3041	0.526	-0.652
9,000	0.2853	0.2996	0.697	-0.566
9,500	0.2818	0.2956	0.856	-0.471
10,000	0.2788	0.2920	1.003	-0.369
11,000	0.2737	0.2858	1.266	-0.160
12,000	0.2697	0.2808	1.495	0.045
13,000	0.2664	0.2767	1.693	0.239
14,000	0.2637	0.2732	1.868	0.419
15,000	0.2614	0.2702	2.021	0.586
20,000	0.2539	0.2603	2.571	1.231
25,000	0.2499	0.2548	2.907	1.655

Appendix II - Data collection sheet for the Ishihara test.



DADOS CLÍNICOS DO PARTICIPANTE N.º \_\_\_\_\_

**Ishihara**

Data: \_\_\_\_\_ Hora: \_\_\_\_\_ Local: \_\_\_\_\_ Experimentador: \_\_\_\_\_

Fonte de luz: \_\_\_\_\_ Observações: \_\_\_\_\_

Resultados:

N.º placa	Visão das cores normal	Deficiência verde-vermelho	Sem visão das cores		Resposta
1	12	12	12		
2	8	3	X		
3	6	5	X		
4	29	70	X		
5	57	35	X		
6	5	2	X		
7	3	5	X		
8	15	17	X		
9	74	21	X		
10	2	X	X		
11	6	X	X		
12	97	X	X		
13	45	X	X		
14	5	X	X		
15	7	X	X		
16	16	X	X		
17	73	X	X		
18	X	5	X		
19	X	2	X		
20	X	45	X		
21	X	73	X		
		Prota		Deuta	
		Severo	Suave	Severo	Suave
22	26	6	2 / 6	2	2 / 6
23	42	2	4 / 2	4	4 / 2
24	35	5	3 / 5	3	3 / 5
25	96	6	9 / 6	9	9 / 6

CLASSIFICAÇÃO VISÃO DAS CORES:



### INFORMAÇÃO AOS VOLUNTÁRIOS E CONSENTIMENTO INFORMADO

**Estudo:** Que combinações de cores que gostamos? – desenvolvimento e implementação de um teste visual com crianças e adultos

**Investigador:** Patrícia Manuela Hilário Oliveira; Departamento de Física, Universidade do Minho; patriciamanuela99@gmail.com

**Responsável:** Sérgio Miguel Cardoso Nascimento; Departamento de Física, Universidade do Minho;  
smcn@fisica.uminho.pt

Este documento visa informar sobre o estudo em que vai participar e obter o seu consentimento informado. O documento presente e os procedimentos deste estudo estão de acordo com a “Declaração de Helsínquia” (1964, Associação Médica Mundial) e foram aprovados pela Comissão de Ética para a Investigação em Ciências da Vida e da Saúde (CEICVS) da Universidade do Minho. Por favor, leia a seguinte informação com atenção.

Este estudo pretende estudar a preferência de cor em amostras coloridas.

O estudo não envolve técnicas invasivas, ou seja, não haverá invasão das barreiras naturais do corpo do observador, não constituindo qualquer risco para a saúde.

Esta experiência tem objetivos científicos e não têm fins comerciais.

Eu, \_\_\_\_\_ declaro:

- Que me foram explicados todos os aspetos relevantes sobre as experiências a serem realizadas;
- Tive oportunidade de questionar o investigador, tendo sido respondida de modo satisfatório;
- Posso recusar a qualquer momento a participação ou continuidade no estudo sem quaisquer consequências;
- Autorizo a que os dados sejam publicados de forma anónima com os fins científicos.

Braga, \_\_\_\_\_ de \_\_\_\_\_ de 20\_\_\_\_

Observador: \_\_\_\_\_

Investigador: \_\_\_\_\_

Campus de Gualtar  
4710-057 Braga –Portugal



Universidade do Minho

Escola de Ciências

## INFORMATION TO VOLUNTEERS AND INFORMED CONSENT

**Study:** Que combinações de cores que gostamos? – desenvolvimento e implementação de um teste visual com crianças e adultos

**Researcher:** Patrícia Manuela Hilário Oliveira; Physics department, University of Minho; patriciamanuela99@gmail.com

**Supervisor:** Sérgio Miguel Cardoso Nascimento; Physics department, University of Minho; smcn@fisica.uminho.pt

This document aims to inform you about the study you are going to participate in and obtain your informed consent. The present document and the procedures of this study comply with the Declaration of Helsinki (1964, World Medical Association) and have been approved by the Ethics Comissão de Ética para a Investigação em Ciências da Vida e da Saúde (CEICVS) at the University of Minho. Please read the following information carefully.

This study aims to investigate color preferences in colored samples.

The study does not involve invasive techniques, meaning there will be no invasion of the observer's natural body barriers, and it poses no risk to health.

This experiment is for scientific purposes and is not for commercial purposes.

I, \_\_\_\_\_ declare:

- I have been provided with an explanation of all relevant aspects of the experiments to be conducted.
- I had the opportunity to ask the researcher questions, and they were answered to my satisfaction.
- I can refuse to participate or continue in the study at any time without any consequences.
- I authorize the data to be published anonymously for scientific purposes.

Braga, \_\_\_\_\_ of \_\_\_\_\_ of 20\_\_\_\_

Observer: \_\_\_\_\_

Researcher: \_\_\_\_\_

Appendix V - Data collection sheet for the single color experiments (Portuguese version)

**Folha de resultados da experiência**

Código observador: \_\_\_\_\_ Duração: \_\_\_\_\_

<b>Amostras</b>	<b>Classificação</b>	<b>Ordem</b>
S 1060-R		
S 2060-Y40R		
S 3060-Y		
S 2060-G40Y		
S 2050-G		
S 2050-B50G		
S 2050-B		
S 1555-R70B		
S 2040-R50B		
S 2050-R30B		
S 3030-R		
S 4020-Y40R		
S 4030-Y		
S 3030-G40Y		
S 3020-G		
S 4020-B50G		
S 3020-B		
S 3020-R70B		
S 3030-R50B		
S 3030-R30B		
S 1030-R		
S 2020-Y40R		
S 2020-Y		
S 2020-G40Y		
S 1020-G		
S 1020-B50G		
S 1020-B		
S 0525-R70B		
S 1030-R50B		
S 1030-R30B		
S 1050-Y		
S 1050-G40Y		
S 1050-Y40R		
S 5030-R		
S 6030-Y40R		
S 6030-Y		

S 5540-G40Y		
S 5030-G		
S 5030-B50G		
S 6020-B		
S 6020-R70B		
S 5030-R50B		
S 5030-R30B		
S 0300-N		
S 4500-N		
S 9000-N		

Appendix VI - Data collection sheet for the single color experiments (English version)

**Data collection sheet of experiment**

Code of observer: \_\_\_\_\_ Duration: \_\_\_\_\_

Samples	Classification	Order
S 1060-R		
S 2060-Y40R		
S 3060-Y		
S 2060-G40Y		
S 2050-G		
S 2050-B50G		
S 2050-B		
S 1555-R70B		
S 2040-R50B		
S 2050-R30B		
S 3030-R		
S 4020-Y40R		
S 4030-Y		
S 3030-G40Y		
S 3020-G		
S 4020-B50G		
S 3020-B		
S 3020-R70B		
S 3030-R50B		
S 3030-R30B		
S 1030-R		
S 2020-Y40R		
S 2020-Y		
S 2020-G40Y		
S 1020-G		
S 1020-B50G		
S 1020-B		
S 0525-R70B		
S 1030-R50B		
S 1030-R30B		
S 1050-Y		
S 1050-G40Y		
S 1050-Y40R		
S 5030-R		
S 6030-Y40R		
S 6030-Y		
S 5540-G40Y		
S 5030-G		
S 5030-B50G		

S 6020-B		
S 6020-R70B		
S 5030-R50B		
S 5030-R30B		
S 0300-N		
S 4500-N		
S 9000-N		





Appendix VIII - Data collection sheet for color combination experiments (English version)

**Data collection sheet of experiment**

**Code of observer:** \_\_\_\_\_ **Duration:** \_\_\_\_\_

Artistic Education: \_\_\_\_\_

Glasses: Yes\_\_\_\_\_ No\_\_\_ CL: Yes\_\_\_\_\_ No\_\_\_\_\_


**Is color preference different in males and females?**

Same samples in different observers = Independent samples

- **All samples**

Analyze normality

Use Smirnov >30:

H0: samples preference is normally distributed

H1: samples preference is normally distributed

**Testes de Normalidade**

Mean	Gender	Kolmogorov-Smirnov <sup>a</sup>			Shapiro-Wilk		
		Estatística	gl	Sig.	Estatística	gl	Sig.
	Male	,189	25	,022	,916	25	,042
	Female	,095	25	,200*	,947	25	,219

\*. Este é um limite inferior da significância verdadeira.

a. Correlação de Significância de Lilliefors

p-value <0.05 Reject H0, this means distribution is not normal and that non-parametric tests have to be performed

Define test

Non-parametric tests and independent samples = Mann-Whitney

H0: median of males = median of females

H1: median of males ≠ median of females

**Estatísticas de teste<sup>a</sup>**

	Mean
U de Mann-Whitney	196,500
Wilcoxon W	521,500
Z	-2,251
Significância Sig. (2 extremidades)	,024

a. Variável de Agrupamento:  
Gender

ET=196.5 p-value =0.024<0.05 so the median of males and females is different

Testes de Normalidade

	Gender	Kolmogorov-Smirnov <sup>a</sup>			Shapiro-Wilk		
		Estatística	gl	Sig.	Estatística	gl	Sig.
S 1060-R	Male	,115	25	,200*	,960	25	,406
	Female	,161	25	,092	,906	25	,025
S 2060-Y40R	Male	,231	25	,001	,864	25	,003
	Female	,096	25	,200*	,964	25	,509
S 3060-Y	Male	,179	25	,039	,947	25	,209
	Female	,147	25	,173	,958	25	,381
S 2060-G40Y	Male	,151	25	,144	,954	25	,302
	Female	,103	25	,200*	,970	25	,636
S 2050-G	Male	,103	25	,200*	,954	25	,312
	Female	,137	25	,200*	,949	25	,233
S 2050-B50G	Male	,132	25	,200*	,952	25	,279
	Female	,147	25	,172	,934	25	,109
S 2050-B	Male	,129	25	,200*	,878	25	,006
	Female	,227	25	,002	,933	25	,101
S 1555-R70B	Male	,172	25	,055	,949	25	,241
	Female	,188	25	,023	,868	25	,004
S 2040-R50B	Male	,123	25	,200*	,958	25	,368
	Female	,172	25	,056	,901	25	,019
S 2050-R30B	Male	,156	25	,118	,959	25	,390
	Female	,153	25	,135	,928	25	,080
S 3030-R	Male	,168	25	,066	,931	25	,091
	Female	,171	25	,057	,868	25	,004
S 4020-Y40R	Male	,144	25	,196	,889	25	,011
	Female	,121	25	,200*	,947	25	,216
S 4030-Y	Male	,201	25	,011	,920	25	,050
	Female	,093	25	,200*	,973	25	,713
S 3030-G40Y	Male	,081	25	,200*	,977	25	,810
	Female	,119	25	,200*	,961	25	,435
S 3020-G	Male	,137	25	,200*	,935	25	,114
	Female	,169	25	,062	,924	25	,062
S 4020-B50G	Male	,093	25	,200*	,978	25	,833
	Female	,141	25	,200*	,938	25	,132
S 3020-B	Male	,124	25	,200*	,966	25	,546
	Female	,147	25	,170	,949	25	,240
S 3020-R70B	Male	,092	25	,200*	,980	25	,894
	Female	,146	25	,176	,940	25	,145
S 3030-R50B	Male	,171	25	,056	,949	25	,240
	Female	,158	25	,110	,953	25	,288
S 3030-R30B	Male	,179	25	,039	,946	25	,201
	Female	,130	25	,200*	,941	25	,158
S 1030-R	Male	,172	25	,055	,917	25	,044
	Female	,177	25	,042	,951	25	,266
S 2020-Y40R	Male	,198	25	,013	,922	25	,058
	Female	,160	25	,096	,907	25	,026
S 2020-Y	Male	,191	25	,019	,943	25	,171
	Female	,126	25	,200*	,965	25	,528
S 2020-G40Y	Male	,132	25	,200*	,976	25	,807
	Female	,117	25	,200*	,950	25	,253
S 1020-G	Male	,121	25	,200*	,942	25	,161
	Female	,185	25	,027	,927	25	,076
S 1020-B50G	Male	,217	25	,004	,911	25	,032
	Female	,184	25	,029	,916	25	,043
S 1020-B	Male	,112	25	,200*	,933	25	,101
	Female	,231	25	,001	,912	25	,033
S 0525-R70B	Male	,179	25	,037	,944	25	,188
	Female	,140	25	,200*	,931	25	,091
S 1030-R50B	Male	,127	25	,200*	,969	25	,627
	Female	,138	25	,200*	,937	25	,125
S 1030-R30B	Male	,137	25	,200*	,975	25	,776
	Female	,106	25	,200*	,931	25	,091
S 1050-Y	Male	,134	25	,200*	,966	25	,551
	Female	,151	25	,147	,952	25	,280
S 1050-G40Y	Male	,115	25	,200*	,961	25	,434
	Female	,197	25	,013	,954	25	,308
S 1050-Y40R	Male	,174	25	,049	,886	25	,009
	Female	,145	25	,187	,949	25	,240
S 5030-R	Male	,123	25	,200*	,960	25	,406
	Female	,129	25	,200*	,968	25	,591
S 6030-Y40R	Male	,125	25	,200*	,951	25	,262
	Female	,116	25	,200*	,962	25	,446
S 6030-Y	Male	,158	25	,106	,869	25	,004
	Female	,135	25	,200*	,957	25	,356
S 5540-G40Y	Male	,132	25	,200*	,968	25	,605
	Female	,136	25	,200*	,969	25	,608
S 5030-G	Male	,096	25	,200*	,960	25	,412
	Female	,181	25	,035	,895	25	,014
S 5030-B50G	Male	,152	25	,137	,946	25	,208
	Female	,145	25	,183	,972	25	,699
S 6020-B	Male	,148	25	,168	,927	25	,074
	Female	,105	25	,200*	,973	25	,726
S 6020-R70B	Male	,133	25	,200*	,962	25	,458
	Female	,082	25	,200*	,963	25	,477
S 5030-R50B	Male	,206	25	,008	,941	25	,154
	Female	,181	25	,035	,928	25	,077
S 5030-R30B	Male	,097	25	,200*	,961	25	,434
	Female	,194	25	,016	,902	25	,020

- **For each sample**  
Analyze normality

Use Smirnov >30:

H0: samples preference is normally distributed

H1: samples preference is normally distributed

p-value <0.05 Reject H0, this means distribution is not normal in some so non-parametric tests have to be performed

Define test

Non-parametric tests and independent samples = non-parametric ANOVA (Kruskal-Walis)

H0: same median in all sample

H1: different median in at least two sample

Samples	Mean		Median		Standard deviation		Significance (p-value)
	Male	Female	Male	Female	Male	Female	
All	1,55	2,49	1,37	2,4	1,91	1,42	<0,05
S 1060-R	0,64	3,12	0	4	5,91	5,70	>0,05
S 2060-Y40R	3,32	2,08	4	2	5,27	3,43	>0,05
S 3060-Y	-2,04	-2,36	-2	-3	4,67	4,34	>0,05
S 2060-G40Y	2,24	1,96	2	1	4,48	4,65	>0,05
S 2050-G	2,64	1,92	3	2	5,11	5,62	>0,05
S 2050-B50G	3,36	4	3	5	4,88	4,56	>0,05
S 2050-B	5,48	4,64	6	5	3,75	3,08	>0,05
S 1555-R70B	3,92	2	4	4	4,00	6,12	>0,05
S 2040-R50B	2,48	4,2	2	5	3,56	3,76	>0,05
S 2050-R30B	0,84	3,36	1	5	5,23	4,83	>0,05
S 3030-R*	1,16	4,76	0	5	3,05	3,38	<0,001
S 4020-Y40R	-0,08	-0,16	0	0	4,05	4,04	>0,05
S 4030-Y	-1,68	-2,68	-3	-3	6,19	4,07	>0,05
S 3030-G40Y	1,8	2,8	2	3	4,82	3,99	>0,05
S 3020-G*	2,08	4,16	1	5	3,62	3,02	<0,05
S 4020-B50G	1,76	4,32	2	4	5,06	3,00	>0,05
S 3020-B	3,08	5,36	3	5	4,44	3,04	>0,05
S 3020-R70B	2,28	4,12	2	4	4,39	3,88	>0,05
S 3030-R50B*	2,56	5,28	2	6	3,61	2,91	<0,05
S 3030-R30B*	0,68	4,52	0	5	4,27	3,84	<0,05
S 1030-R*	0,52	3,36	1	5	4,30	4,06	<0,05
S 2020-Y40R	-0,24	1,52	0	1	4,31	4,25	>0,05
S 2020-Y	0,32	0,96	1	2	4,43	3,86	>0,05
S 2020-G40Y*	0,56	3,52	0	4	4,43	4,21	<0,05
S 1020-G	1,84	3,2	2	4	4,54	3,72	>0,05
S 1020-B50G*	3	5,44	4	6	4,74	2,92	<0,05
S 1020-B*	3,32	6,56	3	8	4,56	2,58	<0,05
S 0525-R70B	1,8	3,56	1	5	4,00	4,72	>0,05
S 1030-R50B*	-0,04	5,36	0	5	4,08	3,13	<0,001
S 1030-R30B*	0,76	3,72	0	4	3,90	4,01	<0,05
S 1050-Y	0,72	2,12	1	2	5,26	4,52	>0,05
S 1050-G40Y	0,8	2,44	0	2	5,27	3,55	>0,05
S 1050-Y40R	3,08	1,84	4	3	5,29	4,80	>0,05
S 5030-R	0,44	1,76	0	1	5,32	3,57	>0,05
S 6030-Y40R	-0,08	-2,68	-1	-3	5,15	3,90	>0,05
S 6030-Y	-4,88	-3,8	-6	-4	4,58	4,30	>0,05
S 5540-G40Y*	1,6	-0,76	1	0	5,02	3,97	<0,05
S 5030-G	3,68	1,88	3	2	3,54	3,60	>0,05
S 5030-B50G	3,48	3,88	3	4	3,64	3,02	>0,05
S 6020-B	3	2,52	3	2	4,50	3,83	>0,05
S 6020-R70B*	3,08	0,2	3	0	4,51	5,11	<0,05
S 5030-R50B	2,48	0,84	2	1	4,32	4,90	>0,05
S 5030-R30B	0,92	2,44	1	4	5,69	4,11	>0,05

The ones marked (\*) have significant statistical differences in males and females.

Appendix X - Statistical analysis.

***Is color preference different in males and females?***

Same samples in different observers = Independent samples

- **All samples**

Analyze normality

Use Smirnov >30:

H0: samples preference is normally distributed

H1: samples preference is not normally distributed

**Testes de Normalidade**

Mean	Sex	Kolmogorov-Smirnov <sup>a</sup>			Shapiro-Wilk		
		Estatística	gl	Sig.	Estatística	gl	Sig.
	Male	,176	25	,045	,919	25	,049
	Female	,125	25	,200 <sup>*</sup>	,950	25	,251

\*. Este é um limite inferior da significância verdadeira.

a. Correlação de Significância de Lilliefors

p-value <0.05 Reject H0, this means distribution is not normal and that non-parametric tests have to be performed

Define test

Non-parametric tests and independent samples = Mann-Whitney

H0: median of males = median of females

H1: median of males ≠ median of females

**Estatísticas de teste<sup>a</sup>**

	Mean
U de Mann-Whitney	266,500
Wilcoxon W	591,500
Z	-,893
Significância Sig. (2 extremidades)	,372

a. Variável de Agrupamento: Sex

ET=266.5 p-value =0.372<0.05 so the median of males and females is the same

Testes de Normalidade							
	Sex	Kolmogorov-Smirnov <sup>a</sup>			Shapiro-Wilk		
		Estatística	gl	Sig.	Estatística	gl	Sig.
S 1060-R	Male	,161	25	,092	,917	25	,043
	Female	,159	25	,105	,918	25	,047
S 2060-Y40R	Male	,146	25	,176	,950	25	,247
	Female	,145	25	,189	,977	25	,811
S 3060-Y	Male	,104	25	,200 <sup>*</sup>	,963	25	,481
	Female	,186	25	,025	,894	25	,013
S 2060-G40Y	Male	,160	25	,100	,929	25	,085
	Female	,137	25	,200 <sup>*</sup>	,957	25	,359
S 2050-G	Male	,107	25	,200 <sup>*</sup>	,964	25	,511
	Female	,092	25	,200 <sup>*</sup>	,962	25	,449
S 2050-B50G	Male	,155	25	,125	,919	25	,050
	Female	,170	25	,061	,944	25	,184
S 2050-B	Male	,128	25	,200 <sup>*</sup>	,916	25	,041
	Female	,140	25	,200 <sup>*</sup>	,953	25	,286
S 1555-R70B	Male	,126	25	,200 <sup>*</sup>	,964	25	,498
	Female	,099	25	,200 <sup>*</sup>	,952	25	,271
S 2040-R50B	Male	,135	25	,200 <sup>*</sup>	,931	25	,092
	Female	,151	25	,145	,914	25	,037
S 2050-R30B	Male	,156	25	,116	,935	25	,116
	Female	,151	25	,144	,910	25	,030
S 3030-R	Male	,127	25	,200 <sup>*</sup>	,972	25	,689
	Female	,143	25	,200 <sup>*</sup>	,947	25	,220
S 4020-Y40R	Male	,118	25	,200 <sup>*</sup>	,973	25	,726
	Female	,143	25	,200 <sup>*</sup>	,958	25	,377
S 4030-Y	Male	,160	25	,099	,918	25	,046
	Female	,142	25	,200 <sup>*</sup>	,920	25	,050
S 3030-G40Y	Male	,142	25	,200 <sup>*</sup>	,972	25	,685
	Female	,101	25	,200 <sup>*</sup>	,968	25	,600
S 3020-G	Male	,119	25	,200 <sup>*</sup>	,971	25	,672
	Female	,156	25	,121	,937	25	,125
S 4020-B50G	Male	,177	25	,041	,926	25	,072
	Female	,165	25	,076	,932	25	,097
S 3020-B	Male	,176	25	,045	,905	25	,024
	Female	,146	25	,181	,899	25	,018
S 3020-R70B	Male	,188	25	,023	,902	25	,020
	Female	,165	25	,077	,902	25	,021
S 3030-R50B	Male	,166	25	,072	,936	25	,117
	Female	,234	25	,001	,815	25	<.001
S 3030-R30B	Male	,155	25	,125	,944	25	,178
	Female	,221	25	,003	,859	25	,003
S 1030-R	Male	,138	25	,200 <sup>*</sup>	,945	25	,189
	Female	,163	25	,084	,935	25	,116
S 2020-Y40R	Male	,108	25	,200 <sup>*</sup>	,965	25	,530
	Female	,103	25	,200 <sup>*</sup>	,968	25	,583
S 2020-Y	Male	,120	25	,200 <sup>*</sup>	,980	25	,890
	Female	,122	25	,200 <sup>*</sup>	,954	25	,310
S 2020-G40Y	Male	,168	25	,068	,924	25	,062
	Female	,216	25	,004	,882	25	,008
S 1020-G	Male	,154	25	,131	,920	25	,050
	Female	,146	25	,176	,899	25	,017
S 1020-B50G	Male	,202	25	,010	,918	25	,047
	Female	,134	25	,200 <sup>*</sup>	,899	25	,017
S 1020-B	Male	,164	25	,082	,873	25	,005
	Female	,148	25	,163	,903	25	,021
S 0525-R70B	Male	,129	25	,200 <sup>*</sup>	,945	25	,191
	Female	,138	25	,200 <sup>*</sup>	,905	25	,024
S 1030-R50B	Male	,175	25	,047	,914	25	,037
	Female	,175	25	,046	,858	25	,002
S 1030-R30B	Male	,160	25	,097	,935	25	,114
	Female	,145	25	,188	,939	25	,143
S 1050-Y	Male	,277	25	<.001	,881	25	,007
	Female	,169	25	,062	,928	25	,080
S 1050-G40Y	Male	,134	25	,200 <sup>*</sup>	,963	25	,477
	Female	,150	25	,152	,944	25	,180
S 1050-Y40R	Male	,124	25	,200 <sup>*</sup>	,950	25	,251
	Female	,156	25	,118	,965	25	,512
S 5030-R	Male	,111	25	,200 <sup>*</sup>	,982	25	,929
	Female	,158	25	,108	,953	25	,287
S 6030-Y40R	Male	,166	25	,073	,940	25	,151
	Female	,135	25	,200 <sup>*</sup>	,933	25	,104
S 6030-Y	Male	,187	25	,025	,864	25	,003
	Female	,206	25	,007	,786	25	<.001
S 5540-G40Y	Male	,195	25	,015	,932	25	,098
	Female	,103	25	,200 <sup>*</sup>	,954	25	,308
S 5030-G	Male	,108	25	,200 <sup>*</sup>	,956	25	,340
	Female	,108	25	,200 <sup>*</sup>	,956	25	,343
S 5030-B50G	Male	,159	25	,104	,922	25	,058
	Female	,150	25	,152	,953	25	,292
S 6020-B	Male	,150	25	,153	,916	25	,042
	Female	,148	25	,163	,901	25	,019
S 6020-R70B	Male	,195	25	,015	,909	25	,029
	Female	,141	25	,200 <sup>*</sup>	,928	25	,077
S 5030-R50B	Male	,119	25	,200 <sup>*</sup>	,971	25	,679
	Female	,133	25	,200 <sup>*</sup>	,933	25	,104
S 5030-R30B	Male	,197	25	,014	,950	25	,254
	Female	,157	25	,115	,939	25	,141
S 0300-N	Male	,173	25	,051	,891	25	,012
	Female	,300	25	<.001	,744	25	<.001
S 4500-N	Male	,151	25	,143	,929	25	,082
	Female	,237	25	<.001	,887	25	,009
S 9000-N	Male	,215	25	,004	,878	25	,006
	Female	,202	25	,010	,861	25	,003

\*. Este é um limite inferior da significância verdadeira.

a. Correlação de Significância de Lilliefors

- **For each sample**

Analyze normality

Use Smirnov >30:

H0: samples preference is normally distributed

H1: samples preference is not normally distributed

p-value <0.05 Reject H0, this means distribution is not normal in some so non-parametric tests have to be performed

Define test

Non-parametric tests and independent samples = non-parametric ANOVA (Kruskal-Walis)

H0: same median in all sample

H1: different median in at least two sample

Samples	Mean		Median		Standard deviation		Significance (p-value)
	Male	Female	Male	Female	Male	Female	
All	1.97	2.33	1.82	2	1.18	1.40	>0.05
S 1060-R	1.40	2.52	3	4	6.23	5.35	>0.05
S 2060-Y40R	2.64	0.84	2	1	3.45	5.08	>0.05
S 3060-Y*	-2.28	-5.28	-3	-6	4.30	3.31	<0.05
S 2060-G40Y	1.96	0.28	3	0	4.08	4.42	>0.05
S 2050-G	1.92	0.12	3	1	4.94	4.87	>0.05
S 2050-B50G	3.44	0.11	3	2	5.53	4.76	>0.05
S 2050-B	4.76	1.14	5	3	3.73	4.11	>0.05
S 1555-R70B	4.56	1.76	4	2	3.22	5.87	>0.05
S 2040-R50B	1.56	4.08	3	5	5.06	4.33	>0.05
S 2050-R30B*	0.28	4.36	2	5	4.92	4.49	<0.05
S 3030-R*	0.76	5.32	1	6	3.59	3.15	>0.05
S 4020-Y40R	-0.32	-1.44	0	0	4.56	4.60	<0.001
S 4030-Y*	-1.76	-5.28	-3	-5	5.56	4.17	<0.05
S 3030-G40Y	3.04	2.88	2	2	3.33	4.60	>0.05
S 3020-G	3.56	4.44	3	5	2.87	4.01	>0.05
S 4020-B50G	3.16	3.44	4	4	4.29	4.27	>0.05
S 3020-B	4.36	5.32	4	6	4.80	3.71	>0.05
S 3020-R70B	3.12	4.72	4	6	3.93	3.81	>0.05
S 3030-R50B*	2.60	5.88	3	7	4.45	3.27	<0.05
S 3030-R30B*	-0.04	4.88	-1	6	4	3.63	<0.001
S 1030-R*	0.64	4.04	0	4	5.26	4.10	<0.05
S 2020-Y40R	0.88	1.32	1	1	3.87	4.44	>0.05
S 2020-Y	2.20	2.24	2	2	4.05	5.28	>0.05
S 2020-G40Y*	2.84	6.12	2	7	2.95	3.78	<0.05
S 1020-G	3.36	5.20	5	6	4.80	4.22	>0.05
S 1020-B50G	4.56	6.36	5	7	4.14	3.29	>0.05
S 1020-B	4.80	6.76	6	7	4.55	2.43	>0.05



S 0525-R70B*	3.04	5.52	3	5	4.48	4.11	<0.05
S 1030-R50B*	2.56	6.64	2	8	3.87	3.40	<0.001
S 1030-R30B*	1.64	6.04	2	6	4.58	2.97	<0.001
S 1050-Y	2.28	2.12	3	4	4.92	5.02	>0.05
S 1050-G40Y	2.24	1.88	3	2	4.42	4.63	>0.05
S 1050-Y40R	1.76	2.44	3	3	5.06	3.95	>0.05
S 5030-R*	-1.12	1.80	-2	3	4.24	4.83	<0.05
S 6030-Y40R	-2.88	-3.28	-2	-3	4.79	5.27	>0.05
S 6030-Y*	-4.40	-7.12	-5	-8	4.78	3.49	<0.05
S 5540-G40Y*	1.12	-2.96	2	-3	4.19	4.98	<0.05
S 5030-G	2.72	-0.56	3	1	3.42	4.37	>0.05
S 5030-B50G	2.64	1.88	3	3	4.16	4.63	>0.05
S 6020-B	2.88	1.88	4	2	4.99	4.81	>0.05
S 6020-R70B*	3.08	-1.08	3	0	5.04	5.53	<0.05
S 5030-R50B	1.16	1	2	2	3.96	5.62	>0.05
S 5030-R30B	0.48	2.16	1	2	4.03	5.01	>0.05
S 0300-N	4.76	4.88	6	7	4.32	4.52	>0.05
S 4500-N	3.16	2.08	3	0	4.85	4.36	>0.05
S 9000-N	5.84	4.64	6	6	3.89	5.70	>0.05

The ones marked (\*) have significant statistical differences in males and females.

**Does artistic education affect color preference?**

Same samples in different observers = Independent samples

- **All samples**

Analyze normality

Use Smirnov >30:

H0: samples preference is normally distributed

H1: samples preference is not normally distributed

**Testes de Normalidade**

		Kolmogorov-Smirnov <sup>a</sup>			Shapiro-Wilk		
Art_education		Estatística	gl	Sig.	Estatística	gl	Sig.
Mean	No	,115	50	,096	,962	50	,107
	Yes	,134	50	,026	,946	50	,023

a. Correlação de Significância de Lilliefors

p-value <0.05 Reject H0, this means distribution is not normal and that non-parametric tests have to be performed

Define test

Non-parametric tests and independent samples = Mann-Whitney

H0: median of observers with art education = median of observers without art education

H1: median of observers with art education ≠ median of without art education

**Estatísticas de teste<sup>a</sup>**

	Mean
U de Mann-Whitney	1147,000
Wilcoxon W	2422,000
Z	-,710
Significância Sig. (2 extremidades)	,478

a. Variável de Agrupamento:  
Art\_education

ET=11147 p-value =0.478<0.05 so the median of observes with or without art education is the same.

Testes de Normalidade							
	Art_education	Kolmogorov-Smirnov <sup>a</sup>			Shapiro-Wilk		
		Estatística	gl	Sig.	Estatística	gl	Sig.
S 1060-R	No	,103	50	,200 <sup>†</sup>	,933	50	,007
	Yes	,141	50	,015	,925	50	,004
S 2060-Y40R	No	,118	50	,079	,959	50	,081
	Yes	,133	50	,027	,962	50	,104
S 3060-Y	No	,130	50	,033	,945	50	,022
	Yes	,137	50	,020	,958	50	,076
S 2060-G40Y	No	,127	50	,042	,948	50	,029
	Yes	,141	50	,014	,963	50	,118
S 2050-G	No	,131	50	,033	,949	50	,030
	Yes	,099	50	,200 <sup>†</sup>	,973	50	,311
S 2050-B50G	No	,139	50	,017	,922	50	,003
	Yes	,128	50	,040	,947	50	,026
S 2050-B	No	,163	50	,002	,931	50	,006
	Yes	,138	50	,019	,939	50	,013
S 1555-R70B	No	,143	50	,013	,925	50	,004
	Yes	,126	50	,044	,950	50	,034
S 2040-R50B	No	,119	50	,077	,945	50	,021
	Yes	,116	50	,088	,934	50	,008
S 2050-R30B	No	,105	50	,200 <sup>†</sup>	,971	50	,245
	Yes	,115	50	,096	,934	50	,008
S 3030-R	No	,140	50	,016	,937	50	,010
	Yes	,105	50	,200 <sup>†</sup>	,973	50	,307
S 4020-Y40R	No	,099	50	,200 <sup>†</sup>	,972	50	,271
	Yes	,096	50	,200 <sup>†</sup>	,971	50	,264
S 4030-Y	No	,118	50	,080	,945	50	,022
	Yes	,132	50	,029	,924	50	,003
S 3030-G40Y	No	,130	50	,034	,935	50	,009
	Yes	,115	50	,094	,972	50	,280
S 3020-G	No	,123	50	,056	,953	50	,045
	Yes	,097	50	,200 <sup>†</sup>	,968	50	,199
S 4020-B50G	No	,195	50	<,001	,917	50	,002
	Yes	,136	50	,022	,937	50	,010
S 3020-B	No	,160	50	,003	,913	50	,001
	Yes	,130	50	,034	,914	50	,001
S 3020-R70B	No	,147	50	,009	,945	50	,022
	Yes	,108	50	,200 <sup>†</sup>	,947	50	,026
S 3030-R50B	No	,137	50	,020	,932	50	,007
	Yes	,152	50	,006	,894	50	<,001
S 3030-R30B	No	,129	50	,035	,955	50	,058
	Yes	,145	50	,010	,927	50	,004
S 1030-R	No	,095	50	,200 <sup>†</sup>	,969	50	,201
	Yes	,091	50	,200 <sup>†</sup>	,962	50	,112
S 2020-Y40R	No	,126	50	,045	,949	50	,033
	Yes	,097	50	,200 <sup>†</sup>	,974	50	,326
S 2020-Y	No	,137	50	,020	,952	50	,041
	Yes	,079	50	,200 <sup>†</sup>	,973	50	,294
S 2020-G40Y	No	,118	50	,077	,949	50	,030
	Yes	,115	50	,095	,952	50	,042
S 1020-G	No	,106	50	,200 <sup>†</sup>	,952	50	,042
	Yes	,147	50	,009	,927	50	,004
S 1020-B50G	No	,134	50	,025	,920	50	,002
	Yes	,157	50	,004	,916	50	,002
S 1020-B	No	,120	50	,072	,944	50	,019
	Yes	,143	50	,012	,861	50	<,001
S 0525-R70B	No	,157	50	,003	,921	50	,003
	Yes	,110	50	,181	,938	50	,011
S 1030-R50B	No	,158	50	,003	,920	50	,002
	Yes	,138	50	,018	,913	50	,001
S 1030-R30B	No	,113	50	,135	,952	50	,040
	Yes	,114	50	,100	,929	50	,005
S 1050-Y	No	,108	50	,200 <sup>†</sup>	,939	50	,013
	Yes	,204	50	<,001	,910	50	,001
S 1050-G40Y	No	,106	50	,200 <sup>†</sup>	,948	50	,027
	Yes	,144	50	,011	,961	50	,100
S 1050-Y40R	No	,115	50	,098	,954	50	,050
	Yes	,139	50	,017	,956	50	,058
S 5030-R	No	,106	50	,200 <sup>†</sup>	,949	50	,030
	Yes	,093	50	,200 <sup>†</sup>	,983	50	,678
S 6030-Y40R	No	,115	50	,097	,957	50	,064
	Yes	,124	50	,053	,945	50	,022
S 6030-Y	No	,095	50	,200 <sup>†</sup>	,949	50	,032
	Yes	,212	50	<,001	,829	50	<,001
S 5540-G40Y	No	,156	50	,004	,938	50	,011
	Yes	,153	50	,005	,964	50	,135
S 5030-G	No	,129	50	,037	,943	50	,018
	Yes	,095	50	,200 <sup>†</sup>	,957	50	,066
S 5030-B50G	No	,199	50	<,001	,897	50	<,001
	Yes	,136	50	,021	,962	50	,104
S 6020-B	No	,178	50	<,001	,869	50	<,001
	Yes	,104	50	,200 <sup>†</sup>	,924	50	,003
S 6020-R70B	No	,202	50	<,001	,887	50	<,001
	Yes	,090	50	,200 <sup>†</sup>	,944	50	,020
S 5030-R50B	No	,094	50	,200 <sup>†</sup>	,939	50	,012
	Yes	,115	50	,096	,960	50	,085
S 5030-R30B	No	,129	50	,036	,940	50	,013
	Yes	,089	50	,200 <sup>†</sup>	,979	50	,494
S 0300-N	No	,217	50	<,001	,779	50	<,001
	Yes	,225	50	<,001	,834	50	<,001
S 4500-N	No	,178	50	<,001	,940	50	,013
	Yes	,165	50	,002	,926	50	,004
S 9000-N	No	,164	50	,002	,847	50	<,001
	Yes	,180	50	<,001	,868	50	<,001

\*. Este é um limite inferior da significância verdadeira.

a. Correlação de Significância de Lilliefors

- **For each sample**

- Analyze normality

- Use Smirnov >30:

- H0: samples preference is normally distributed

- H1: samples preference is not normally distributed

- p-value <0.05 Reject H0, this means distribution is not normal in some so non-parametric tests have to be performed

- **Define test**

- Non-parametric tests and independent samples = non-parametric ANOVA (Kruskal-Walis)

- H0: same median in all sample

- H1: different median in at least two sample

Samples	Mean		Median		Standard deviation		Significance (p-value)
	Without art education	With art education	Without art education	With art education	Without art education	With art education	
All	2.17	2.53	1.92	1.3	1.18	2.07	>0.05
S 1060-R*	1.96	-1.58	3	-1.74	5.77	6.37	<0.05
S 2060-Y40R	1.74	2.62	2	3.5	4.39	5.14	>0.05
S 3060-Y*	-3.78	-1.22	-5	-1	4.09	6.01	<0.05
S 2060-G40Y	1.12	0.68	2	2	4.30	4.85	>0.05
S 2050-G	1.02	-0.66	2	-0.5	4.94	6.01	>0.05
S 2050-B50G	2.76	1.90	2.5	3	5.16	5.88	>0.05
S 2050-B	3.8	0.89	5	3.5	4	5.37	>0.05
S 1555-R70B	3.16	3.46	4	5	5.21	4.93	>0.05
S 2040-R50B	2.82	3	4	4	4.84	5.21	>0.05
S 2050-R30B	2.32	1.12	3	2	5.10	5.04	>0.05
S 3030-R	3.04	2.56	3	4	4.06	4.71	>0.05
S 4020-Y40R	-0.88	0.76	0	1	4.57	4.30	>0.05
S 4030-Y	3.52	-2.22	-5	-2	5.18	5.73	>0.05
S 3030-G40Y*	2.96	4.26	2	5	3.98	3.80	<0.05
S 3020-G	4	3.32	4	4	3.48	4.28	>0.05
S 4020-B50G	3.30	4.20	4	5	4.24	4.24	>0.05
S 3020-B	4.84	5.32	5.5	6	4.28	3.67	>0.05
S 3020-R70B	3.92	4.48	4	5	3.91	3.79	>0.05
S 3030-R50B	4.24	3.84	5	5	4.21	4.98	>0.05
S 3030-R30B	2.42	2.74	2.5	3.5	4.53	4.10	>0.001
S 1030-R*	2.34	-0.24	3	0	4.98	5.38	<0.05
S 2020-Y40R	1.1	0.80	1	0	4.13	4.3	>0.05
S 2020-Y	2.22	3.22	2	4	4.66	4.23	>0.05
S 2020-G40Y	4.48	3.26	5	4	3.75	4.13	>0.05
S 1020-G*	4.28	1.96	5.50	2	4.57	5.56	<0.05
S 1020-B50G*	5.46	3.08	6.50	4	3.81	5.40	<0.05
S 1020-B	5.78	4.36	6	5	3.75	4.27	>0.05
S 0525-R70B	4.28	5.22	5	6	4.44	3.89	>0.05
S 1030-R50B	4.60	3	5	3	4.15	4.79	>0.05
S 1030-R30B*	3.84	0.66	4	2	4.42	5.68	<0.05
S 1050-Y	2.2	3.6	3	4	4.92	4.6	>0.05
S 1050-G40Y	2.06	1.8	2	2.5	4.49	5.24	>0.05
S 1050-Y40R	2.1	0.7	3	0.5	4.51	5.96	>0.05
S 5030-R*	0.34	3.92	1	4	4.74	4.28	<0.001
S 6030-Y40R*	-3.08	-0.58	-2.5	0	4.99	4.21	<0.05
S 6030-Y*	-5.76	-1.58	-7	-1	4.37	5.7	<0.001
S 5540-G40Y*	-0.92	2.74	0	4	5	4.27	<0.001
S 5030-G	1.98	2.66	2	3	3.96	4.7	>0.05
S 5030-B50G*	2.26	4.3	3	6	4.37	4.74	<0.05
S 6020-B*	2.38	6	3	7	4.88	4	<0.001
S 6020-R70B*	-0.6	4.84	2	7	5.64	4.57	<0.001
S 5030-R50B*	1.08	3.68	2	4	4.81	4.8	<0.05
S 5030-R30B*	1.32	3.66	1	4	4.58	4.61	<0.05
S 0300-N	4.82	5.68	6	7	4.38	4.40	>0.05

S 4500-N	2.62	2.42	3	1	4.6	4.68	>0.05
S 9000-N	5.24	6.18	6	7	4.87	3.88	>0.05

The ones marked (\*) have significant statistical differences in observers with or without art education